APPROVED FOR PUBLIC RELEASE. CASE 06-1104.

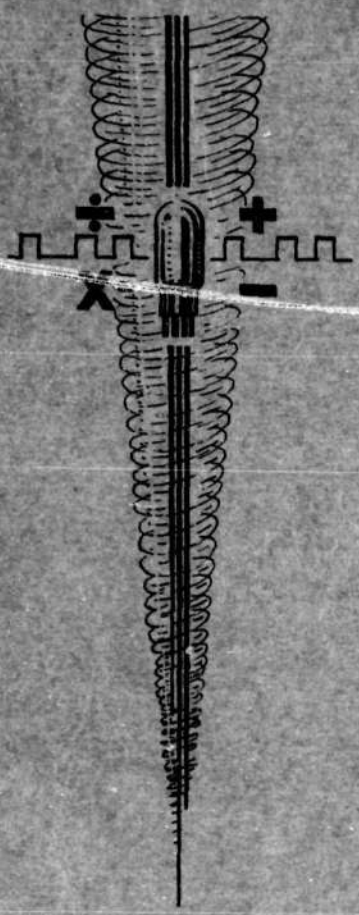

PROJECT WHIRLWIND

Contract N5ori60

SUMMARY REPORT NO. 2

VOLUME 18

PULSE TRANSFORMERS

SERVOMECHANISMS LABORATORY
MASSACHUSETTS INSTITUTE OF TECHNOLOGY

Copy 30

SPECIAL DEVICES CENTER

APPROVED FOR PUBLIC RELEASE. CASE 06-1104.

PROJECT WHIRLWIND
Summary Report No. 2
November, 1947

PULSE TRANSFORMERS

Volume 18 of 22 Volumes

Servomechanisms Laboratory
Massachusetts Institute of Technology
Cambridge, Massachusetts

APPROVED FOR PUBLIC RELEASE. CASE 06-1104.

CONTENTS

APPROVED FOR PUBLIC RELEASE. CASE 06-1104.

INTRODUCTION

Pulse transformers are important components of the Whirlwind computers. Their use as impedance transformers and for pulse inversion greatly reduces the number of tubes required and simplifies circuit design.

Commercial pulse transformers suitable for use with the pulse shape and power level of the Whirlwind computers have not been obtainable. Report, R-122, contained in this volume is the result of a study of pulse transformers undertaken by T. F. Winett which occupied his full time for more than a year. The report contains an analysis of pulse-transformer operation, with particular reference to impedance transformation and transformers for pulse inversion of the pulses used in the Whirlwind computers. A discussion of transformer design follows the section on analysis.

An up-to-date discussion of pulse transformers and pulse-transformer development, including a brief discussion of pulse-transformer operation and design, appears in M-132 of this volume.

Transformers for Whirlwind I have been designed by C. G. Hoberg, who has also made a study of pulse-transformer applications for Whirlwind I. At present, two transformer types are adequate for all applications. One type is a one-to-one inverter transformer and the other is a three-to-one impedance transformer intended primarily for coupling vacuum tubes to low-impedance cables. These transformers are for 0.1 microsecond, half-sine-wave pulses.

Several pulse-transformer applications are discussed in other volumes. The pulse transformer as a one-to-one inverter in the plate-load circuit of a gate tube is described in volume 16, R-73. The pulse transformer for impedance transformation in coupling an amplifier to the low-impedance digit-transfer bus is discussed in volume 19, R-131. The use of a three-to-one transformer as a voltage step-up transformer is discussed in volume 19, R-60.

APPROVED FOR PUBLIC RELEASE. CASE 06-1104.

REFERENCE INDEX

M Series Memorandums

REF.	VOL.	REF.	VOL.	REF.	VOL.
M-32	8	M-95	8	M-133	18
M-46	9	M-96	9	M-134	7
M-56	9	M-99	15	M-135	7
M-58	15	M-100	8	M-136	7
M-61	8	M-101	11	M-137	7
M-62	4	M-103	16	M-138	15
M-63	4	M-105	19	M-140	4
M-64	4	M-106	11	M-141	7
M-65	14	M-107	19	M-142	8
M-66	4	M-109	16	M-143	9
M-68	15	M-110	15	M-144	10
M-69	4	M-111	7	M-145	11
M-71	8	M-112	9	M-146	12
M-72	16	M-113	7	M-147	13
M-74	14	M-114	19	M-148	14
M-76	4	M-116	16	M-149	15
M-77	15	M-117	7	M-150	16
M-78	8	M-118	16	M-151	17
M-80	16	M-119	16	M-152	18
M-81	16	M-121	9	M-153	19
M-82	16	M-123	7	M-154	20
M-83	16	M-124	8	M-155	21
M-85	14	M-127	7	M-156	22
M-89	11	M-128	16	M-157	11
M-91	15	M-129	7	M-158	7
M-92	15	M-130	9	M-159	9
M-94	8	M-131	16	M-160	8
		M-132	16	M-161	7

APPROVED FOR PUBLIC RELEASE. CASE 06-1104.

REFERENCE INDEX

E Series Memorandums

C Series Memorandum

REF.	VOL.	REF.	VOL
E-7	14	E-52	19
E-24	7	E-53	13
E-31	10	E-54	19
E-32	10	E-55	19
E-33	19	E-56	15
E-37	15	E-57	15
E-38	19	E-58	19
E-39	15	E-59	19
E-41	15	E-60	19
E-42	15	E-61	16
E-44	19	E-63	19
E-45	19	E-64	16
E-47	15	E-68	13
E-48	19	E-69	15
E-49	19	E-71	19
E-50	16	E-73	16
C-15	14		

APPROVED FOR PUBLIC RELEASE. CASE 06-1104.

REFERENCE INDEX

R Series Memorandums

REF.	VOL.	REF.	VOL.
R-36	14	R-115	4
R-49	14	R-116	4
R-63	14	R-117	16
R-64	3	R-118	16
R-89	19	R-120	10
R-90	4	R-121	19
R-94	14	R-122	18
R-98	14	R-123	17
R-100	14	R-124	11
R-103	14	R-125	14
R-104	16	R-126	19
R-106	15	R-127	5
R-108	15	R-127	6
R-109	19	R-128	10
R-110	9	R-129	12
R-111	15	R-130	9
R-113	15	R-131	10
R-114	8	R-132	10

APPROVED FOR PUBLIC RELEASE. CASE 06-1104.

Project Whirlwind
Servomechanisms Laboratory
Massachusetts Institute of Technology
Cambridge, Massachusetts

SUBJECT: PULSE TRANSFORMERS, REVIEW OF DEVELOPMENT

To: J. W. Forrester

From: G. G. Hoberg

Date: November 5, 1947

Introduction

A pulse transformer is fundamentally similar to any other kind of electromagnetic transformer in construction and operating principles. It consists of primary and secondary windings through which passes a closed loop of magnetic material, and functions in accordance with the elementary laws of induction. However, the requirement that it pass short-duration pulses of energy, preferably without distortion, imposes a need for rather precise design which justifies special analysis and treatment.

Two broad classes of pulse transformers exist: (1) those in which heating and insulation problems are of prime importance, such as the transformers used to deliver high-energy, high-voltage pulses to magnetrons in radar transmitters, and (2) those which may be designed without consideration of these factors, since only low-energy, low-voltage pulses need be handled.

Pulse transformers used in the circuits of high-speed electronic digital computers are of the latter type. They are quite small and of simple construction. Primary and secondary are usually wound as two concentric solenoids about one leg of a rectangular core of thinly-laminated, high-permeability ferromagnetic alloy. Overall dimensions are of the order of $1'' \times 1\frac{1}{2}'' \times \frac{1}{2}''$.

History of Development

During the recent war a great deal of research was conducted at the Radiation Laboratory, M.I.T., and at a number of establishments in Great Britain, on the analysis, design, and techniques of construction of pulse transformers. Reports on this work are available in the Radiation Laboratory Document Room, M.I.T. Practically all of the Radiation Laboratory research and much of the British work was on the high-power variety of transformers for magnetron modulators. Although the broad principles of analysis are similar in both cases, relatively little work was done specifically on low-power transformers, and those British reports which do treat them separately are still highly classified. An abstract of a paper, "Low-Power Pulse Transformers", given

APPROVED FOR PUBLIC RELEASE. CASE 06-1104.

by N. H. Moody before the British Radiolocation Convention in 1946 appears in the Journal of the I.E.E. (Vol. 93. Part IIIA, No. 1, March-May, 1946), but most of his work remains unpublished.

A rigorous general treatment of pulse transformers has been prepared by Dr. W. H. Bostick of the D.I.C. Staff, M.I.T., for Volume 5 of the Radiation Laboratory Series ("Pulse Generators", Glasoe and Lebacqz; McGraw Hill), but this book will not be available until early 1948.

All in all, the topic has received remarkably little treatment in the literature. The most pertinent discussions currently available are to be found in the following references:

1. A. G. Ganz, "Applications of Thin Permalloy Tape in Wide-Band Telephone and Pulse Transformers", A.I.E.E. Transactions, April, 1946.

2. L. N. Ridenour, "Radar System Engineering", Vol. 1, Radiation Laboratory Series, pp. 384-6; McGraw Hill.

3. M.I.T. Radar School, "Principles of Radar", 2-73 to 2-82; McGraw Hill.

Research on Project Whirlwind

Soon after digital methods were adopted for the Whirlwind computers, it became apparent that electronic circuit design could in many cases be simplified if satisfactory pulse transformers were available. Early in 1946 T. F. Wimett undertook an investigation of the problem. Experiments with commercially manufactured transformers soon disclosed the fact that none were particularly suitable, and that in general a given transformer was good for only one specific application. It became apparent that pulse transformers would have to be custom-designed for each computer use.

Wimett then studied the work which had already been done on the subject and began a series of experiments to achieve optimum designs for proposed operating conditions. Much of the work which followed is a real contribution to the field of pulse transformer analysis and design. It is comprehensively treated in his report "Low-Power Pulse Transformers" R-122 which was written in the summer of 1947.

Since the guiding principles are firmly established and successful transformers have already been built, work currently in progress and foreseen for the near future consists merely of extrapolating proven designs to cover new circuit conditions and pulse lengths.

APPROVED FOR PUBLIC RELEASE. CASE 06-1104.

Applications in Computer Circuits

In computer circuits pulse transformers are used for one or more of the following reasons:

1. Impedance matching (to obtain optimum power transfer between source and load).

2. Polarity reversal (to convert a negative pulse to a positive pulse or vice versa).

3. DC isolation (to permit source and load to operate at different direct-voltage levels).

4. Reduction of DC resistance (to prevent buildup of DC bias).

Wimett's report describes transformers capable of adequately performing these functions in dealing with low-energy pulses (peak power of the order of 25 watts) of very short duration (1/20 to $\frac{1}{4}$ microsecond).

They are most commonly used in the plate circuit of a pentode tube. Since the control grid of the tube is usually biased below cut-off voltage, and driven toward cathode potential by positive pulses, negative pulses appear at the plate terminal (i.e., across the transformer primary). If the output is to be used to drive other tubes, as usually required, it should be positive pulse. Hence the transformers are almost invariably connected to give phase reversal, and because tubes need never conduct except during pulses, power dissipation is held at a minimum and component life increased.

If the output is to be used at a nearby point so that transmission line is unnecessary, a simple inverting transformer with unity turns ratio is commonly employed. However, when the output from tube and transformer is to appear at a remote point, a step-down transformer is used to match more closely the tube source to the low-impedance cable which must be used to transmit the pulse.

A problem arises here, for by conventional transformer theory, the impedance reflected back to the plate of the tube is then the impedance looking into the cable multiplied by the square of the transformer turns ratio. The rate of rise of the pulse can then never exceed that permitted by the time constant of this reflected impedance and the output capacitance of the tube. The turns ratio is therefore limited in magnitude, for the short pulses used demand rapid rates of rise and fall. But, insofar as the pentode tube is approximately a constant-current source over a limited operating range, a high step-down ratio is desirable in many cases because current output of the transformer is then multiplied by the turns ratio, and for constant load impedance

APPROVED FOR PUBLIC RELEASE. CASE 06-1104.

this represents an increase in voltage. Both the above effects, together with the fact that the pentode loses its constant-current properties at low plate voltages, must be considered and appropriate compromises made in deciding upon the ratio to be used. In some cases it is possible to use a step-up transformer at the remote end of the transmission line where usually the highest attainable voltage is desired.

The isolating properties of the transformer are utilized in many cases where the secondary feeds the grid of a tube. One terminal of this winding may be connected to the grid-bias supply and the other to the grid; coupling condensers and grid resistors are then unnecessary.

Effect on Pulse Shape

If an equivalent circuit for a pulse transformer is derived (as is done in practically all the aforementioned references) it will be found that the leakage inductance appears in series between source and load, while stray capacitances and the magnetizing inductance are effectively in parallel with the load. Ideally the leakage inductance and stray capacitances should be zero and the magnetizing inductance infinite. The fact that they can never be made so results in several undesirable effects of the transformer on pulse shape:

1. The leakage inductance acts in conjunction with the stray capacitance and the series resistance of source and load to slow the rate of rise of the pulse. This is in addition to the limit on the rate of rise mentioned previously, which is intrinsic to the circuit, rather than the transformer, and would therefore exist even if the transformer were ideal.

2. Although by Lenz's law current cannot flow through the magnetizing inductance during the first instant, current builds up in this element approximately in a linear fashion for the duration of the pulse. Since most transformers are operated from constant-current sources, the current flowing through the load is decreased by the amount diverted to the magnetizing inductance, and a droop occurs in the top of the pulse. After the pulse, again by Lenz's law, flow of current through the magnetizing inductance cannot cease instantaneously. Since the driving tube is then cut off, its impedance is very high, and the equivalent circuit is such that for current to continue flowing in the inductance it must flow through the load in a direction opposite to the original pulse current. This phenomenon represents an undesirable "overshoot".

APPROVED FOR PUBLIC RELEASE. CASE 06-1104.

3. If the pulses recur at high frequency, the load voltage may not fully recover from the negative overshoot of one pulse before the next pulse begins. The next pulse will then not rise to the same absolute amplitude as the preceding one. This process is cumulative, causing undesirable amplitude loss, or objectionable differences in amplitude if the pulses do not come at a regular rate.

4. Various combinations of inductances and capacitances of the equivalent circuit can give rise to oscillations on the top of the pulse or the backswing. Although generally undesirable, such oscillations may occasionally be used to advantage, as in the case of very short pulses whose length corresponds approximately to a half-period.

5. Components of the input current diverted to supply hysteresis and eddy-current losses add to the droop described in 2. above.

Design and Construction

Mention has already been made of the need to choose a value of turns ratio which represents a compromise between conflicting requirements. A similar compromise must be made to meet the contrasting requirements of (1) fast rise and fall of the pulse (interpretable as good transient response), which demands a low value of leakage inductance and effective capacitance to ground, and (2) little droop of the top of the pulse, and hence little overshoot (interpretable as good low-frequency response), for which the magnetizing inductance must be high. All three of these parameters increase with increasing winding length; for a given core the magnetizing inductance cannot be increased to meet the requirement (2) without increasing the other quantities and defeating requirement (1). If conditions (1) are established, improvements in (2) can be realized only by using a better core, whose reluctance must be low if the magnetizing inductance is to be high. Pulse length and pulse repitition frequency must be considered and an appropriate balance of transformer characteristics achieved. Wimett discusses these design problems in detail.

The core found most suitable for use in Whirlwind pulse transformers is constructed by winding a continuous ribbon of a high-quality magnetic alloy about a rectangular mandrel. This process results in essentially a rectangular core which may then be cut across its width, forming two C-shaped halves. Cores used in these transformers are manufactured by Westinghouse from .001" x $\frac{1}{4}$" hipersil ribbon.

The low-voltage winding of the transformer is wound on a paper tube whose inside dimensions correspond to the cross-section of the core. A proper thickness of paper is then placed over it and the high-voltage winding placed on this. Both solenoids are close-wound to the same length, the correct turns ratio being achieved by using different wire sizes. Parameters of the equivalent circuit are determined by winding length, number of turns, interwinding spacing, winding circumference, etc.

APPROVED FOR PUBLIC RELEASE. CASE 06-1104.

Core halves are inserted at both ends of the paper tube such that a butt joint is formed. They are held together under pressure by a steel band. Terminal lugs and a suitable mounting base are then put on, and the transformer finished by application of a protective coating.

G. G. Hoberg

GGH:b

APPROVED FOR PUBLIC RELEASE. CASE 06-1104.

6345
Report R-122

Project Whirlwind
Servomechanisms Laboratory
Massachusetts Institute of Technology
Cambridge, Massachusetts

SUBJECT: LOW-POWER TRANSFORMERS

Written by: Thomas F. Minett

Date: July 15th, 1947

TABLE OF CONTENTS

APPROVED FOR PUBLIC RELEASE. CASE 06-1104.

APPROVED FOR PUBLIC RELEASE. CASE 06-1104.

SUMMARY

Analysis and design procedures are derived for application to low-power pulse transformers including, in particular, the types expected to be employed in many circuits of the electronic digital computer of Project Whirlwind. Pulse lengths considered are between a twentieth and a quarter microsecond. Although optimum reproduction of pulse shape is assumed to be a leading requirement, the procedures given are presumably general enough to be extended to applications for which faithful reproduction of input voltage or current waveform is not necessary.

Two different equivalent circuits are presented, by means of which good approximate response calculations may be made for most circuits which include pulse transformers. One is a lumped-parameter circuits which is almost identical to those used for audio transformers. The other replaces the transformer by a "delay" or "lag" line, and is useful when the turns ratio between windings is unity. Curves and special techniques are presented to aid in the analysis of these circuits, and sample calculations of elements in the equivalent circuits are given in an appendix. Applicability of the equivalent circuits is demonstrated by comparisons of observed pulse responses with those calculated from the equivalent circuits for various pulse transformers. By means of these circuits, pulse distortion produced by transformers is analyzed and methods for its elimination are derived. Experimental results are presented in the form of photographs of response waveforms as displayed on an oscilloscope.

In the discussion will be found a new method which takes into account non-linear effects of core material in treating magnetizing inductance and low-frequency response. For example, the decay of voltage across a winding is shown to follow very nearly the exponential law

APPROVED FOR PUBLIC RELEASE. CASE 06-1104.

$e^{-k\sqrt{t}}$, where k is a constant, rather than the usual $e^{-\frac{Rt}{L}}$ which holds for the linear case.

Although each pulse transformer application requires, in general, a design and construction procedure different from any other, a few general design rules may be summarized as follows:

Core

a. Material

The core material should have the highest possible permeability and should produce the lowest possible eddy current and hysteresis losses; hence it should be a laminated iron alloy (Hypersil, etc.)

b. Size and Shape.

The core should present the shortest possible magnetic path length and therefore should be in the form of a loop just long enough to hold the windings. Cross-section area should be maximum consistent with other conditions such as minimum wire length in a winding.

Windings

a. Number of turns.

For a given core, the number of turns per winding determines the rate of amplitude decay in the pulse response. The number of turns should be great enough, therefore, to limit the decay to a specified maximum. The upper limit on number of turns is determined by distortion due to excessive leakage inductance and distributed capacitance, each of which is proportional to the number of turns.

APPROVED FOR PUBLIC RELEASE. CASE 06-1104.

b. Wire size.

The winding layer with the greatest number of turns should usually have the smallest wire size that may be safely used without danger of breaking. There are some instances, however, where wire size is determined by impedance level (see d. below) and larger sizes may be required.

c. Geometry.

If an adequate selection of core sizes is available, the most satisfactory arrangement of windings is that with a single-layer primary and a single-layer secondary.

d. Spacing between windings.

Everything else being held constant, the spacing (layer of paper) between windings determines the "characteristic impedance" (Z_o), or impedance into which the transformer will deliver the least-distorted output. For a two-winding pulse transformer, the relationship is

$$Z_o = \frac{377}{\sqrt{\epsilon f}} \left(\frac{\ell_i}{D}\right) \text{ ohms}$$

where ϵ is the dielectric constant of the paper spacer, f, is a factor depending on geometry, ℓ_i is the spacing in cm, and D is the wire diameter.

2. INTRODUCTION

The electronic digital computer of Project WHIRLWIND will consist of circuits which must be capable of handling fractional-microsecond pulses of voltage or current. Important components of these circuits are pulse transformers of types which, unfortunately, are not yet commercially available. In fact, the development of transformers capable of faithfully reproducing fractional-microsecond pulses appears to be in a very early stage.

The most advanced information currently available on the subject

APPROVED FOR PUBLIC RELEASE. CASE 06-1104.

of pulse transformer design is found in declassified M. I. T. Radiation Laboratory documents (Refs. 2, 3, 4, 6, 10). For the most part, these reports cover the analysis and design of high-voltage, high-power transformers of the type used for driving magnetrons, whereas the computer circuits of Project WHIRLWIND will employ the low-voltage, low-power variety, which require a somewhat different design procedure. Problems of insulation and core saturation, for example, will be of little or no importance.

Though there are many more uses for pulse transformers, the principal functions which they will perform in the computer are the following:

a. impedance transformation

b. phase inversion

c. reduction of d-c resistance

This report is concerned with pulse transformers to be used only for the above functions, and in circuits where the average power level is of the order of one watt and instantaneous power less than one hundred watts. Analysis and design techniques discussed in the references are summarized, modified, and extended with particular attention to the applications mentioned above. In some instances, new approaches are introduced, as, for example, the application of the delay-line concept to response analysis in Section 3.4. Various kinds of pulse distortion introduced by transformers are explained, and design procedures for minimizing objectionable distortion are outlined. Limitations are pointed out in order to make clear the performance which may reasonably be expected from a pulse transformer.

APPROVED FOR PUBLIC RELEASE. CASE 06-1104.

3. ANALYSIS

The photographs in Figs. 1 and 2 show transformers of the type to be discussed in this report. The sketch in Fig. 3 shows details of the physical positions of windings, etc. A discussion of the details of construction is presented in Section 4.

Briefly, a p.t. (pulse transformer) consists of two or more coaxial solenoids which are separated by cylindrical paper spacers, and through which passes one side of a closed loop of ferromagnetic metal (core).

Because of the physical arrangement, undesired capacitance exists between adjacent turns in a solenoid, or winding, and between windings. Also, when current is applied in one winding, there will be leakage magnetic flux, in the region between windings, which does not encircle all turns. These effects and the inherent non-linearity of the core are difficult to take into account. However, simplified equivalent circuits provide the basis for a sufficiently accurate analysis.

3.1 Equivalent Circuits.

A two-winding pulse transformer, which is the principal type to be considered, is shown in the schematic representation of Fig. 4. Distributed core and interwinding capacitances are shown as lumped parameters, C_0 and C_1, which are the capacitances that would be found by direct measurement at low frequency (60 cycles) between the core and inner winding, and between windings, respectively.

An equivalent circuit for an audio transformer is derived by simple circuit theory in Ref. 1. An extension of that procedure to obtain a closer approximation to a p.t. yields the slightly more complicated circuit of Fig. 5. All quantities are referred to the primary, and an ideal transformer is added in order to realize the proper voltage transformation. Wire resistance is neglected, since it is usually less than fifteen ohms.

APPROVED FOR PUBLIC RELEASE. CASE 06-1104.

Capacitance between adjacent turns of a winding is ignored since an analysis similar to one used in Ref. 9 shows it to be negligible.

3.11 Elements of the Equivalent Circuit of Fig. 5.

Capacitance C_C'. The effect of energy storage in the capacitance between the primary winding and the core (which is assumed at ground potential) is represented by C_C'. (prime indicates reference to the primary) Energy calculations show that C_C' is equal to one-third of the measured capacitance C_o. (This assumes that the winding nearest the core is called the primary). Because C_o can usually be made small with little sacrifice of other characteristics, and because the energy stored in it can be held to a relatively low value by placing the low-voltage winding next to the core, in most cases C_C may be omitted from the equivalent circuit.

Capacitance C_D. The effect of energy storage in the distributed capacitance between windings is represented by C_D.

"Squirt" Inductances, L_C' and L_D'. The effects of so-called "squirted" flux (Ref. 2), which is due to currents charging C_C' and C_D' through the winding inductances, are represented by L_C' and L_D'. Though included for completeness, L_C' and L_D' will be assumed negligible compared to L_L' and will be replaced by short circuits for the purposes of this report.

Coupling Capacitance, C_{ps}'. The coupling effect of the inter-winding capacitance is represented by C_{ps}', which is given approximately by $\mathcal{E}_i/n^2$ for the pulse transformer of Fig. 4.

Primary Inductance, L_p. The effect of that current which is not used to charge any capacitance (But which flows into the primary, yet not out of the secondary terminals) is represented by L_p, the primary self-inductance. The current drawn by L_p may be called magnetizing current since most of it is used in maintaining flux in the core. Actually, this

APPROVED FOR PUBLIC RELEASE. CASE 06-1104.

current has a real component which provides hysteresis and eddy current loss, and its effect may be represented separately by resistances R_e and R_h. (See Ref. 3). However, for reasons which will appear in Section 3.21 the effect of the core will be represented in this report by one element, L_p; which acts as a very non-linear inductance..

Leakage Inductance, L'_L The effect of energy storage in the leakage flux is represented by L_L, which is usually defined by $2(L_p - M)$ or $(1 - k^2) L_p$, where M is the mutual inductance and k is the coefficient of coupling. The concept of a coupling coefficient is not used in this report, however, because its definition involves the assumption that L_p is an inductance of fixed value. That this cannot be assumed will be shown in Section 3.21.

3.2 A Simplified Equivalent Circuit.

Removal of the negligible elements mentioned above from the circuit of Fig. 5 leaves the more easily analyzed circuit shown in Fig.6. The ideal transformer is omitted because it is not necessary for a frequency analysis.

3.21 Evaluation of the Elements.

Leakage Inductance, L'_L. Because L'_L represents the effect of leakage flux, which, by definition, is flux which strays from the core and meets with reluctance due primarily to air, it is independent of the core and is a function only of the geometry of winding. Energy considerations may be used to calculate L'_L as shown in App. 7.2, where it is obtained for the simple case of two single-layer windings: If wire diameter

APPROVED FOR PUBLIC RELEASE. CASE 06-1104.

is assumed to be negligible compared with spacing between windings, the expression for L'_L becomes

$$L'_L = \frac{4\pi N_p^2 U \lambda_i}{\ell_w} 10^{-9} \text{ henries} \qquad (3\text{-}1)$$

in which N_p = number of turns in the primary winding,

U = average circumference of the two windings (cm),

ℓ_w = winding length (cm),

λ_i = spacing between windings (cm).

This neglects wire diameter, which is assumed small compared to λ_i. Expressions for L'_L derived by a similar method are given for more involved winding geometries in Refs. 1 and 5. A comparison of leakage inductance calculated from Eq. 3-1 with the measured value is given in App. 7.5 for a one-to-one p.t.

Distributed Capacitance and C'_D. The capacitance between windings may be calculated by considering the windings as solid cylindrical sheaths. Since the spacing is usually constant between them, the capacitance may be computed by considering the sheaths as parallel plates with areas equal to the average area of the two sheaths. The capacitance between two adjacent windings is thus found to be

$$C_i = 0.0885 \frac{\epsilon U \ell_w}{\lambda_i} \mu\mu f. \qquad (3\text{-}2)$$

Now C'_D may be calculated by determining the voltage distribution along the length of the windings. The total energy, W, stored in all interwinding capacitances may be found and set equal to the energy stored in equivalent capacitor C'_D, which will have the primary voltage, V_p, impressed across it (or V_S if C''_D is to be determined) in the equivalent circuit. Then

$$W = \sum' W_i = \frac{1}{2} C'_D V_P^2 \qquad (3\text{-}3)$$

APPROVED FOR PUBLIC RELEASE. CASE 06-1104.

whence $$C_D' = \frac{2W}{V_P^2} \qquad (3\text{-}4)$$

where W is a different function of the ratio of secondary turns to primary turns, n, for each winding arrangement. Expressions for C_D' in terms of n are derived in App. 7.3 for two p.t. circuits.

For the simple two-winding p.t., the above formula gives (assuming a linear voltage distribution along the length)

$$C_D' = \frac{C_i}{3 V_P^2} (V_{AB}^2 + V_{AB} V_{CD} + V_{CD}^2) \qquad (3\text{-}5)$$

Here V_{AB} and V_{CD}, which are functions of n, are the voltage differences between adjacent winding ends as shown in Fig. 60.

For an inverter transformer of the type shown in Fig. 32, one obtains, on substituting for V_{AB} and V_{CD} in Eq. 3-5,

$$C_D' = \frac{C_i}{3} (n^2 + n + 1) \qquad (3\text{-}6)$$

Substitution for n in this expression shows that C_D' is just equal to the interwinding capacitance for a one-to-one inverting p.t., and for a two-winding voltage-step-down inverter approaches one-third of this value as n becomes small.

Primary Self-Inductance, L_p. The magnetizing inductance, or primary self-inductance, is the most difficult element to evaluate in the equivalent circuit. As defined in Section 3.11, L_p is a function not only of core material, but also of primary turns (N_p), pulse length (τ), primary voltage (E_p), and duty factor.

If the core material were linear, i.e. had constant permeability (μ), the general formula for inductance of a winding would hold, giving

$$L_p = \frac{4\pi N_p^2 A\mu}{\ell_m} 10^{-9} \text{ henries,} \qquad (3\text{-}7)$$

where A is the cross-sectional area of the core (cm^2), and ℓ_m is the mean

APPROVED FOR PUBLIC RELEASE. CASE 06-1104.

magnetic path length (cm).

However, since the above assumption does not hold, it is customary to define an "effective" incremental permeability, μ_e, which takes into account non-linearity, as follows:

$$\mu_e = \frac{\Delta B}{\Delta H}, \qquad (3\text{-}8)$$

where ΔB and ΔH are total increments of flux density and magnetic field strength traversed in a pulse loop (hysteresis loop obtained with pulse excitation).

If there were no eddy currents, μ_e could be substituted into the formula for L_p, and the resulting expression would be found to represent adequately the effect of the core. The quantities, ΔB and ΔH, are functions of core material and N_p, τ, E_p, etc., however, so curves would have to be constructed to show the dependence of μ_e on the different variables. Ref. 6 discusses the variation of μ_e with maximum flux density and rate of change of flux density, each of which are functions of the variables mentioned above. From fundamental considerations,

$$\frac{dB}{dt} = \frac{E_p}{N_p A} 10^8 \quad \frac{\text{gauss}}{\text{sec}} \qquad (3\text{-}9)$$

$$B_{max} = \frac{10^8}{N_p A} \int_0^\tau E_p dt \quad \text{gauss}, \qquad (3\text{-}10)$$

where E_p is the instantaneous voltage across the winding. Thus $\frac{dB}{dt}$ is proportional to the pulse voltage, and B_{max} is proportional to the voltage time area of the pulse. Rough plots of μ_e vs $\frac{dB}{dt}$ for different values of B_{max} show the following:

APPROVED FOR PUBLIC RELEASE. CASE 06-1104.

1. At low $\frac{dB}{dt}$ (small E_p), μ_e approaches the d-c permeability.
2. At high $\frac{dB}{dt}$, μ_e approaches zero.
3. At high $\frac{dB}{dt}$, μ_e is higher for thinner laminations.
4. Below saturation, μ_e is proportional to B_{max}.

Now, if such curves could be obtained more accurately at the low flux densities to be considered here, they could be used to calculate the magnetizing inductance, L_m, which would have to be shunted by a resistance to represent the effects of eddy currents and hysteresis. Ref. 3 discusses a method for representing eddy currents and hysteresis losses for a known pulse loop, but this is impractical unless the form of the hysteresis loop is known. A more simple method, which is suggested in Ref. 2, is to include hysteresis effects in L_m and add a shunt resistance R_e to account for eddy currents. An expression for R_e in terms of transformer constants derived by an approximation method in Ref. 3 is (for a laminated core)

$$R_e = \frac{12 \rho N_p^2 A}{d^2 \ell_m} \text{ ohms} \qquad (3\text{-}11)$$

where ρ is the core resistivity (ohms-cm)

d is the lamination thickness (cm)

If it is assumed that the effect of the core may be represented by L_m in parallel with R_e instead of by one element, L_p, it should be possible to make pulse measurements of the low-frequency response and obtain the data necessary to make plots of μ_e vs $\frac{dB}{dt}$ and B_{max}. For this purpose, μ_e may be defined by the equation

$$\mu_e = \frac{L_m \ell_m}{4\pi N_p^2 A} 10^{-9}, \qquad (3\text{-}12)$$

APPROVED FOR PUBLIC RELEASE. CASE 06-1104.

which is obtained from Eq. 2-7 with L_m substituted for L_p.

The value of L_m may be obtained by comparing the observed pulse response of the primary in the ciurcuit of Fig. 7 with that calculated for the circuit of Fig. 8. The waveform across the winding is a pulse with exponentially decaying amplitude. The rate of decay is determined by both L_p and the added resistance, R_p, so the value of L_m may be calculated (knowing R_p and R_e) from the amount of decay in a given time. Equations 3-9 and 3-10 may be used to determine $\frac{dB}{dt}$ and B_{max} for each set of data taken with the circuit of Fig. 7.

Curves A and B in Fig. 9 show plots of $\log \mu_e$ vs $\log B_{max}$ for two values of $\frac{dB}{dt}$ obtained by using the above procedure with a winding of thirty-six turns on a Hipersil core with two-mil laminations. Curves of constant $\frac{dB}{dt}$ (i.e. constant amplitude at termination of pulse) were obtained by varying R_p, pulse length and input pulse amplitude, the amplitude at the end of the pulse being held constant. Integration of the voltage-time area for finding B_{max} was achieved by counting grid squares included within the output pulse curve as displayed on an oscilloscope. That curves A and B are meaningless and of little use may be concluded from the fact that they have unusual curvatures and even intersect at two points.

If the primary inductance is to be represented by one element, L_p, as in Fig. 7, instead of by the arrangement of Fig. 8, much more consistent results would be obtained. Thus, L_p may be calculated from the decay by using Fig. 7 as the equivalent circuit, and μ_e may be calculated from L_p by Eq. 3-12 with L_p inserted in place of L_m. Using this scheme for calculating μ_e and the same data used for curves A and B yields straight-line curves, C and D, Fig. 9. Results of further experiments verify the fact that these curves are straight lines at least within the range of flux

APPROVED FOR PUBLIC RELEASE. CASE 06-1104.

densities and $\frac{dB}{dt}$ used in the experiments (also in the range of most computer applications).

Plots of log μ_e vs log $\frac{dB}{dt}$ for constant B_{max}, as shown in Fig. 10, are also found to be straight lines. These curves were obtained directly from those of Fig. 9, and extended by extrapolation. However, measurements made on other sizes of cores and with other valves of N_p were found to check reasonably well with these curves even in the extrapolated regions.

A further justification for lumping the effect of the core into a single element is brought out in a study of the law of decay for the voltage across L_p in Fig. 7. The decay is not exponential, as would be expected if the equivalent circuit of Fig. 8 were used. This may be shown by calculating the value of inductance L_m required to produce the observed decay at different values of pulse duration. Plots of such results show that L_m increases with time, but not according to any simple consistent law.

Again, if the circuit of Fig. 7 is considered as the equivalent circuit, and values of L_p which will produce the measured decay are calculated, the results when plotted disclose a very simple relationship between L_p and pulse duration. The curves of Figs. 11 and 12 show L_p plotted against time or pulse duration for several different cases as noted on the curves. Plots of μ versus pulse duration are shown in Fig. 13. All plots, when made on log-log paper, show nearly straight lines. Moreover, the lines all exhibit slopes equal to or slightly greater than one-half. Only near the high ends do some of the curves bend away from a straight line. The dependence of L_p, hence μ_e, on time t after pulse initiation, may therefore be expressed within the straight line regions of the plots as follows:

$$L_p \sim \mu_e \sim t^r \qquad (3\text{-}13)$$

APPROVED FOR PUBLIC RELEASE. CASE 06-1104.

where $r \geq \frac{1}{2}$

These experimental results appear to agree with the purely theoretical results of Dr. L. A. MacColl in Ref. 7, where the calculated variation of μ_e with time is shown plotted on log-log scaled. That curve has a slope of exactly one-half up to long pulse durations, where the curve bends away slightly from a straight line.

3.3 Response of the Equivalent Circuit Including External Elements.

In operation, a p.t. will be driven by a source having a certain amount of resistance and shunt capacitance to ground, and the transformer will be terminated usually by shunting resistance and capacitance. Since the effects of these external elements is generally appreciable, investigation of the p.t. response alone would be pointless. Therefore the circuit of Fig. 14, which includes external elements, will be analyzed.

Replacing the p.t. by its equivalent circuit and omitting the ideal transformer by referring elements to the primary side, the circuit of Fig. 15 is obtained. The elements of Fig. 15 are obtained from those of Fig. 14 as follows:

$$C_1 = C_p + C_c \text{ (if } C_c' \text{ is significant)}$$

$$R_1 = R_p$$

$$C_2 = n^2 C_s + C_D' = C_s' + C_D'$$

$$R_2 = \frac{R_S}{n^2} = R_s'$$

For simplicity, C_{ps}' is omitted because its effect will be negligible in most cases to be considered.

APPROVED FOR PUBLIC RELEASE. CASE 06-1104.

3.31 Influence of Each Element on Response

Leakage Inductance, L_L'. Because L_L' presents a series impedance which increases with frequency, its effect is to attenuate the output at high frequencies. Consequently, it has a delaying effect on pulse response.

Output Capacitance, C_2. High frequencies are likewise attenuated by C_2 because of its shunting action which increases with frequency. It also contributes to pulse delay.

Primary Inductance, L_p. For very high frequencies L_p acts as an open circuit and may be neglected. For low frequencies, however, it presents a shunting impedance which produces attenuation. It is thus to be considered only with regard to "low-frequency" response.

Elements C_1, R_1, R_2. Resonances will occur at certain frequencies between C_1, C_2, and L_L', and oscillations or "ringing" will appear in the pulse response. This ringing may be damped by R_1 and R_2.

3.32 Square-Wave or Pulse Response

For purposes of analysis it is convenient to reduce the circuit of Fig. 15 to its equivalent circuit, Fig. 16, for response to frequencies below the pass-band center, and a different one, Fig. 17, for response to frequencies above the band center.

3.321 Long-Time Response.

The response to low frequencies may best be determined by a study of the long-time response to a step-function applied to the "low-frequency" equivalent circuit of Fig. 16.

If L_p were a pure inductance, the pulse response of the low-frequency circuit would be simply a pulse with amplitude decaying exponentially with a time constant given by L_p/R_L. Because L_p is a function of time as given by Eq. 3-13, the actual observed decay may be expressed

APPROVED FOR PUBLIC RELEASE. CASE 06-1104.

by the equation

$$\frac{E_o}{n} = I_1 R_1 e^{-\frac{R_L t (1-T)}{L_o}} \simeq I_1 R_L e^{-\frac{R_L \sqrt{t}}{L_o}} \qquad (3\text{-}14)$$

where L_o is a constant and I_1 is the input current amplitude.

Figure 18 shows a curve (A) of the response given by Eq. 3-14 and superimposed on it a curve (B) of ordinary exponential decay with time constant L/R_L, where L is the inductance producing the same decay in one microsecond as curve A. Examination of the curves shows that they intersect at $t' = 1$, but exhibit different amounts of decay for other values of t'.

The general effect of a decay of the type shown in Curve A is seen to be a peaking of the early portion of the pulse. This may be explained by noting that the amplitude follows a parabola at the beginning (when $t << L_o/R$, $E_o \sim \sqrt{t}$) instead of a straight line as for ordinary exponential decay.

The voltage backswing or overshoot at the termination of a pulse also shows decay of the same form as that during the pulse, but the value of L_p is less at each value of time measured from the time of termination than at the same value of elapsed time during the pulse.

Curve D of Fig. 11 shows L_p, for a particular transformer primary, plotted on log-log coordinates against time measured from the beginning of the pulse. Curve E is a plot of L_p on the same scale during the backswing decay. For Curve E, time is measured from the time of pulse termination.

The effect of a lower L_p after the backswing is to cause the overshoot to decay faster. This is usually a welcome effect.

Oscillograms F-6-6-8 (Fig. 54) and F-7-1 (Fig. 55) show decay (of the type discussed above) in the pulse response of primary windings

APPROVED FOR PUBLIC RELEASE. CASE 06-1104.

connected as in the circuit of Fig. 16.

3.322 Transient Response.

Since the high-frequency response of a network determines its transient behavior, it follows that the high-frequency equivalent circuit of Fig. 17 may be used to study the transient response of a p.t.

As it is practically impossible to obtain a general transient solution for such a circuit, the best procedure is to find approximations to the response for particular combinations of component values. However, some important facts are brought to light by a study of roots of the cubic equation which is obtained in the exact analysis. For example, a general analysis shows that oscillations, or at least overshoots, will appear in the step-function response for most values of loading. It also shows that only when

$$C_2 \geq 8\, C_1$$

and

$$L \geq \frac{27}{64} R_2^2\, C_1 \qquad (3\text{-}15)$$

will it be possible to realize critical damping.

The case of transitional frequency response (first, second and third derivatives vanish at origin) for the circuit of Fig. 17 is considered in Ref. 8. Relations between the different elements obtained therein for the two solutions to the transitional case are presented in graphical form in Figs. 19 and 20. The overshoot produced by step-function excitation is 8.1% for this case as calculated by S. A. Wingate.

A satisfactory approximation to the actual response may be made for the cases where either capacitor is less than half the other by neglecting the smaller of the two. If

$$C_1 < \frac{C_2}{2}$$

and

$$R_1 < \frac{1}{2}\sqrt{\frac{L_L}{C_1}}$$

APPROVED FOR PUBLIC RELEASE. CASE 06-1104.

the circuit of Fig. 21 will yield practically the same rise time as that of Fig. 17, although the overshoot and ringing may be slightly different.

Curves of the step function response of this circuit are given in Fig. 23 for several values of the damping factor, D, where

$$D = \left[\frac{R_1}{L_L'} + \frac{1}{R_2 C_2}\right] \sqrt{\frac{L_L' C_2}{1 + R_1/R_2}} \qquad (3\text{-}17)$$

By application of the reciprocity theorem and general circuit theory, these curves may be applied to many variations of the original circuit. For example, they apply to the circuit of Fig. 22 if R_2 is allowed to go to infinity. For this case,

$$D = R_1 \sqrt{\frac{C_2}{L_L'}} \qquad (3\text{-}18)$$

and the circuit time constant, used as a measure of time in Fig. 23, becomes

$$T = 2\pi \sqrt{L_L' C_2}$$

Critical damping occurs for any of these circuits when D = 2. As the damping factor decreases toward zero, the overshoot increases toward one hundred percent. In general ringing becomes damped very quickly, as may be seen in the extended curve for D = 0.3.

3.33 "Low-frequency Analogues".

Unfortunately, a great many pulse transformer circuits are such that one may not make the assumptions of Section 3.32 and obtain the response by the use of the set of curves discussed, but must actually solve the general equivalent circuit of Fig. 17. In order to obtain the transient response of this circuit, a computer would be required to solve the cubic equation involved for each set of circuit constants. The most suitable computer for solving such a system is clearly the equivalent circuit itself with step-function excitation.

APPROVED FOR PUBLIC RELEASE. CASE 06-1104.

If such a circuit were built however, it would be found that control of capacitance values is limited by stray capacitances which, in many cases are of the same order of magnitude as the actual circuit values. It is therefore advantageous to make a frequency transformation in the equivalent circuit by multiplying inductance and capacitance values by a factor, k, which will make circuit capacitance large compared with strays. This is equivalent to multiplying the time scale by K also. What should happen in one microsecond in the actual circuit will thus require K microseconds in the transformed circuit or "low-frequency analogue".

Photographs F-103-5, -7, -8, (Fig. 56) are oscillograms of pulse responses of the low-frequency analogues for three p.t. equivalent circuits, and Photographs F-103-1, -2, -4 show responses of the p.t.'s for comparison. Values used for L_L' and C_D' in the analogues were obtained by direct measurement as discussed in Section 5. Data concerning characteristics of the p.t.'s and circuit values for the analogues are given in Section 7. The frequency transformation factor K was chosen equal to the ratio of oscilloscope sweep speeds used. Thus the analogue photographs give the response to a 5.3-microsecond pulse displayed on a 5.3-microsecond-per-inch sweep, while for the p.t. photographs a pulse of 0.23 microseconds is used and the output displayed on a 0.23-microsecond-per-inch sweep.

Amplitudes were adjusted for the photographs by variation of input current, which was supplied by a pulsed pentode (6AG7). Since this adjustment was made with the camera in place, there are discrepancies in amplitude which must be taken into account in comparing the photographs. Thus, the response of analogue T39 is nearly identical with that of p.t. T39, although photographs F-103-2 and F-103-5 show an amplitude difference which might be interpreted incorrectly as a difference in transient response.

APPROVED FOR PUBLIC RELEASE. CASE 06-1104.

Photographs F-103-1 and F-103-8 for T52D5 exhibit the greatest discrepancy found between analogue and p.t. Ringing appears in the analogue but not in the p.t. Attempts to introduce the loading due to eddy currents by shunting a resistance equal to R_o (see Section 3.21) across the input of the analogue failed to damp the ringing sufficiently. However, if this resistance were shunted across L_L', fairly good damping could be achieved and the rise time made more nearly equal to that of the p.t. It should be noted also that T52D5 has a tapered spacer between windings which may account for the lack of ringing.

3.4 Special Case of n = 1; Analysis by Delay-Line Theory.

The equivalent circuits for high-frequency or transient response discussed in Section 2.3 are found to be inadequate to predict satisfactorily the response of a p.t. with a turns ratio of unity. To illustrate this, the response of a one-to-one p.t. will be compared to that calculated for the equivalent circuit obtained as in Section 2.2.

For example, consider operation of T16 in the circuit of Fig. 24 with $R_p = R_s = 1900$ ohms, $C_p = 0$, $C_s = 10$ μμf. The characteristics of T16 are as follows:

$N_p = N_s = 118$ turns
$L_L = 33\mu h$ (measured)
$C_o = 10\mu\mu f$ "
$C_1 = 30\mu\mu f$ "

Since the primary and secondary voltages are equal, C_D' is zero C_{ps}' is just equal to C_1, and the equivalent circuit becomes that of Fig. 25 if C_c' (+ 3.3 μμf) is neglected. A transient analysis of this circuit yields the response plotted in Fig. 26 (Curve A). On the same graph, the experimental p.t. response shown in photograph F-5-7, Fig. 51, is sketched (Curve B). A comparison of the two curves discloses no similarity

APPROVED FOR PUBLIC RELEASE. CASE 06-1104.

in the rising parts of the responses.

The staircase effect in the experimental response suggests existance of some sort of reflection in the p.t. windings similar to a reflection in a transmission line. That a two-winding one-to-one p.t. (or any pair of adjacent windings in a p.t.) does have some of the properties of a delay line is easily provad.

3.41 Delay-Line Features of a P.T.

Two windings may be shown to act as a delay or lag line if a pair of adjacent winding ends are considered as input terminals, and the other pair of windihg ends considered as output terminals. The necessary condition that a line possess both a series inductive reactance and a distributed shunt capacitive reactance is realized by a p.t., as illustrated in the equivalent circuit of Fig. 6, if the windings have the same number of turns and are in the same sense (wound in the same direction). It is certainly true that an open-circuit impedance measurement on the two-winding line does yield a capacitance equal to the distributed capacitance, and a short-circuit measurement finds an inductance equal to a sum of the winding self-inductances minus twice the mutual inductance, which is, by definition, equal to the leakage inductance, L_L'.

Further verification of the existance of delay line action may be found in Ref. 9, where delay lines are discussed which are constructed in the same manner as two-winding p.t.'s but with windings wound in opposite senses and with no iron core. The reason for the former is to obtain, for the series inductance per unit length, the sum of the winding self-inductance plus twice the mutual inductance. This provides a much greater inductance, and hence delay, than if the windings were in the same sense. The effect of the core will be discussed in Sec. 3.421.

APPROVED FOR PUBLIC RELEASE. CASE 06-1104.

3.411 Delay

According to transmission line theory the delay per unit length, τ_d, is defined by the following:

$$\tau_d = \sqrt{LC}$$

where L and C are respectively inductance and capacitance per unit length. It follows from this definition that the total time delay, τ_d, of a pair of transformer windings with total capacitance C_1 between them and leakage inductance L_L will be given by

$$\tau_d = \sqrt{L_L C_1} \qquad (3\text{-}19)$$

Since for a two-winding transformer with N turns in each winding

$$L_L = \frac{4\pi N^2 U \lambda_1}{\ell_w} 10^{-9} \text{ henries}$$

and

$$C_1 = \frac{0.0885 \epsilon U \ell_w}{\lambda_1} 10^{-12} \text{ farads,}$$

on substitution for L_L and C_1 the delay becomes

$$\tau_d = \sqrt{0.0885 \cdot 4\pi N^2 U^2 \epsilon \cdot 10^{-21}}$$

$$= \frac{N U \sqrt{\epsilon}}{c}, \qquad (3\text{-}20)$$

where c is the velocity of light.

Note that the product NU is the average length of wire in a winding and $c/\sqrt{\epsilon}$ is the velocity of propagation of electromagnetic waves in a medium of dielectric constant ϵ and permeability unity. Therefore, the delay may be said to be equal to the time of wave propoagation through a length of the interwinding dielectric equal to the average length of wire used in a winding, or

APPROVED FOR PUBLIC RELEASE. CASE 06-1104.

$$\tau_d = \frac{\text{wire length}}{\text{velocity}} = \frac{NU}{c/\sqrt{\epsilon}} = \frac{NU\sqrt{\epsilon}}{c}$$

3.412 Characteristic Impedance

Carrying the delay-line concept further, the characteristic impedance, Z_o, of a pair of windings is given approximately by the square root of the ratio of series inductance per unit length to shunt capacitance per unit length. Taking the transformer winding length as the unit of length, this gives for the pair of windings described above

$$z_o = \sqrt{\frac{L_L}{C_1}} \qquad (3\text{-}21)$$

Substituting again for L_L and E_1:

$$z_o = \sqrt{\frac{4\pi N^2 \lambda_1^2 \cdot 10^{-9}}{\ell_w \cdot 0.0885\, \epsilon\, \ell_w \cdot 10^{-12}}}$$

$$= \sqrt{\frac{4\pi}{.0885} \cdot 1000}\ \frac{N}{\ell_w \sqrt{\epsilon}}$$

$$= \frac{377}{\sqrt{\epsilon}} \left(\frac{\lambda_1}{D}\right) \text{ ohms.} \qquad (3\text{-}22)$$

Here D is the wire diameter.

This means that it should be possible to eliminate reflections in such a pair of windings by providing a resistance of z_o ohms between adjacent winding ends. Oscillogram 3-11, Fig. 54 (see page 49 for discussion), illustrates the effect of varying termination resistance of a pair of p.t. windings.

3.42 Delay-Line Theory Applied to a One-to-One P.T. With Windings In the Same Sense.

3.421 One-to-One Non-Inverter. The staircase type of response shown in Fig. 26 and oscillogram F-5-7 (Fig. 51) may be predicted with remarkable success by application of the delay-line concepts of the foregoing section. The circuit of Fig. 24 which produces this pulse response may be redrawn as in Fig. 27 to illustrate better the delay-line effect. The characteristic impedance of p.t. T16 is of the order of a thousand ohms as

APPROVED FOR PUBLIC RELEASE. CASE 06-1104.

calculated from Eq. 3-21

By transmission line theory the impedance seen looking into the p.t. between ends A and B is a resistance equal to the characteristic impedance, Z_o, until the short circuit at the far end, CD, is reflected to end AB. Thus if a voltage step, E_i, is applied at time $t = 0$, the circuit may be represented by the equivalent circuit of Fig. 28 until twice the one-way delay time has elapsed ($2\tau_d$). The part of the output waveform sketched in Fig. 30 for $t < 2\tau_d$ is obtained from an analysis of this circuit. Since E_o is equal to the potential across C_s, it must be an exponentially rising voltage with time constant

$$\frac{R_s (R_p + Z_o)}{R_p + R_2 + Z_o} (C_s) = 0.0067 \ \mu\text{secs}$$

and must rise toward the potential

$$\left(\frac{R_s}{R_p + R_s + Z_o} \right) E_1 = \frac{E_1}{3} ,$$

where E_1 is the step-function amplitude and $R_p = R_s = Z_o$. The input current, I_p, will approach $\frac{E_1}{3 Z_o}$.

At time $t = 2\tau_d$, the reflection from short-circuited end CD will arrive at end AB and see across AB the network of Fig. 29. The current wave reflected from CD will have the same magnitude $\frac{E_1}{3 Z_o}$ and will be in the same direction as the initial current. Neglecting the effect of C_s, the reflection coefficient at end AB will be

$$\frac{(R_p + R_s) - Z_o}{(R_p + R_s) + Z_o}, \text{ or } \frac{I}{3} .$$

Thus a current wave of $\frac{1}{3} \left(\frac{E_1}{3 Z_o} \right)$ flowing in the opposite direction from the initial current will be reflected back toward CD, and the current at AB will increase by

APPROVED FOR PUBLIC RELEASE. CASE 06-1104.

$$\frac{2}{9}\left(\frac{E_1}{3\,Z_o}\right) = \frac{2}{9}\left(\frac{E_1}{Z_o}\right).$$

This means that E_o will increase by

$$\frac{2}{9}\left(\frac{E_1}{Z_o}\right) R_s = \frac{2}{9}\,E_1.$$

The output thus becomes stepped up to $\frac{5}{9}\,E_1$. The current wave of amplitude $\frac{1}{9}\frac{E_1}{Z_o}$ which is propagated toward end CD is reflected, returns to end AB, and decreases the current at that end to

$$\frac{4}{9}\left(\frac{E_1}{Z_o}\right) + \frac{1}{27}\left(\frac{E_1}{Z_o}\right) = \frac{13}{27}\left(\frac{E_1}{Z_o}\right).$$

Then E_o becomes $\frac{13}{27}\,E_1$, which is so close to the final value of $\frac{E_1}{2}$ that further reflections need not be considered.

The effect of C_s on the response is shown in the sketch of Fig. 30. The waveform of the second step, beginning at $t = 2\tau_d$, may be determined by finding the response of the circuit of Fig. 31 by ordinary delay-line theory. The input is twice the first reflected voltage wave, which has the same exponential form as the current taken from the source during the interval $0 < t < 2\tau_d$. The response E_o' of this circuit will be the waveform of Fig. 30 with the origin shifted to point $0'$. Each succeeding reflection will have a longer rise time than the previous one because of the charging action of C_s.

Circuit values used in the above analysis are not exactly equal to those used in obtaining photograph F-5-7, Fig. 51. For example, the measured value of Z_o is about 1200 ohms, R_1 = 1100 ohms, and C_s is somewhat less than 10 $\mu\mu$F. Although values were rounded off for simplicity in the analysis, comparison of the calculated and experimental waveforms shows very good agreement. Rise time (0-95%) of the first step is about 0.02 microseconds experimentally and 2.9 x 0.0067 = 0.019 microseconds as calculated. The amplitude of the first step is three-tenths that of the input pulse (shown in F-4-0, Fig.50) as compared to the calculated value of one third. However

APPROVED FOR PUBLIC RELEASE. CASE 06-1104.

if the exact experimental values of R_1 and Z_o were used in the calculation, the value of one-third would be obtained.

That the second step appearing in F-5-7 (Fig. 51) is actually a reflection from end CD, ad discussed above, may be substantiated by attempting to remove it experimentally. If delay-line theory applies, proper termination at end CD could be achieved by inserting a resistance equal to Z_o between C and D, and the reflections would be eliminated. To do this, the circuit producing the pulse response shown in F-5-7 may be revised by adding a resistance of 1000 ohms ($= Z_o$) between end D and ground. The resulting output at B appears in F-4-23, Fig. 50, and shows that the step has been completely eliminated. Waveforms appearing at A and D are shown in F-4-22 and F-4-24. The pulse at D is delayed by the one-way p.t. delay as shown by the small negative pulse coupled directly from the input pulse preceding the main positive pulse in F-4-24.

The foregoing delay-line analysis ignores the fact that potentials are set up between ends of the same winding. Even in the G.E. coaxial-solenoid type of delay-line discussed in Ref. 9, such potentials would induce appreciable magnetizing current and lead to very poor low-frequency response. However, the iron core in a transformer type of line acts to minimize such magnetizing current by providing a high self-inductance in the winding.

In an analysis of the circuit of Fig. 24 taking into account the low frequency effects mentioned above, the magnetizing current flowing for $0<t<2\tau_d$ will be neglected since it is small. For $t>2\tau_d$ the voltage drop between ends A and B is very nearly zero, so it will be assumed that the potentials across the two windings are equal, i.e. that all reflections are completed. This means that the output voltage, $E_o = E_1/2$, appears across both windings. For this potential to exist, a magnetizing current must flow in the primary winding. This current should increase

APPROVED FOR PUBLIC RELEASE. CASE 06-1104.

according to the function $\frac{E_1}{R_p}\left\{1 - e^{-(R/L_p)t}\right\}$, where R is the resistance of the parallel combination of R_p and R_s. This becomes, as in Section 3.32,

$$\frac{E_1}{R_p}\left\{1 - e^{-(R/L_o)\sqrt{t}}\right\}$$

where L_o is a constant. Since the magnetizing current must flow through the primary to ground, I_p will be greater than I_s by the amount of the magnetizing current I_m. This I_p will increase and I_s will decrease according to the law mentioned above until the pulse is terminated or until no voltage drop appears across the windings.

3.422 One-to-One Inverter.

If a one-to-one p.t. with windings wound in the same sense is used with secondary connections reversed, as in Fig. 32, it will act as a phase inverter. Again, transmission-line action is exhibited, as may easily be seen from the same circuit redrawn in Fig. 33 with C_p and C_s omitted for simplicity.

Referring to Fig. 33, operation may be analyzed by transmission-line theory with R_p acting as the source impedance and R_s as the line termination. It will be noted that this circuit differs from the usual line circuit in that the conductor grounded at the input end is not the same one as is grounded at the output. With the General Electric Company, coaxial-solenoi type of delay line, this would lead to very poor low-frequency response, but the transformer line adapts itself easily to such operation by virtue of its iron core, which, as shown before, makes it possible for a potential to exist across each winding for a reasonable time.

If the input voltage E_i, Fig. 33, is a step function beginning at time t = 0, and current $I = \frac{E_1}{R_p + Z_o}$ will flow into the p.t., producing a voltage drop $\left(\frac{Z_o}{R_p + Z_o}\right)E_1$ between A and B. This voltage will be propagated down the so-called transmission line toward end CD, which it will reach at

APPROVED FOR PUBLIC RELEASE. CASE 06-1104.

time τ_d. Now if $R_s = Z_o$ there will be no reflection from end CD, and current I_p will flow through R_s, producing a negative voltage of magnitude $\left(\frac{R_s}{R_p + R_s}\right) E_1 = \left(\frac{Z_o}{R_p + Z_o}\right) E_1$ at D. Because end B is rounded, a potential of that magnitude must appear across each winding. Again, I_p will split up at junction D, allowing magnetizing current I to be diverted from the load, R_s, and flow directly to ground.

This will cause the output amplitude to decay according to the law discussed in Section 3.21. The output voltage, E_o, is thus a decaying step function which is delayed by time τ_d. This delay is shown in photographs F-5-16 and F-5-17, Fig. 53, which are double exposures showing the input waveform (negative pulse) at A and the output waveform (positive pulse) at D superimposed on the same time axis.

Oscillogram F-5-1 (Fig. 51) shows the response of T16 connected as in the circuit of Fig. 52 with R_p = 1100 ohms, R_s = 1000 ohms, C_p = 0 C_s = 7 μμf. Because of the high value of N in T16, very little decay can be noticed.

3.43 Effects of Capacitive Loading on a One-to-One Inverter.

In most applications, capacitance C will exist across R due to tube input capacitances, etc. connected across the output. This means a travelling wave front will not see the characteristic impedance at end CD for any value of R_s. Instead, capacitance C_s will effectively charge through the line impedance in parallel with R_s, and an inverted reflection will be sent back toward end AB. If $R_p = Z_o$, the reflection will see the proper termination and no further reflections will ensue. The output will be an exponentially rising voltage with time constant $R_s Z_o (C_s)/(R_s + Z_o)$. Oscillogram F-5-15 (Fig. 52), shows the waveforms at A and D for T16 in the circuit of Fig. 52 with $R_p = R_s$ + 1200 ohms, C_p + 0, C_s + 7 μμf. The

APPROVED FOR PUBLIC RELEASE. CASE 06-1104.

reflection due to capacitance C_s may be seen on the negative pulse which appears at A. The output (positive pulse) exhibits only a slow rise. This rise time (0 to 95%) is of the order of 0.05 microseconds, which checks well with that calculated. $(R_s Z_o C_s/(R_s + Z_o)$ = .0162 μsec, giving a rise time of 2.9 x 0.162 = 0.047 μsec).

Now if $R_p \neq Z_o$ and/or a capacitance C_p exists across R_p, further reflections occur which lose their square step-like edges, and in the extreme case the reflections will appear as damped oscillations in the output. In other words, the delay-line and capacitances tend to form a resonant circuit which produces sine waves when excited by a voltage step. Such oscillations may be seen in oscillograms F-118-20, Fig. 57, F-118-24, Fig. 58 and F-12-19, Fig. 54.

3.44 Elimination of Oscillations in a One-to-One Inverter.

In most applications of a one-to-one inverter, oscillations such as those above are undesirable in the output. However it is possible to eliminate them without serious loss in amplitude or rise time in most circuits by the method described below.

Usually an inverter will be connected in the plate circuit of a pentode as in Fig. 34, and hence will be driven by what is essentially a current source. The circuit may be redrawn as in Fig. 35 to illustrate delay line action. Obviously, the line is not terminated properly at either end, and unwanted reflections are apt to result. If it were possible to terminate the line in its characteristic impedance at just one end, there would be, at the most, one reflection. This may be accomplished at end CD by an artifice as discussed below.

Instead of connecting point C directly to B+ (or pulse ground), let it be connected to B+ through the parallel combination of an inductance L and a resistance R_R as in Fig. 36. The resulting delay-line circuit is then

APPROVED FOR PUBLIC RELEASE. CASE 06-1104.

that of Fig. 37.

Now if $R_s = R_R = Z_o$, and L_R is made equal to $Z_o^2 C_s$, the external impendance across end CD is a resistance of Z_o ohms at all frequencies, and the line is terminated properly.

The transient response may be calculated by using the equivalent circuit of Fig. 38. Because the L_R-R_R-R_S-C_s network acts as a pure resistance equal to Z_o, the current I_s may be easily calculated to be

$$I_s = I_1 (1 - e^{-t/Z_o C_p})$$

where I_1 is the amplitude of I_p, which is assumed to be a step function.

Photographs of pulse responses of two inverter p.t.'s with and without such compensating networks are shown in Fig. 57 and 58. Photograph F-118-24 shows the output waveform of T66C with a 0.2 microsecond input current pulse and no compensation. The circuit is that of Fig. 34 with C_s = 19 μμf and R_s = 1000 ohms. The characteristic impedance of T66C is approximately 1000 ohms. Photograph F-118-25 is the output with the proper compensating network as in Fig. 36. Photographs F-118-20 and F-118-23 show the corresponding output pulses of T63C2 with an input pulse of 0.05 microseconds duration.

3.45 One-to-One P.T. with Windings in Opposite Senses.

If one of the windings of a two-winding one-to-one p.t. is wound in the opposite sense from the other, the delay-line effect is not found. This may be shown to be a reasonable outcome by attempting to consider such a p.t. as a delay line. If it acted as a delay line, its series element would be, as in Ref. 9, an inductance equal to the sum of the two self-inductances plus twice the mutual inductance, or altogether about four times the primary inductance. This amounts to several hundred times the leakage inductance which acted as the series element in Section 3.42, so the characteristic impedance and delay would be very much higher

APPROVED FOR PUBLIC RELEASE. CASE 06-1104.

for the same interwinding spacing than for the p.t. of Section 3.42. As a result, the coupling effect of the interwinding capacitance completely overshadows its effect as part of a line.

The coupling effect of the interwinding capacitance is illustrated in Fig. 39 through 41 for the p.t. discussed above when connected as in Fig. 32. In these figures, each arrow represents a portion of current.

Fig. 39 represents the situation shortly after a voltage step is applied at the input. Of four units of current entering the primary at A, one unit is coupled via interwinding capacitance to B and ground, one unit flows down the primary toward C, and two units are coupled across to the other winding and proceed along the path of least impedance toward end D. Of the latter two, one unit flows through R_s to ground, and the other is coupled back to the primary by the interwinding capacitance near end CD.

Fig. 40 shows the current distribution a short time later while the current in the load, R_s, is still increasing. At this time current in the interwinding capacitance is beginning to decrease because that capacitance is now almost fully charged. Ordinary transformer action now starts to become evident, i.e. the amount of current flowing in the secondary approaches that in the primary.

Fig. 41 depicts the quasi-steady-state condition which occurs after the interwinding capacitance has become fully charged and the p.t. is acting as an ordinary transformer. (Magnetizing current is neglected.)

These diagrams indicate that for a p.t. with windings in opposite senses the current in the load, R_s, begins to build up immediately after application of voltage to the primary. No delay occurs as for the p.t. of Section 3.41, since current can flow into the load before all interwinding capacitance is charged.

APPROVED FOR PUBLIC RELEASE. CASE 06-1104.

Although the delay-line analysis technique is not applicable, the equivalent-circuit method of Section 3.3 may be used for a p.t. with one reversed winding, provided C_{ps} is included in the equivalent circuit. In fact, application of this method suggests a scheme for minimizing the effect of interwinding capacitance.

If a p.t. of the type mentioned above is connected as in the circuit of Fig. 24, and a positive pulse applied to point A, a negative pulse of the same amplitude will appear at B. The interwinding capacitance at end AB therefore has impressed across it a pulse voltage equal to twice that of the output, while at end CD, which is connected to ground, there is no voltage across the interwinding capacitance. Accordingly, energy stored per unit length near end AB is large and contributes greatly to the total energy storage, while energy stored near end CD contributes very little. If the interwinding capacitance per unit length at end AB could be made sufficiently less than at end CD, a more uniform distribution of energy storage and perhaps a decrease in total storage may be achieved.

In practice, this may be accomplished by merely increasing the spacing between windings at end AB, Fig. 24, and gradually decreasing it toward end CD. This may be done in such a way that the leakage inductance will not be affected but that capacitance C'_D, which is determined by energy storage, will be appreciably decreased. Experimental p.t.'s constructed in this fashion exhibit the same pulse delay and rise time as an inverter p.t. which does not have a reversed winding, but has the same leakage inductance and number of turns. Ringing, however, is generally of different amplitude for the two cases.

The non-uniform spacer discussed above may also be used in many other types of p.t.'s in which the pulse voltage across the interwinding capacitance varies from one end to the other. By this means, C'_D may be decreased by as much as thirty per cent.

APPROVED FOR PUBLIC RELEASE. CASE 06-1104.

4. DESIGN AND CONSTRUCTION

4.1 Requirements

For the purpose of this report it is assumed that a p.t. should reproduce an input pulse shape with the best possible accuracy. Accordingly, a p.t. must be designed to meet the following pulse-response requirements:

a. Minimum decay of output amplitude during the pulse (good low-frequency response)

b. minimum rise and fall times (good high-frequency response)

c. minimum of ringing and general distortion.

Requirement (a) may be realized, according to Section 3.31, by making L_p as large as possible. Reference to the formula for L_p, Eq. 3-7, shows that this may be done by making N_p, A, and μ_e large, and by minimizing ℓ_m. Photograph F-7-3, Fig. 55, illustrates the effect of μ_e on decay. For the upper waveform, μ_e is high due to the iron core, while for the lower trace, it is only that of air.

Requirement (b) may generally be realized by making both L_L' and C_i as small as possible, thus minimizing the product $L_L' C_i$. For a given turns ratio and type of winding geometry, this product is proportional to $N_p^2 U^2$, which is the square of the wire length used in the primary winding. Rise and fall times may therefore be minimized by using the shortest possible length of wire.

Requirement (c) may be realized for a given circuit application by obtaining the proper ratio of L_L' to C_D' in addition to minimizing them. A good general rule to follow is to satisfy at least one of the following relationships:

$$\sqrt{\frac{L_L'}{C_D'}} = Z_o' = R_p \qquad (4\text{-}1)$$

$$\sqrt{\frac{L_L''}{C_D''}} = Z_o'' = R_s \qquad (4\text{-}2)$$

where Z'_o and Z''_o are respectively the characteristic impedance of the primary and the secondary. Substitution of L_L' and C_D' yields, for a two-winding p.t.,

$$Z'_o = \frac{377}{\sqrt{\epsilon_r}} \left(\frac{\lambda_i}{D_p}\right) \text{ ohms} \qquad (4\text{-}3)$$

APPROVED FOR PUBLIC RELEASE. CASE 06-1104.

where f_1 is the capacitance ratio C'_p/C_i as derived in App. 7.3 and given in the curves of Fig. 62.

It should be noted that the product $L'_L\ C'_D$ is a function only of wire length and is independent of the variables λ_i and D_p which determine Z_o. This suggests a scheme for finding more accurately the optimum ratio of L'_L to C'_D. As soon as the low-frequency response and winding length are fixed, the product $L'_L\ C'_D$ is determined. It is therefore possible to set up a low-frequency-analogue circuit as discussed in Section 3.33 and vary the ratio of L'_L to C'_D in that circuit, holding their product constant. The values of L'_L and C'_D which produce the optimum response in the analogue circuit should then be correct ones to design for in the p.t.

Unfortunately, (a) and (b) are conflicting requirements. The first requires a large N_p while the second requires a small N_p; the first requires a large core cross-sectional area, A, while the second requires a small winding circumference, U. For a specified maximum decay of pulse amplitude there is, therefore, a lower limit on the rise time which may be obtained for a given impedance level.

4.2 Limitations

In formulating design specifications it is important to keep in mind the fact that an actual p.t. can in general perform no better than an ideal transformer. For example, consider a voltage step-up p.t. ($n > 1$) to be used in the circuit of Fig. 14. Let R_p = 1000 ohms, $R_s = \infty$, C_p = 10 μμf, C_s = 15 μμf, (a 6AG7 feeding a 6AG7, for instance), and n = 2. Considering the p.t. as an ideal transformer, a calculation of rise time (0-95%) gives 0.2 microseconds, hardly short enough for a 0.05 microsecond pulse. It would not be sensible, therefore, to specify a rise time any less than 0.2 microseconds for a p.t. used in this circuit.

The conflicting requirements mentioned in Section 4.1 also impose a serious limitation on reasonable specifications for p.t. response.

APPROVED FOR PUBLIC RELEASE. CASE 06-1104.

It is generally impossible, for example, to design a p.t. which will pass satisfactorily both a very short pulse and a very long one.

An exception to the above limitations may be found in the one-to-one-ratio p.t. discussed in Section 3.41. The response rise time for step-function excitation is practically independent of the product $L'_L C'_D$ and hence of N_p for this type of p.t. Accordingly, the conflict mentioned in Section 4.1 does not apply, and N_p may be made as large as necessary without sacrifice of rise time. However, the time delay, τ_d, introduced by the p.t. will be a function of $L'_L C'_D$, and, in those cases where a long delay is as objectionable as a long rise time, a conflict still exists.

4.3 Core

4.31 Material

From the discussion of Section 4.1, it is seen that the core should have the highest possible effective permeability (u_e). This means that the core material should provide both a high incremental permeability and low losses. (According to the definition used in Section 3.21, $\mu_e = \frac{L_p \ell_m}{4\pi N_p^2 A} 10^{-9}$, where L_p is determined from the droop in pulse response.)

Low core loss is achieved by using laminated cores with very thin insulated laminations made of high-resistivity material. The effect of lamination thickness (d) on core loss may be seen by examination of Eq. 3-11, in which d appears in the denominator of the expression for R_e. The smaller the value of d the larger will be R_e, hence the lower the core loss with its accompanying objectionable attenuation.

Several different alloys have been developed for producing a high resistivity and high permeability at low flux densities. Some of these are: Molybdenum Permalloy(4% Mo, 79% Ni, 17% Fe); Numetal (71% Ni, 20% Fe, 5% Cu, 1% Mn); Nicaloi and 45 Permalloy (Iron with 45-50% Ni); Hipersil

APPROVED FOR PUBLIC RELEASE. CASE 06-1104.

(Iron with about 3.5% Si). Special annealing and rolling processes have been developed to improve further the characteristics of these alloys. Rolling orients crystals of the metals in a preferred direction so that the edges are essentially parallel. Magnetizing force is thus considerably reduced and permeability increased.

The curves of Fig. 13 provide a comparison of three core materials tested under identical pulse conditions. These show that Mumetal is somewhat superior to both Nicaloi and Hipersil, at least for the particular impedance level, pulse lengths, etc., used in the tests.

A good qualitative comparison between Mumetal and Hipersil cores is found in Photographs F-6-6 and F-6-8, Fig. 54. The first is the pulse response of a winding with a core of Mumetal. The second is the response of the same winding with a Hipersil core of the same cross section. These photographs show a decidedly greater pulse droop for the Hipersil than for the Mumetal core.

P.t.'s for the computer of Project Whirlwind will probably use Hipersil cores exclusively because of their good mechanical design and availability, even though they do not have the best electrical properties. Hipersil cores produced by Westinghouse Electric Corporation are formed in closed core loops which are cut into c-shaped halves whose cut ends are ground smooth. It is then a simple matter to insert them into preformed windings and apply a metal band to hold the butt ends together under pressure. A mounting plate is also easily attached with the band (Fig. 3).

Mumetal core material is usually manufactured in the form of single c-type laminations (examples shown in Fig. 1) which must be applied to a winding by interleaving one by one. Photograph FB-20, Fig. 1, shows steps in the construction of a p.t. with Mumetal laminations.

APPROVED FOR PUBLIC RELEASE. CASE 06-1104.

4.32 Size of Core.

The core size is determined by the requirements mentioned in Section 4.1. Size must be such as to present the shortest possible magnetic path length, ℓ_m, and the greatest cross-sectional area consistent with a minimum length of wire per winding. Calculations for determining optimum shape are difficult because of the non-linearity of the core material; an experimental procedure is much more practical.

A direct experimental method for selecting the proper core is to choose a length of wire as close as possible to that which will be used in the primary winding of the p.t. to be designed. It must also be of the same diameter or gauge as that used in the p.t. This length of wire is then wound in a single layer (assuming that the primary will have a single layer) on the available types of cores having different sizes and shapes (some of which may be eliminated because they do not have sufficient window length for the winding). The resulting inductors are then compared in the circuit of Fig. 7 by applying a pulse of the length to be employed in the p.t. being designed. The value of R_p should be such as to represent both primary and secondary loading to be used. Responses are judged according to the amount of droop exhibited: the inductor giving the least droop has the most satisfactory core.

Tested by the above procedure, the best core will be the one which has a window just long enough to enclose the winding. This, however, assumes that all possible sizes and shapes of cores are available for the test, while actually only a limited number are obtainable at this time. The best assortment is supplied in Hipersil material (which is a further reason for using Hipersil cores in the computer of WWI).

APPROVED FOR PUBLIC RELEASE. CASE 06-1104.

4.33 Lamination Thickness (d)

It is well known that eddy currents in a core tend to decrease flux density at the center, thereby decreasing the permeability; that laminating the core counteracts this effect; and that increasing the resistivity of the laminations lowers core losses due to eddy currents. For pulse applications it is found that, other things being equal, there is an optimum lamination thickness for each pulse length. For example, a Hipersil core with 2-mil laminations is better for a 2-microsecond pulse than one with 1-mil laminations, while for a 0.05-microsecond pulse the 1-mil laminations are superior.

As the lamination thickness is decreased, the ratio of iron cross-sectional area to total core cross-sectional area (stacking or space factor) becomes reduced because of an increase in number of laminations necessary. This lowers the core efficiency and tends to counteract the improvement mentioned above. The latter effect is negligible, however, for the cores that are currently available, as may be seen from the stacking factors specified for the Hipersil material: for 2-mil material, the stacking factor is given as 89%; for 1-mil material, it is 88%.

The optimum lamination thickness may be determined experimentally by exactly the same procedure as suggested in Section 3.22 for finding the optimum core size. For present computer applications this will involve merely the comparison of two different Hipersil lamination thicknesses, 1-mil and 2-mil.

4.4 Windings

4.41 Number of turns per winding, N_p

The number of turns in a winding is determined by requirement (a) of Section 4.1. For a given core, the value of N_p may be calculated approximately by using curves as in Fig. 9 and 10. The procedure is to sketch the desired pulse response, with its allowable droop, for the

APPROVED FOR PUBLIC RELEASE. CASE 06-1104.

winding connected as in Fig. 7 and obtain its voltage-time area and amplitude. These quantities may be substituted into Equations 3-9 and 3-10 to get B_{max} and $\frac{dB}{dt}$, using a trial value of N_p. The graphs of Fig. 9 or 10 are then entered to obtain μ_e, which may be substituted into Eq. 3-7 to find L_p. Using this value of L_p, the droop is calculated. If it does not check with that of the sketch, a new value of N_p is assumed and the whole procedure repeated until a check is obtained.

The final value of N_p may be obtained by experimental measurements of the response. In many cases the above procedure for finding an approximate N_p may be replaced by a good estimate based on experience or by testing a number of windings.

The number of turns in the secondary winding (N_s) obviously will be nN_p. It is important to note here that for purposes of analysis either winding may be called the primary.

4.42 Wire Size

For a given N_p, the wire diameter, D_p, determines the length of winding, ℓ_w ($=N_pD_p$), and ℓ_w determines ℓ_m, which must be large for large ℓ_w. Therefore, in order to minimize ℓ_m for requirement (a), the wire should be made as small as possible. The lower limit on wire size is fixed by mechanical strength, the smallest reasonable size being about 39 A.W.G. In general, the wire used in the winding with the greater number of turns should be about this minimum size.

Wire size also appears in the expression for characteristic impedance, Z_o, given in Eqs. 3-22 and 4-3, and in many cases it will be determined by Z_o rather than by requirement (a), as discussed above.

4.43 Geometry

By winding geometry is meant the arrangement of windings in the primary and secondary. The secondary may consist of two windings, for example, one on either side of a single primary winding, opposite

APPROVED FOR PUBLIC RELEASE. CASE 06-1104.

ends of the two windings being connected; or the primary and secondary may have windings on both legs of the cores with appropriate interconnections. Only the fundamental case of a single primary winding and a single secondary winding will be considered here; more windings are added only for the purpose of obtaining a higher value of L_p, and in this report it is assumed that sufficiently high values of L_p can be obtained by proper choice of cores.

4.44 Spacing between windings (λ_i)

Winding spacing is important in determining the characteristic impedance. For a given wire size, Z_o is directly proportional to λ_i. For a desired Z_o, Eq. 4-3 may be solved to give the value of λ_i. Spacing λ_i is controlled by the number of layers of paper and the thickness of the paper placed between windings. In low-voltage p.t.'s, insulation considerations rarely determine the type of paper and value of λ_i.

Section 4.1 discusses a method for determining the best ratio of L_L' to C_D' and hence Z_o. Section 5.4 describes a procedure for measuring the value of Z_o and thus for determining whether or not the spacing in a particular p.t. is correct.

4.45 Spacing between Inner Winding and Core (λ_o)

The layers of paper applied between the inner winding and the core govern the core capacitance, C_o. As pointed out in Section 3.11, this capacitance may be made negligible by reducing it to the point where one-third of it (C_C') is negligibly small for the impedance level of the primary or inner winding. To facilitate this, it is usually best to make the inner winding the one of fewer turns.

4.46 Construction of Windings

In constructing a p.t., the first step is to obtain a mandril with a cross-section slightly larger than that of the core to be used in the p.t. A total thickness of paper equal to λ_o is then applied by

APPROVED FOR PUBLIC RELEASE. CASE 06-1104.

winding on at least two layers of paper (usually Kraft or other paper of equivalent low loss and low dielectric constant). The inner winding is next applied by turning it on the mandril, forming a close-wound solenoid. Another thickness (λ_1) of paper is applied, and, on top of that, the outer winding. Protective paper is wound on top of this, and strips of clear celulose-acetate tape ("Scotch" tape) with good electric properties are used to hold windings and paper in place. Finally, the mandril is removed and the core is inserted and banded. If terminal lugs are used, they may be taped on and soldered to the winding ends.

The outer winding layer must be placed with its ends flush with those of the inner layer. If the layers are not flush, leakage inductance is increased and the response is distorted. Oscillogram F-7-4, Fig. 55, shows distortion produced by windings displaced with respect to each other.

5. MEASUREMENT

5.1 Primary Inductance

Because of the non-linearity of the core material, a sine-wave measurement of L_p is meaningless. The only measurement that is useful employs a pulse of the length to be used in the actual operation of the p.t. The circuit of Fig. 46 may be used for this purpose and the output at point E displayed on an oscilloscope. The value of L_p may be calculated from the amount of decay observed at the end of the pulse, or the measurement may be used only qualitatively.

5.2 Leakage Inductance

Leakage inductance may be determined either from pulse measurement or by sine-wave technique. If the secondary terminals are shorted together, the impedance seen looking into the primary terminals will be practically equal to the reactance of L_L' at frequencies for which C_{ps}' presents a reasonably high impedance. This may be seen by examining the equivalent circuit of Fig. 6 with the output terminals shorted together.

APPROVED FOR PUBLIC RELEASE. CASE 06-1104.

It will be noted that L_L' appears in parallel with L_p across the input, but since $L_p >> L_L'$, L may be neglected.

Photograph F-5-31, Fig. 53, shows the pulse response of a primary with the secondary short-circuited. Knowing the loading across the primary, it is a simple matter to calculate L_L' from the rate of decay of the pulse so obtained.

A simple method for measuring L_L' independent of the value of C_{ps}' and other stray capacitance across the primary terminals is to use a Q-meter. The procedure is to find the resonant frequencies f_1 and f_2 of the primary with shorted secondary when paralleled with two different external capacitances, C_1 and C_2, each of which is considerably larger than stray shunt capacitances. Then L_L' may be calculated from the following formula:

$$L_L' = \frac{f_1^2 - f_2^2}{(2\pi f_1 f_2)^2 (C_2 - C_1)} . \qquad (5\text{-}1)$$

5.3 Distributed Capacitance

Capacitances C_o and C_i may be measured directly on any capacitance bridge at frequencies in the region of 60 cycles. The low frequency is necessary so that inductance reactances will be negligible.

5.4 Characteristic Impedance

The circuit of Fig. 45 with pulse excitation may be used for measuring the characteristic impedance of a winding. The procedure is to observe the waveform at A for different values of R_t. The value of R_t which causes no reflections or produces least distortion at A is the characteristic impedance, Z_c, of winding AC. Photographs F-4-25,-28,-29, Fig. 50 and 51, show steps in measurement of Z_o for a one-to-one ratio p.t. (T16). Photographs F-5-21,-22, Fig. 52, show steps in measuring Z_o for the low-voltage winding of a two-to-one-ratio p.t. (T24).

APPROVED FOR PUBLIC RELEASE. CASE 06-1104.

It is important that R_p be different from Z_o in this measurement in order to exaggerate pulse distortion due to improper values of R_t. An advantage inherent in this measuring technique is that no capacitance which would interfere with such a measurement is introduced across R_t.

6. OSCILLOGRAMS

All test circuits for oscilloscope photographs (Fig. 50 through 58) were mounted within two inches of the upper vertical deflection plate of the cathode ray tube in a Model 5 synchroscope. This made possible the use of very short connecting leads which reduced to less than 7 μμf the shunt capacitance added to the circuit by the oscilloscope. This capacitance has negligible effect except where indicated. The low inductance of the short leads permitted observation of steep wave fronts, as in F-4-0, Fig. 50, without objectionable ringing.

It was impossible to illuminate the grid on the face of the oscilloscope adequately with the camera attachment used for oscillograms in the F-4,-5,-6,-7, and -12 series, but it is hoped that gaps due to grid lines showing in the beam traces will serve the purpose. A scale showing grid spacing is also provided at the bottom of each plate. Sweep speeds (or horizontal scale factors) are specified by the time necessary for the beam to traverse the distance between grid lines (0.1 inch on actual grid).

Fig. 50.

F-4-0. Input voltage pulse (1/4 μ sec) used for all photographs in the F-4 and F-5 series. It is the pulse voltage which appears across R_o of Fig. 42 with R_{se} disconnected. Accordingly, it is the input voltage for the circuit of Fig. 43, which will be referred to in discussions of the F-4 and F-5 photographs even though the experimental circuit has the input of Fig. 42.

APPROVED FOR PUBLIC RELEASE. CASE 06-1104.

F-4-22,-23,-24. Waveforms at points A, B, and D for the circuit of Fig. 44 with p.t. T16, which is described in Sec. 2.4 and App. 6.5, R_p = 1100 ohms, $R_s = R_t$ = 1000 ohms, C_p = 0. When the oscilloscope is connected to A, C_p = 6.6 μμf.

F-4-25,-28,-29. (-29 in Fig. 51) Waveforms at A in the circuit of Fig. 45 with T16. R_p = 1100 ohms, R_t = 500, 1500, 4700 ohms. These photographs demonstrate the delay-line action of the windings and show that the characteristic impedance of T16 is somewhat less than 1500 ohms.

Fig. 51.

F-4-29. Discussed above.

F-5-1. Waveform at D with B grounded. T16 with R_p = 1100, R_s = 1000 ohms. The p.t. acts as a phase inverter.

F-5-5,-7. Waveforms at A and B, D grounded, Fig. 43 with T16. R_p = 1100, R_s = 1000 ohms. For F-5-7, C_s = 6.6 μμf, C_p = 0. For F-5-5, C_s = 0, C_p = 6.6 μμf.

F-5-10. Waveform at A, Fig. 45. T16 with R_p = 1100 ohms, R_t = 0. This shows delay-line action with short-circuit termination. Input end has approximately the characteristic impedance across it (Z_o = 1200 ohms).

F-5-12. Double exposure showing the waveform at A superimposed on that across R_o with the circuit of Fig. 45 (if the voltage source is replaced by the actual current source shown in Fig. 42). T16 with R_p = 1300 ohms.

APPROVED FOR PUBLIC RELEASE. CASE 06-1104.

Fig. 52.

F-5-14. Double exposure showing waveforms at E in Fig. 46 with switch S_1 open (b) and with S_1 closed (a). The sloping waveform (a) illustrates poor low-frequency response.

F-5-16. Waveforms at A and D, Fig. 43, shown in double exposure. P.t. is T16, B grounded, $R_p = R_s = 1200$ ohms. Except for stray capacitance added by the oscilloscope, $C_s = 0$. A delay between input pulse and inverted output is demonstrated.

F-5-17. Same as F-5-16 except C_s is increased by 20 $\mu\mu$f. The dip in waveform A is due to a reflection in the p.t. arising from the impedance mismatch at CD introduced by the added capacitance.

F-5-18. Waveform at D with B grounded in Fig. 43. T31 with $R_p = 1100$, $R_s = 1000$ ohms. The characteristic impedance of T31 is 1000 ohms, and there are 88 turns per winding as compared to 118 for T16. Consequently there is less delay than in T16, which is evidenced by the shorter negative "undershoot" preceding the pulse.

The waveforms of F-5-21 through F-5-32 are obtained with p.t. T24. Specifications for T24 are:

N_p = 44

N_s = 88

A = 0.0625 square inches

λ_i = 0.021 inch

ℓ_w = 0.437 inch

C_i = 35 $\mu\mu$f (measured)

L_L' = 7.3 μh. "

APPROVED FOR PUBLIC RELEASE. CASE 06-1104.

F-5-21. Double exposure showing waveforms at A, Fig. 45, with R_t = 220 and 1000 ohms, R_p = 500 ohms. Winding AC is the 44-turn winding. Proper termination is obviously somewhere between the two values of R_t used for these oscillograms.

F-5-22. Same as F-5-21 with R_t = 470 ohms. This is apparently the correct termination for the low-voltage winding since no reflection can be seen in the response.

Fig. 53.

F-5-24. Same as F-5-21 except that winding AC is the 88-turn winding of T24, and R_t = 500 ohms for one exposure and 1000 ohms for the other. The rectangular pulse (b) is the waveform for which R_t = 1000 ohms, indicating that this is approximately equal to the characteristic impedance for the high-voltage winding.

F-5-25. Waveform at D, Fig. 43, with B grounded. Winding BD is the higher-turn winding of T24. R_p = 1100, R_s = 2200 ohms. This photograph demonstrates step-up inversion. (The poor leading edge is relatively independent of the value of R_s.)

F-5-27. Waveform at B, Fig. 43, with D grounded. Remaining circuit elements are the same as for T-5-25. This demonstrates step-up action without inversion.

F-5-31. Waveform at A, Fig. 45, with AC the low-voltage winding of T24. R_t = 0, R_p = 500 ohms. This shows the effect of leakage inductance or, using delay-line theory, it shows reflections arising from a short-circuit across one end (CD) of the p.t.

APPROVED FOR PUBLIC RELEASE. CASE 06-1104.

F-5-32. Waveform at D, Fig. 44, with the high-voltage winding of T24 as winding BD. R_p = 500, R_s = 1100, R_t = 1200 ohms. The output is much more rectangular than that of F-5-25, showing the effect of proper termination at end CD.

Fig. 54.

F-6-5. A 5-microsecond pulse which is the input voltage, E_i, for response patterns shown in F-6-6 and F-6-8.

F-6-6. Waveform at A, Fig. 46, with switch closed. R_p = 3000 ohms. The p.t. is T17 with a Mumetal core (110 laminations). The number of turns per winding is 118 (the same as for T16 of Sec. 2.4). The cross-sectional area of the core is 0.0625 square inches.

F-6-8. Same as for F-6-6 except that the Mumetal core was replaced by a Hipersil core without a metal banding strap. The Hipersil core has the same cross section and its magnetic path length is about equal to that of the Mumetal core.

F-12-19. Illustration of oscillations in p.t. output due to insufficient primary damping. The oscillating waveform (a) is observed at point D, Fig. 42, with B grounded. R_{se} = 0, R_s = ∞, C_s = 6.6 $\mu\mu$f, C_p = 0, R_o = 100 ohms. The more rectangular pulse (b) is obtained at the same point with R_{se} = 390 ohms. The p.t. is Westinghouse unit 166 AW.

F-12-4. Double exposure showing waveforms at both A and D in the circuit of Fig. 43 with T19, which is the same p.t. as T31 except that one winding is wound in the opposite sense from the other. Point B is grounded, R_p = 100 ohms, R_s = 1000 ohms, and capacitances are zero except where the oscilloscope introduces about 7 $\mu\mu$f. This photograph clearly shows that no delay is introduced by this type of transformer.

APPROVED FOR PUBLIC RELEASE. CASE 06-1104.

Both pulses begin to rise at the same point even though the output pulse at D exhibits a slower rise than that at A.

3-11. Triple exposure showing waveforms at A of Fig. 43 with B grounded. The p.t. is Westinghouse's 132 AW 2. Points A, B, C and D of Fig. 43 correspond to terminals 1, 3, 2, and 4 respectively of the p.t. R_p = 500, R_s = 0, ∞, and 180 ohms. The waveform for R_s = 0 shows a short pulse of duration equal to twice the one-way delay of the p.t. followed by a few rapidly damped reflections, and another similar pulse with opposite polarity at the termination of the input pulse. Since 180 ohms is the characteristic inpedance of the p.t., this value when used for R_s eliminates reflections and allows a perfectly rectangular pulse to appear at A. For $R_s = \infty$, reflections add, and produce a staircase effect. The decrease in amplitude beginning near the middle of the waveform is due to poor low-frequency response. It will be noted that all three waveforms trace the same initial step just as would be expected if the p.t. were acting as a delay line.

Fig. 55.

F-7-1. Waveform at A, Fig. 46, with the switch closed. The p.t. is T17 with a Hipersil core. R_p = 3000 ohms. Pulse duration is 1 μ sec.

F-7-3. Double exposure showing waveforms at D, Fig. 43, with B grounded. The p.t. is T17, R_p = 1100, R_s = 1100 ohms. Pulse duration is 1/2 μ sec. The upper trace was made with a Hipersil core in T17. The lower trace shows the effect of removing the core entirely. It will be noticed that rise-time or high-frequency response is unaffected.

F-7-4. The upper trace is the same as the lower trace of F-7-3. The lower trace was obtained when one winding was displaced longitudinally 5/32 inch from the other. It may be seen that the effect of this is to introduce a larger negative voltage (which is in phase with the input pulse) during the delay interval preceding the inverted pulse.

APPROVED FOR PUBLIC RELEASE. CASE 06-1104.

F-7-11. Triple exposure showing waveforms at A, Fig. 43, with B grounded. The p.t. is T19. R_p = 1100 ohms. The top trace is made with R_s = 470 ohms, the middle trace with R_s = 1100 ohms, the bottom trace with R_s = 2200 ohms. This indicates that there is an optimum terminating resistance, in this case 1100 ohms.

F-7-12. Waveform at D for the same circuit as used for photograph F-7-11. R_s = 1100 ohms.

F-7-13. Waveforms at B with D grounded. Otherwise same circuit as for F-7-12. The upper trace is made with $R_s = \infty$, the lower with R_s = 1100 ohms.

Fig. 56.

Photographs F-103-1,-2,-4 on the left in Fig. 56, show pulse responses of three different p.t.'s in the circuit of Fig. 47, while the photographs opposite them are output waveforms of their low-frequency analogues. Because the input, E_i, is a positive pulse for both circuits, the output waveforms are positive for the actual p.t. (inverter) and negative for the analogue. Comparison was therefore facilitated by printing photographs F-103-5,-7,-8 with the negatives reversed, thus producing a mirror image of the actual output pulse which appears like a pulse of opposite polarity. The input amplitude and bias voltage of the 6AG7 driver tube in the analogue circuit were adjusted to account for the voltage step-up in the p.t. and to make the analogue output amplitude equal to that of the actual p.t. circuit.

APPROVED FOR PUBLIC RELEASE. CASE 06-1104.

F-103-1. Output waveform of the circuit of Fig. 47 with T52D5, which has the following specifications:

N_p = 177

N_s = 37

ℓ_w = 3/4 inch

λ_i increases from 0.003" at one end to 0.025" at the other

L_L' = 35 μh. (measured)

C_i = 100 μμ f. (measured)

n = 0.21

F-103-2. Output waveform of the circuit of Fig. 47 with T39.

Specifications for T39 are:

N_p = 58

N_s = 12

ℓ_w = 5/16 inch

λ_i = 0.03 inch

L_L' = 52 μ h.

C_i = 9 μμ f

n = 0.207

F-103-4. Output waveform of the circuit of Fig. 47 with T53A.

Specifications for T53A are:

N_p = 120

N_s = 30

ℓ_w = 5/8 inch

λ_i = 6.014 inch

L_L' = 32 μ h

C_i = 30 μμ f

n = 0.25

APPROVED FOR PUBLIC RELEASE. CASE 06-1104.

F-103-5. Response of T39 analogue. Referring to the circuit of Fig. 48,

$k = 23$

$C_1 = 10$ μμf. (Output capacity of 6AG7 plus strays)

$C_2 = C_D' = 5$ μμf.

$kL_L' = 1.2$ mh

$R_2 = 1000$ ohms

$kL_p = 30$ mh

$R_e = 4500$ ohms

(The eddy current resistance R_e has very little effect on the transient response for this p.t.)

F-103-7. Response of T53A analogue. Referring to the circuit of Fig. 48,

$k = 23$

$C_1 = 10$ μμf

$C_2 = C_D' = 13$ μμf

$kL_L' = 750$ mh

$R_2 = 1100$ ohms

$kL_p = \infty$

$R_e = 20{,}000$ ohms

F-103-8. Response of T52D5 analogue. Referring to the circuit of Fig. 48,

$k = 23$

$C_1 = 10$ μμf

$C_2 = C_D' = 28$ μμf

$kL_L' = 0.8$ mh

$R_2 = 1000$ ohms

$kL_p = \infty$

$R_e = 7{,}500$ ohms

APPROVED FOR PUBLIC RELEASE. CASE 06-1104.

(The primary inductance L_p was omitted in these last two analogues because low-frequency response was of no particular interest. It is true, however, that the addition of L_p would make for a better duplication of pulse shape.)

Oscillograms in the F-118 series demonstrate a ringing-compensating network which is shown in Fig. 49 and discussed in Sec. 3.4. Characteristics of p.t.'s used in these photos are:

T630-2

$N_p = 98$ $A = 1/4" \times 3/8"$

$N_s = 98$ $\ell_m = 8$ cm.

$\ell_w = \frac{17}{32}$ inch

$\lambda_i = 0.003$ inch

$n = 1$

$Z_o = 1400$ ohms (measured)

T660

$N_p = 19$ $A = 3/16" \times 1/4"$

$N_s = 19$ $\ell_m = 6.5$ cm.

$\ell_w = 3/16$ inch

$\lambda_i = 0.049$ inch

$n = 1$

$Z_o = 1100$ ohms (measured)

Fig. 57

F-118-20. Response (E_o) to a 1/20-msec pulse of the circuit of Fig. 49 with p.t. T660. Switch S_1 is open and S_2 closed. $R_s = 1100$ ohms, $C_s = 9$ $\mu\mu$f.

F-118-21. Output waveform of the same circuit as for F-118-20, except with S_1 closed. $R_R = 500$ ohms, $L_R = 10$ μh.

F-118-22. Output waveform of the same circuit as for F-118-20, except with S_1 closed and S_2 open. $R_p = 550$.

APPROVED FOR PUBLIC RELEASE. CASE 06-1104.

F-118-23. Output waveform of the same circuit as for F-118-20, except with S_2 open.

Fig. 58.

F-118-24. Response (E_o) to a 1/4 μsec pulse of the circuit of Fig. 49 with p.t. T6302. Switch S_1 is open and S_2 closed. R_s = 1200 ohms, C_s = 19 μμf.

F-118-25. Output waveform of the same circuit as for F-118-24 except with S_2 open. R_R = 1000 ohms, L_R = 25 μh.

F-118-26. Output waveform of the same circuit as for F-118-24 except S_1 closed and S_2 open. R_p = 0.

F-118-27. Output waveform of the same circuit as for F-118-24 except with S_1 closed.

APPROVED FOR PUBLIC RELEASE. CASE 06-1104.

7 APPENDIX

7.1 List of Symbols

Symbol	Definition
p.t.	Pulse transformer
A	Cross-sectional area of core
B	Flux density
B_{max}	Maximum flux density
c	Velocity of light
C_C'	Equivalent capacitance referred to the primary. Represents effect of C_o
C_o	Capacitance between inner winding and core
C_D'	Equivalent capacitance (referred to primary) representing C_i
C_i	Interwinding capacitance
C_1	First shunt capacitance in equivalent circuit
C_2	Second shunt capacitance in equivalent circuit
D	Wire Diameter
D_p	Diameter of wire used in primary winding
D_s	Diameter of wire used in secondary winding
d	Lamination thickness
E_i	Input voltage
E_o	Output voltage
E_p	Voltage across primary winding.
E_s	Voltage across secondary winding
E_1	Amplitude of input voltage
E_2	Amplitude of output voltage
ϵ	Dielectric constant (CGS)
f_1	Factor by which C_1 is multiplied to obtain C_D'
I_i	Input current
I_1	Amplitude of input current

APPROVED FOR PUBLIC RELEASE. CASE 06-1104.

List of Symbols (continued)

Symbol	Definition
I_m	Magnetizing current
I_p	Current in primary winding
I_s	Current in secondary
k	Frequency conversion factor
L'_L	Leakage inductance referred to primary
L_m	Magnetizing inductances
L_o	An inductance constant giving effective primary inductance at t = 1
L_p	Primary inductance
L_R	Inductance used in ringing-compensating network
ℓ_m	Mean magnetic path length
ℓ_w	Winding length
n	Ratio of secondary to primary turns
N_p	Number of turns in primary winding
N_s	Number of turns in secondary winding
R_e	Equivalent resistance representing effect of eddy currents
R_h	Equivalent resistance representing effect of hysteresis
R_L	Total resistance paralleling primary inductance
R_o	Source resistance
R_p	Primary shunting resistance
R_s	Secondary shunting resistance
R_{se}	Series resistance between generator and transformer
R_1	First shunting resistance in equivalent circuit
R_2	Second shunting resistance in equivalent circuit

APPROVED FOR PUBLIC RELEASE. CASE 06-1104.

List of Symbols (continued)

Symbol	Definition
S_1, S_2	Switches
t	Time variable
U	Mean circumference of windings
V_{AB}	Pulse voltage difference between adjacent winding ends, A and B
V_{CD}	Pulse voltage difference between adjacent winding ends, C and D
V_p	Amplitude of pulse voltage across primary
V_s	Amplitude of pulse voltage across secondary
W	Stored energy
W_i	Energy stored in interwinding capacitance
x	Variable used for distance along a winding
Z_o	Characteristic impedance
λ_{AB}	Separation between windings at end AB
λ_{CD}	Separation between windings at end CD
λ_i	Separation between windings in a two-winding transformer
λ_o	Separation between core and inner winding
μ	D-C permeability (gauss per oersted)
μ_e	Effective incremental permeability (gauss per oersted)
ρ	Resistivity of core material (ohm-cm)
τ	Pulse duration
τ_d	Delay time
Single prime (')	Refers a quantity to the primary side
Double prime (")	Refers a quantity to the secondary side
Rise time (0-95%)	Time necessary for voltage or current to reach 95% of its final asymptotic value.
Duty factor	Product of pulse duration and pulse repetition frequency.

APPROVED FOR PUBLIC RELEASE. CASE 06-1104.

7.2 Calculation of Leakage Inductance

To demonstrate the procedure used for calculating leakage inductance, the simple two-winding p.t. will be considered. Assuming that the ampere-turns are equal in the two windings, primary and secondary, and that the length of the windings is large compared to the spacing between them ($\ell_w \gg \lambda_1$), the field in the space between them should be nearly the same as that within a solenoid having the same number of ampere-turns as one of the windings. If it is assumed that there is uniform current distribution across the layer thickness, the field is as shown in Fig. 59, and its magnitude is as follows:

In the primary

$$H_1 = \frac{4\pi N_p I_p}{\ell_w} \left(\frac{x_p}{D_p} \right) \text{ oersteds,}$$

where x_p is measured from the side of the primary next to the core.

Between layers

$$H_2 = \frac{4\pi N_p I_p}{\ell_w} .$$

In the secondary

$$H_3 = \frac{4\pi N_p I_p}{\ell_w} \left(1 - \frac{x_s}{D_s} \right) ,$$

where x_s is measured from the inside of the secondary.

Since the interwinding space has the same permeability as air ($\mu = 1$), the energy in magnetic field H is given by $W = \frac{H^2}{8\pi}$ ergs per cc. Therefore, the energy stored in the field between layers is given by

$$W = \frac{U \ell_w}{8\pi} \left[\int_0^{D_p} H_1^2 \, dx_p + H_2^2 \lambda_i + \int_0^{D_s} H_3^2 \, dx_s \right]$$

$$= \frac{2\pi N_p^2 I_p^2}{\ell_w} \left[\lambda_i + \frac{D_s + D_p}{3} \right]$$

APPROVED FOR PUBLIC RELEASE. CASE 06-1104.

Setting this expression equal to an expression for energy stored in L_L' which has I_p flowing in it in the equivalent circuit gives

$$\frac{1}{2} L_L' \quad I_p^2 = \frac{2\pi \quad N_p^2 \quad I_p^2}{\ell_w} \left[\lambda_i + \frac{D_s + D_p}{3} \right],$$

from which,

$$L_L' = \frac{4\pi \quad N_p^2 \quad U}{\ell_w} \left[\lambda_i + \frac{D_s + D_p}{3} \right] \text{ abhenries} \quad (7\text{-}1)$$

7.3 Calculation of C_D'.

If the winding layers of a two-winding p.t. are considered as parallel plates of a condenser with length ℓ_w, width U, and separation λ_i, the total capacitance between windings is given by

$$C_i = 0.0885 \frac{\varepsilon \quad U \quad \ell_w}{\lambda_i} 10^{-12} \text{ farads.} \quad (7\text{-}2)$$

The energy stored in a section of width U and length dx (Fig. 60) is

$$dW = \frac{C_i}{2 \ell_w} \left[\Delta V_x \right]^2,$$

where ΔV_x is the voltage between windings at height x measured from the lower end. Letting V_{AB} represent the voltage rise from end A to adjacent end B, and V_{CD} the rise from C to D, and assuming a linear voltage distribution along the windings,

$$\Delta V_x = \left[(V_{AB} - V_{CD}) \frac{x}{\ell_w} + V_{CD} \right]$$

Substituting this into the expression for dW yields

$$dW = \frac{C_i}{2 \ell_w} \left[(V_{AB} - V_{CD}) \frac{x}{\ell_w} + V_{CD} \right]^2.$$

Integrating over the range from 0 to ℓ_w gives for the total energy stored

APPROVED FOR PUBLIC RELEASE. CASE 06-1104.

$$W = \frac{C_i}{6} \left[V_{AB}^2 + V_{AB} V_{CD} + V_{CD}^2 \right].$$

The value of C_D' may now be determined by setting this energy equal to that stored in C_D' and solving. This gives

$$C_D' = \frac{C_i}{3 V_p^2} \left[V_{AB}^2 + V_{AB} V_{CD} + V_{CD}^2 \right], \quad (7\text{-}3)$$

where V_p is the voltage across the primary winding, AC.

Now if ends B and C are grounded, or the p.t. is used as an inverter, the voltages across the ends are given by

$$V_{AB} = -V_p$$

$$V_{CD} = -nV_p$$

Substituting these into Eq. 7-3 yields

$$C_D' = \frac{C_i}{3} (1 + n + n^2).$$

The ratio $f_1 = C_D'/C_i$ is plotted against n in Fig. 62.

If ends C and D are grounded and the p.t. is used as a non-inverter, the end voltages become

$$V_{AB} = (n - 1) V_p$$

$$V_{CD} = 0.$$

Substituting as above,

$$C_D' = \frac{C_i}{3} (n - 1)^2,$$

which is also plotted in Fig. 62.

APPROVED FOR PUBLIC RELEASE. CASE 06-1104.

7.4 Capacitance Calculations for a Tapered Spacer between Windings.

In many cases where the pulse voltage across one end of a p.t. is much greater than that across the other end, interwinding capacitance effects may be greatly reduced by using a tapered spacer between windings. The wide end of the taper will increase spacing and reduce capacitance at the high-voltage end, while the narrow taper end will decrease spacing at the low-voltage end.

It is desired to compute C_i when such a spacer is used. Letting λ_{CD} be the spacing at the narrow end and λ_{AB} that at the wide end (See Fig. 61), the following analysis may be used to determine the total capacitance between windings which would be found by direct measurement.

Let C_x = Capacitance of section with width U and height dx at x

$$= \frac{0.0885\ \varepsilon\ U\ dx}{\lambda_x} \quad \mu\mu f,$$

where λ_x = spacing at height x

U = average circumference of tapered windings.

From Fig. 61,

$$\lambda_x = (\lambda_{AB} - \lambda_{CD}) \frac{x}{\ell_w} + \lambda_{CD}$$

Integrating over the range from 0 to ℓ_w gives for the total capacitance

$$C_i = 0.0885\ \varepsilon\ U \int_0^{\ell_w} \frac{dx}{(\lambda_{AB} - \lambda_{CD})\ \frac{x}{\ell_w} + \lambda_{CD}}$$

$$= \left(\frac{0.0885\ \varepsilon\ U \ell_w}{\lambda_{AB} - \lambda_{CD}}\right) \log\left(\frac{\lambda_{AB}}{\lambda_{CD}}\right) \quad \mu\mu f. \qquad (7\text{-}4)$$

Now if it is desired to find C_D' for the case where ends C and D are grounded and the p.t. acts as a step-up non-inverter, the following procedure, which is similar to that of Section 7.3, applies. Thus

APPROVED FOR PUBLIC RELEASE. CASE 06-1104.

$$V_{AB} = (n-1)\ V_p$$

and

$$V_{CD} = 0,$$

giving

$$V_x = (n-1)\ V_p \left(\frac{x}{\ell_w}\right)$$

From the foregoing analysis

$$C_x = \frac{0.0885\ \varepsilon\ U\ dx}{(\lambda_{AB} - \lambda_{CD})\ \frac{x}{\ell_w} + \lambda_{CD}} \quad 10^{-12} \text{ farads.}$$

Therefore

$$W = \frac{0.0885\ \varepsilon\ U\ (n-1)^2\ V_p^2}{2\ \ell_w^2}\ 10^{-12} \int_0^{\ell_w} \frac{x^2\ dx}{(\lambda_{AB}-\lambda_{CD})\ \frac{x}{\ell_w} + \lambda_{CD}}$$

$$= \frac{0.0885\ \varepsilon\ U\ (n-1)^2\ V_p^2\ \ell_w\ \lambda_{CD}^2}{2\ (\lambda_{AB} - \lambda_{CD})^3}\ 10^{-12}$$

$$\cdot \left\{ \frac{\left(\frac{\lambda_{AB}}{\lambda_{CD}} - 3\right)\left(\frac{\lambda_{AB}}{\lambda_{CD}} - 1\right)}{2} + \log_e \left(\frac{\lambda_{AB}}{\lambda_{CD}}\right) \right\}$$

Setting this energy equal to $\frac{1}{2}\ C_D'\ V_p^2$ and solving gives

$$C_D' = \frac{0.0885\ \varepsilon\ U\ (n-1)^2\ \ell_w\ \lambda_{CD}^2}{(\lambda_{AB} - \lambda_{CD})^3} \left\{ \frac{\left(\frac{\lambda_{AB}}{\lambda_{CD}} - 3\right)\left(\frac{\lambda_{AB}}{\lambda_{CD}} - 1\right)}{2} + \log_e \left(\frac{\lambda_{AB}}{\lambda_{CD}}\right) \right\} \mu\mu f. \qquad (7\text{-}5)$$

Now, to get C_D' from measured capacitance C_1, the ratio $\frac{C_D'}{C_1}$ must be found. Dividing Eq. 7-5 by Eq. 7-4 gives.

$$\frac{C_D'}{C_i} = f_1 = \frac{(n-1)^2}{\left(\frac{\lambda_{AB}}{\lambda_{CD}} - 1\right)^2} \left\{ \frac{\left(\frac{\lambda_{AB}}{\lambda_{CD}} - 3\right)\left(\frac{\lambda_{AB}}{\lambda_{CD}} - 1\right)}{2 \log \frac{\lambda_{AB}}{\lambda_{CD}}} + 1 \right\}$$

APPROVED FOR PUBLIC RELEASE. CASE 06-1104.

This factor may then be used in place of that in Fig. 62 to obtain C_D' from the measured value, C_i.

7.5 Sample calculations of Leakage Inductance and Distributed Capacitance for T16.

The specifications for T16 are as follows:

$A = \frac{1}{4}" \text{ by } \frac{1}{4}"$

$\lambda_o = 0.021" = 0.053$ cm.

$D_p = D_s = 0.005" = 0.0127$ cm.

$\lambda_i = 0.021" = 0.533$ cm.

$U = 1.5"$ (measured) $= 3.8$ cm.

$w = 0.625" = 1.58$ cm.

$\varepsilon = 3.5$ (paper)

$N_p = N_s = 118$ turns

Substituting in Eq. 7-1,

$$L_L' = \frac{4\pi \cdot (118)^2 \cdot 3.8}{1.58} (0.0533 + \frac{0.0254}{3}) \text{abhenries}$$

$= 26 \mu h$ (Actual measurement by the method of Section 4 gave 33 μ h.)

Substituting in Eq. 7-2,

$$C_D' = C_i = \frac{0.0885 \cdot 3.5 \cdot 1.58 \cdot 3.8}{0.0533} = 35 \mu\mu f.$$

(Actual measurement on 60-cycle bridge gave 30 $\mu\mu$f.)

APPROVED FOR PUBLIC RELEASE. CASE 06-1104.

7.6 Typical Designs and Applications

7.61 One-to-One Inverters

The most useful application of an inverting p.t. is in the plate circuit of a pentode amplifier. A typical circuit is that of Fig. 49, in which C_s represents the input capacitance of a succeeding stage. If a droop of 10-15% can be tolerated, T6302 of Fig. 58 is about an optimum design for a 1/4-microsecond pulse at an impedance level of 1000 ohms. Referring to oscillogram F-118-25, the pulse rise time (0-95%) is about 3.5 divisions or 0.08 microseconds for the circuit of Fig. 49, whereas an ideal transformer would give a rise time of 0.1 microseconds (assuming 10 μμf output capacitance for the 6AG7). The p.t. introduces a delay of about 0.02 microseconds, which makes up the difference. The L_R-R_R corrective network described on page 54 and shown in Fig. 49 must be used if ringing is to be eliminated in such a circuit.

For a 1/20-microsecond pulse, T66C of Fig. 57 represents a good design at a 1000-ohm impedance level for application in the circuit of Fig. 49. The total capacitance in the circuit used for F-118-22,-23 (Fig. 57) is 19 μμf, giving a rise time for an ideal transformer of 0.06 microseconds. Rise and fall times measured in the oscillograms of Fig. 57 are all less than this.

If more precise reproduction of pulse shape is desired, the impedance level may be lowered by applying resistive loading in both primary and secondary. For this application, T16, T17, and T31 are all good designs for 1/4-microsecond pulses with 1000 ohms across each side. Oscillograms F-5-1 (Fig. 50), F-5-18 (Fig. 52), and F-7-3 (Fig. 55) show responses of these transformers as inverters with both primary and secondary loading.

APPROVED FOR PUBLIC RELEASE. CASE 06-1104.

7.62 Current Step-Up Inverters

The problem of introducing high-current pulses into low-impedance loads such as transmission lines is one for which a p.t. is well adapted. An example of such a p.t. application is that of driving a 93-ohm transmission line terminated at both ends. With a p.t. connected in the plate circuit of a 6AG7 as in Fig. 47, 1/4-microsecond pulses of amplitudes as high as 26 volts may be obtained across such a load (47 ohms). (See oscillograms on left in Fig. 56) This means that the pulse currents are of the order of 0.5 ampere, which could not ordinarily be obtained in a 6AG7.

The best design for such an application if T52D5, which is described on page 52. The droop in 1/4 microsecond is only about 3% for this p.t. to satisfy a requirement which involves operating seven p.t.'s in parallel. To obtain this very small droop, a large number of turns are used in the windings of T52D5. Because of this, a tapered spacer is employed to aid in reducing the L'_L-C'_D product as discussed on page 62. Nevertheless, a loss is taken in rise time in order to satisfy the stringent requirement on droop. (The overshoot seen in F-103-1, Fig. 56, is not to be confused with droop.)

7.63 Non-Inverters

An example of a one-to-one p.t. which may be used solely for d-c isolation is T19, which is discussed on page 49. When used as a non-inverter at an impedance level of about 500 ohms, its response to a 1/4-microsecond pulse is as shown in F-12-4, Fig. 54. The use of windings in opposite senses in T19 eliminates the delay-line type of distortion which would be present if the windings were in the same sense. Compare waveform (D) of F-12-4 with that of F-5-7, Fig. 51, for example. The latter waveform was obtained using T16 (with windings in the same sense)

APPROVED FOR PUBLIC RELEASE. CASE 06-1104.

as a non-inverter with the same loading as for T19 of F-12-4. It will be noted that rise time is much less for T19.

For other than one-to-one p.t.'s nothing is gained by using windings in opposite senses, as may be shown by calculating C_D' for those cases. It will be found that f_1 (see App. 6.3) is higher for the same L_L' and C_i with opposite-sense windings than with windings in the same sense.

An example of a p.t. which may be used as a step-up non-inverter is T24, discussed on page 48. Oscillogram F-5-27, Fig. 53, shows the response of T24 used in this way.

APPROVED FOR PUBLIC RELEASE. CASE 06-1104.

7.7 References:

1. EE Staff, M.I.T., Magnetic Circuits and Transformers, New York: John Wiley and Sons, 1943, pp. 486-494.

2. W.H. Bostick, in Radiation Laboratory Technical Series, Vol 5. "Pulse Generators", New York: McGraw-Hill Book Company, Inc. (Expected to be published in late summer, 1947) Chapters 11, 12, 13.

3. H.L. Rehkopf, "Equivalent Circuit of a Pulse Transformer Core," M.I.T. Radiation Laboratory Report 666, PB 2719 from "Scientific and Industrial Reports" prepared by the Office of Technical Services, United States Department of Commerce.

4. Gillette, Bostick, and Rehkopf "Leakage Inductance and Distributed Capacitance for Various Types of Pulse Transformer Windings," PB 2478.

5. F.E. Terman, Radio Engineers' Handbook, New York: McGraw-Hill Book Company, Inc., 1943, pp. 96-100.

6. Rehkopf, Bostick, and Gillette, "Pulse Transformer Core Measurements", PB 2736.

7. A.G. Ganz, "Applications of Thin Permalloy Tape in Wide-Band Telephone and Pulse Transformers", AIEE Technical Paper 46-27, December, 1945.

8. S.A. Wingate, "The Steady-state and Transient Response of a Coupling Network", Bachelor's Thesis, M.I.T. Electrical Engineering Department, 1943.

9. Blewett, Langmuir, Nelson and Rubel, "Delay Lines", General Electric Co., Internal Report 214, 1943.

10. Bostick, Gillette, Rehkopf, and Zeller, "The Evaluation of an Equivalent Circuit for a Pulse Transformer", PB 2559.

APPROVED FOR PUBLIC RELEASE. CASE 06-1104.

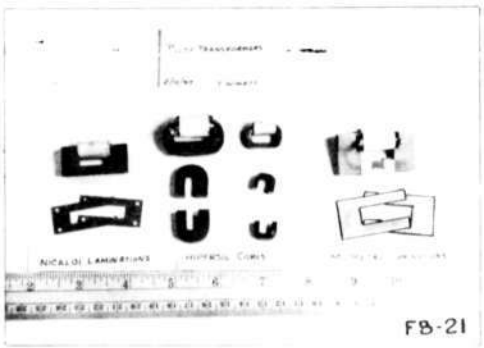

PULSE TRANSFORMERS WITH NICALOI, HIPERSIL, AND MUMETAL CORES.

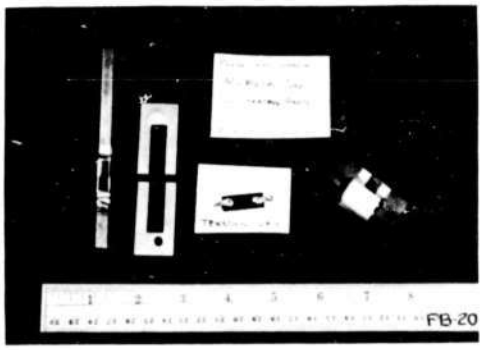

CONSTRUCTION OF A TRANSFORMER WITH MUMETAL LAMINATIONS. FROM LEFT TO RIGHT — WINDING BEING FORMED ON MANDRIL, LAMINATIONS, TERMINAL STRIP, AND COMPLETED TRANSFORMER

FIG. 1

A-30730

APPROVED FOR PUBLIC RELEASE. CASE 06-1104.

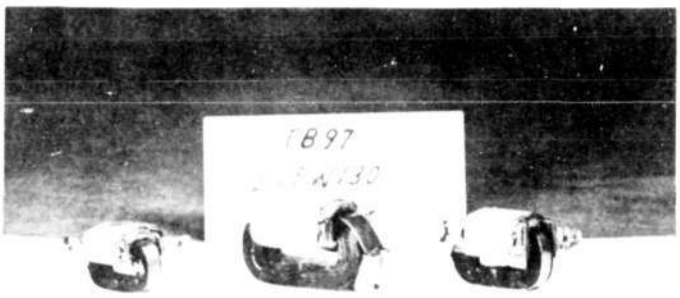

EXPERIMENTAL PULSE TRANSFORMERS
ILLUSTRATING VARIOUS SIZES OF HIPERSIL CORES.

FIG. 2

A-30731

APPROVED FOR PUBLIC RELEASE. CASE 06-1104.

A-30631

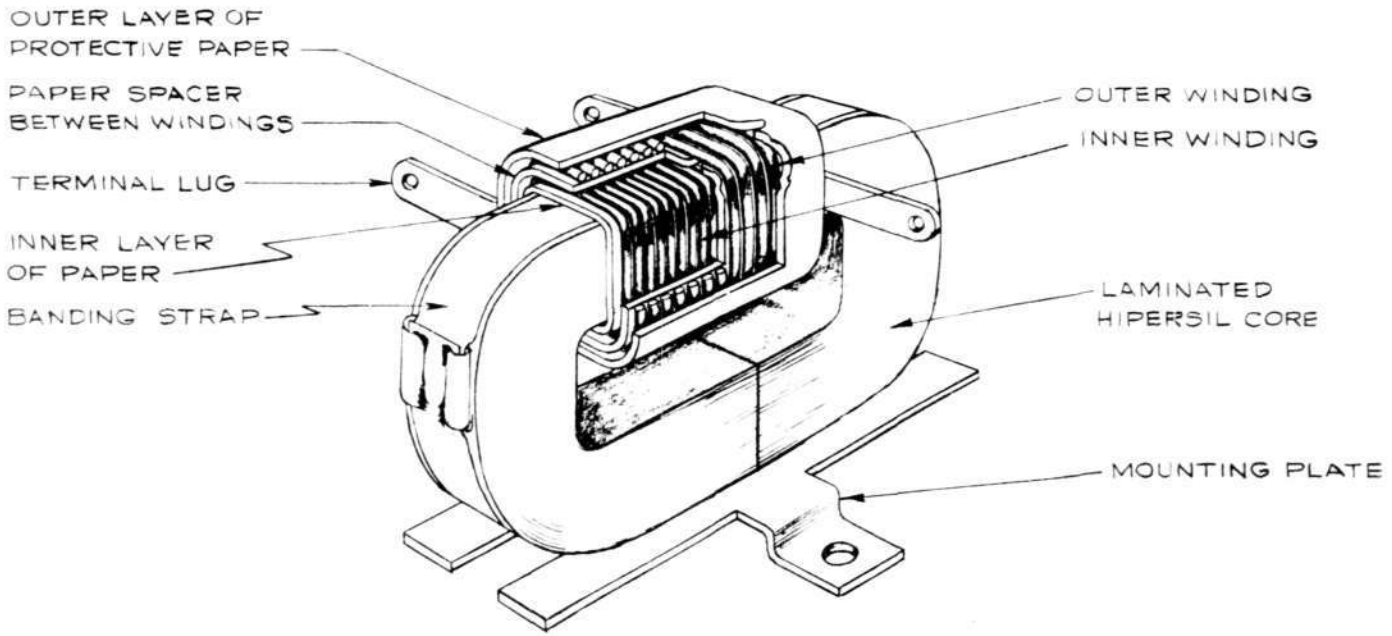

FIG. 3 CUTAWAY VIEW OF A PULSE TRANSFORMER

APPROVED FOR PUBLIC RELEASE. CASE 06-1104.

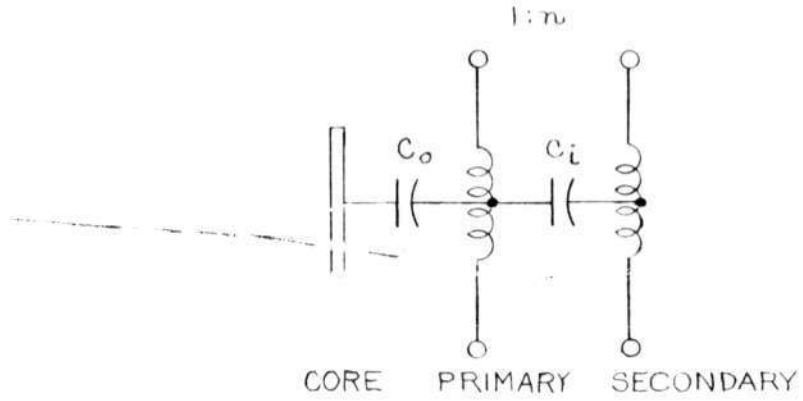

FIG 4 DIAGRAM OF A PULSE TRANSFORMER SHOWING DISTRIBUTED CAPACITANCES AS LUMPED ELEMENTS.

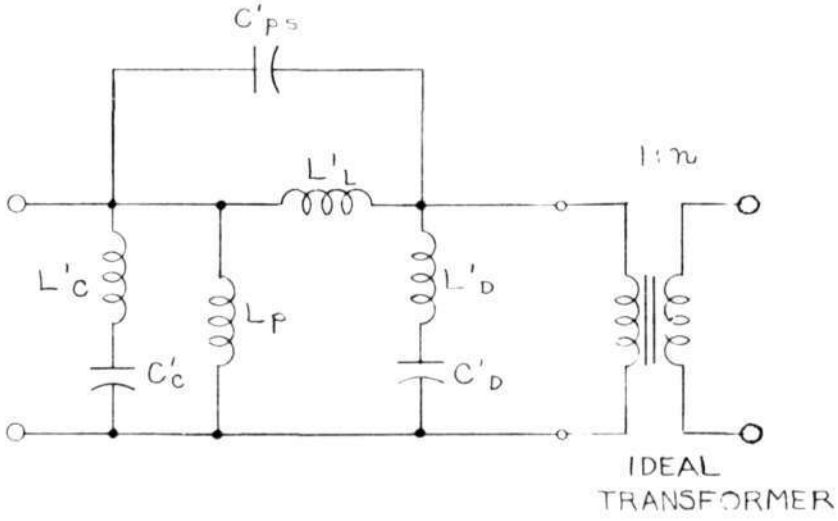

FIG. 5 EQUIVALENT CIRCUIT OF A PULSE TRANSFORMER WITH QUANTITIES REFERRED TO THE PRIMARY.

A-30632

FIGS. 4 & 5

APPROVED FOR PUBLIC RELEASE. CASE 06-1104.

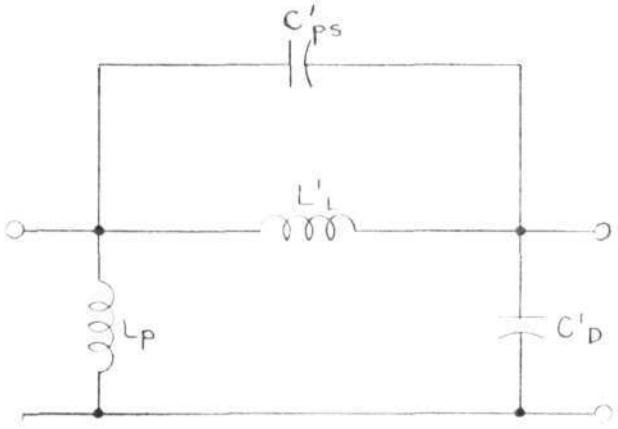

FIG. 6 SIMPLIFIED EQUIVALENT CIRCUIT OF A PULSE TRANSFORMER

A-30623

APPROVED FOR PUBLIC RELEASE. CASE 06-1104.

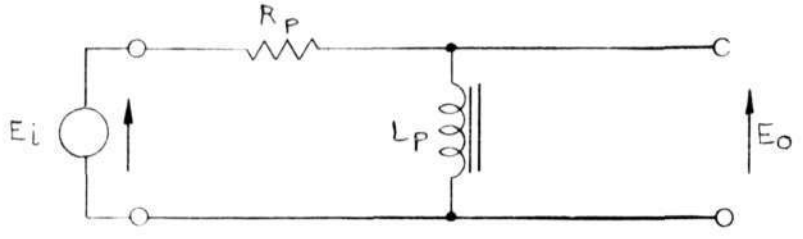

FIG. 7. CIRCUIT FOR MEASURING CHARACTERISTICS OF CORE.

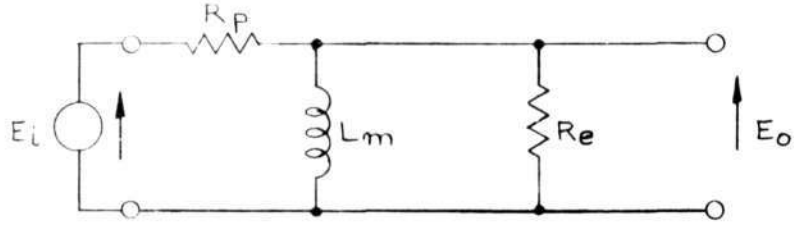

FIG. 8 PROPOSED EQUIVALENT CIRCUIT OF FIG. 7

FIGS. 7 & 8

A-3142-34

APPROVED FOR PUBLIC RELEASE. CASE 06-1104.

A-30760

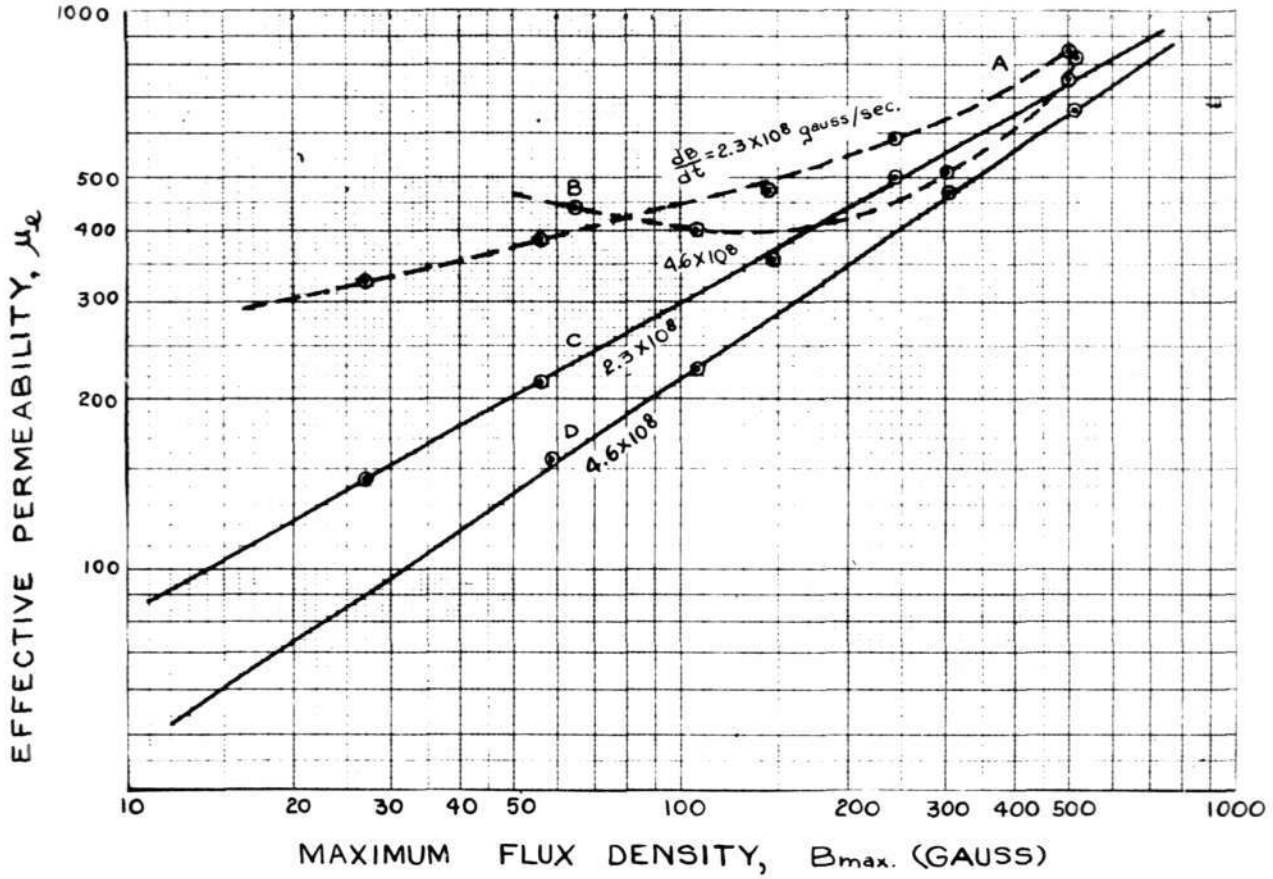

FIG. 9. EFFECTIVE PERMEABILITY OF 2-MIL HIPERSIL CORES (CALCULATED FROM EXPERIMENTAL PULSE RESPONSE) PLOTTED AGAINST MAXIMUM FLUX DENSITY. DATA 2TW 149

APPROVED FOR PUBLIC RELEASE. CASE 06-1104.

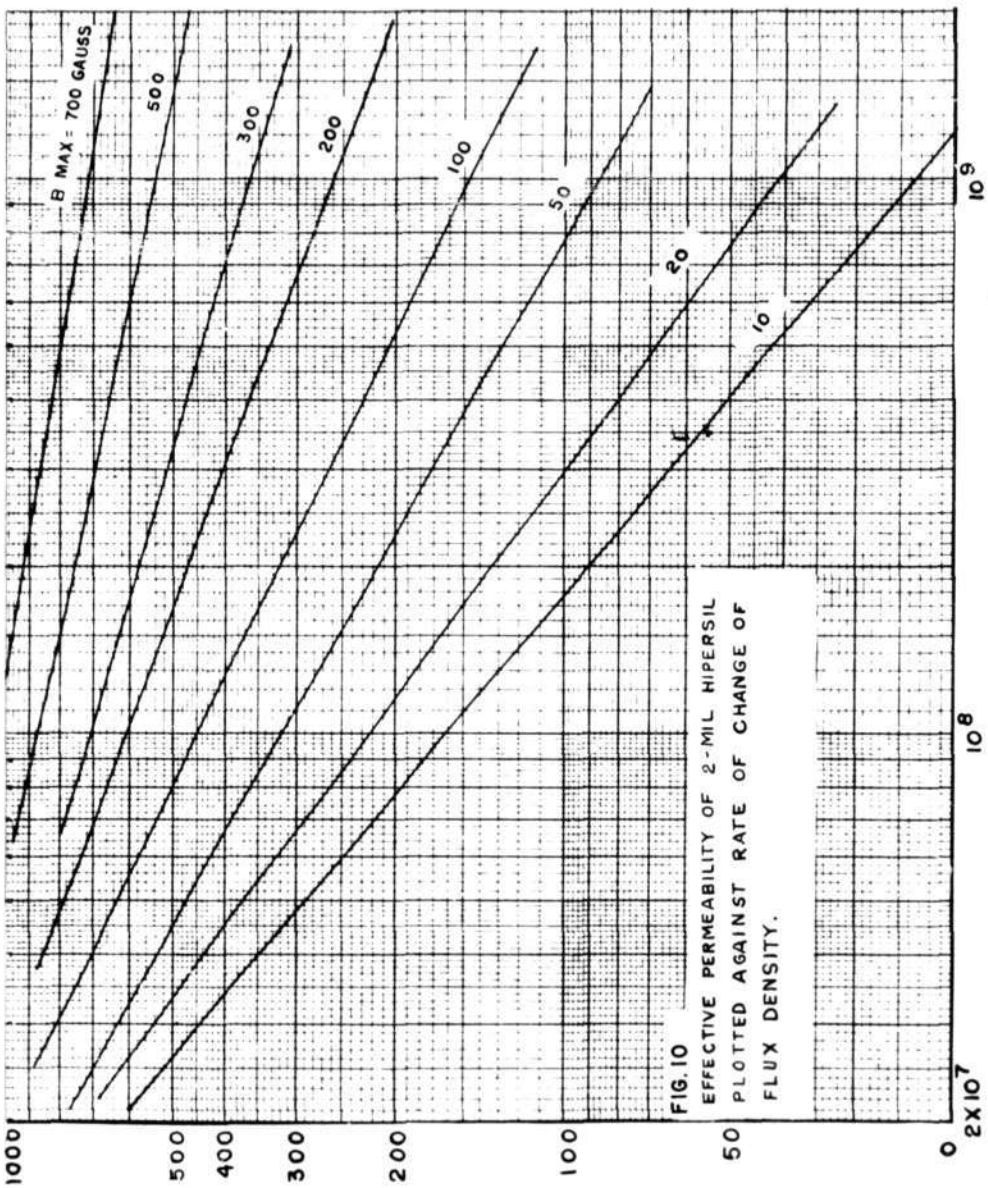

FIG. 10
EFFECTIVE PERMEABILITY OF 2-MIL HIPERSIL PLOTTED AGAINST RATE OF CHANGE OF FLUX DENSITY.

A-30761

A-30762

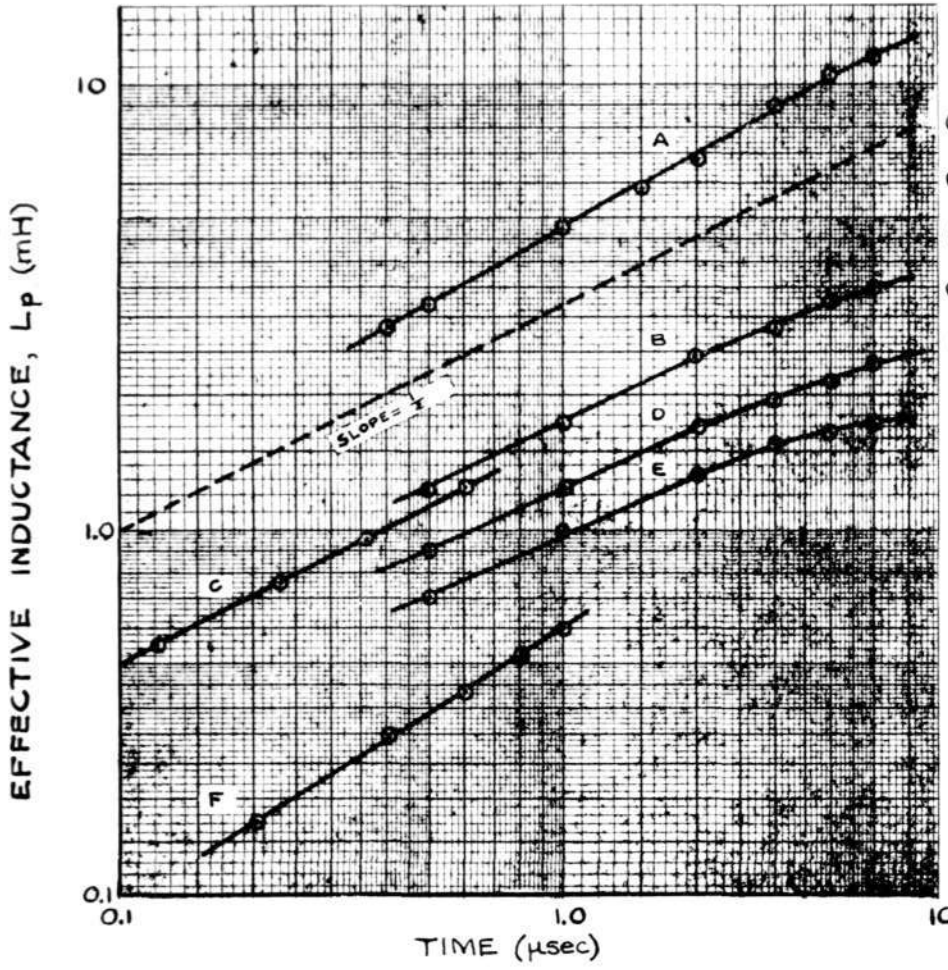

(A) 2-MIL HIPERSIL, N=80, CROSS SECTION $\frac{1}{4}$" X $\frac{1}{4}$". R_p = 3000 OHMS DATA - 2TFW 76

(B) 1-MIL HIPERSIL, N=70, CROSS SECTION $\frac{1}{4}$" X $\frac{3}{16}$". R_p = 2600 OHMS DATA 2TFW 136

(C) 1-MIL HIPERSIL, N=70, CROSS SECTION $\frac{1}{4}$" X $\frac{3}{16}$". R_p = 1050 OHMS DATA 2TFW 142

(D) 1-MIL HIPERSIL, N=70, CROSS SECTION $\frac{1}{4}$" X $\frac{3}{16}$" R_p = 580 OHMS DATA 2TFW 136

(E) BACKSWING DECAY FOR 5 μsec. PULSE OF D DATA 2TFW 136

(F) 2-MIL HIPERSIL, N=48, CROSS SECTION $\frac{1}{4}$" X $\frac{1}{8}$" R_p = 430 OHMS DATA 2TFW 105

FIG. 11 EFFECTIVE INDUCTANC VS. TIME FOR WINDING ON HIPERSIL CORES.

APPROVED FOR PUBLIC RELEASE. CASE 06-1104.

APPROVED FOR PUBLIC RELEASE. CASE 06-1104.

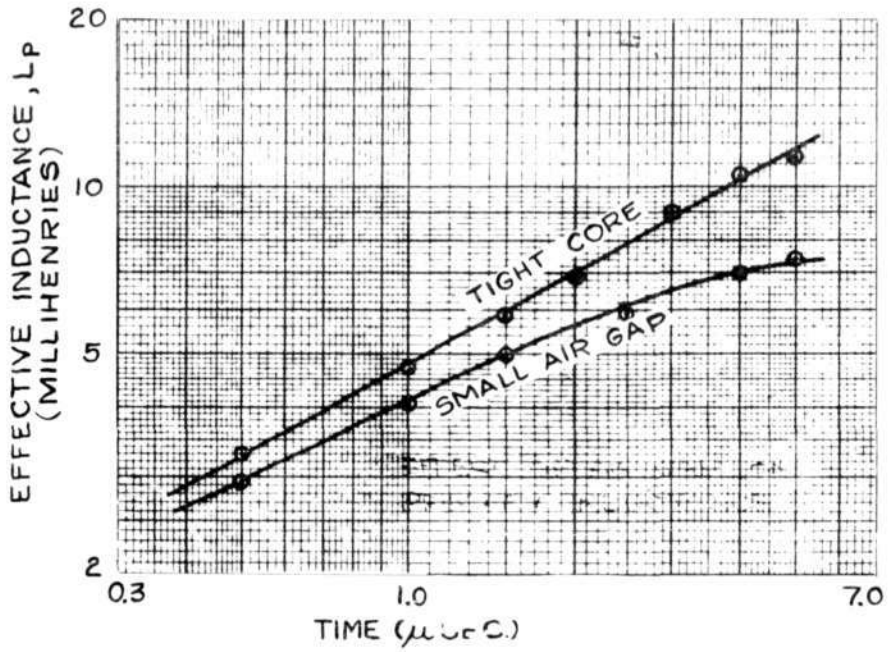

FIG. 12 EFFECT OF AIR GAP ON PRIMARY INDUCTANCE

DATA CALCULATED FROM WAVEFORMS IN 2TFW56; PULSE TRANSFORMER USED WAS T17 WITH $R_P = 3000\Omega$.

A-30763

APPROVED FOR PUBLIC RELEASE. CASE 06-1104.

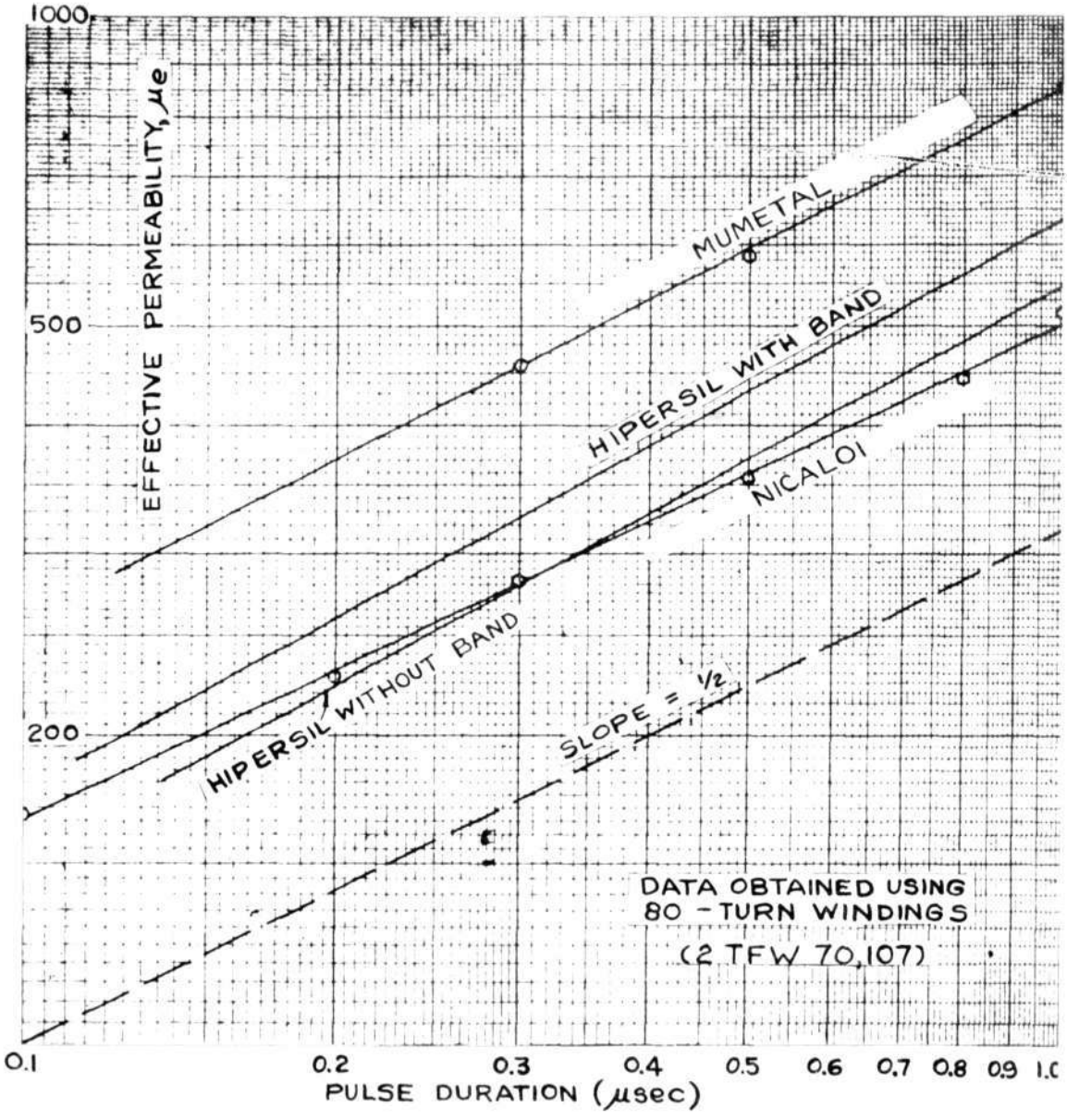

FIG. 13 EFFECTIVE PERMEABILITY vs. PULSE DURATION FOR THREE DIFFERENT CORES

A-30764

APPROVED FOR PUBLIC RELEASE. CASE 06-1104.

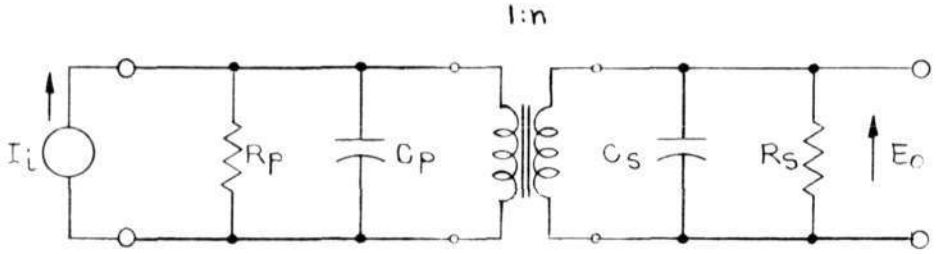

FIG. 14 GENERAL PULSE TRANSFORMER CIRCUIT

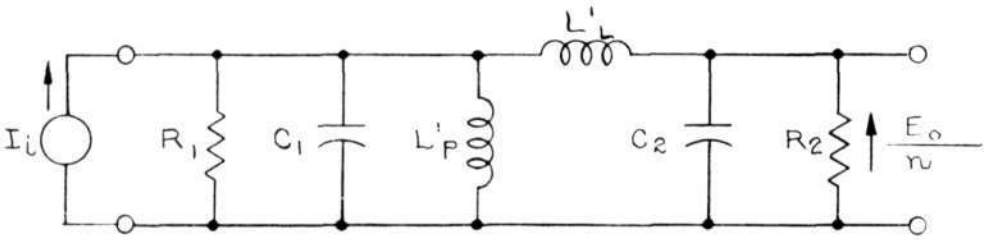

FIG. 15 AN EQUIVALENT CIRCUIT FOR FREQUENCY ANALYSIS OF THE CIRCUIT IN FIG 14.

FIGS. 14 & 15

A-30635

APPROVED FOR PUBLIC RELEASE. CASE 06-1104.

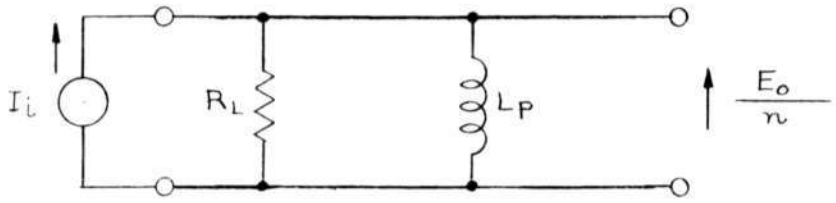

FIG. 16. EQUIVALENT CIRCUIT FOR FREQUENCIES BELOW THE BAND CENTER OF THE CIRCUIT IN FIG. 15.

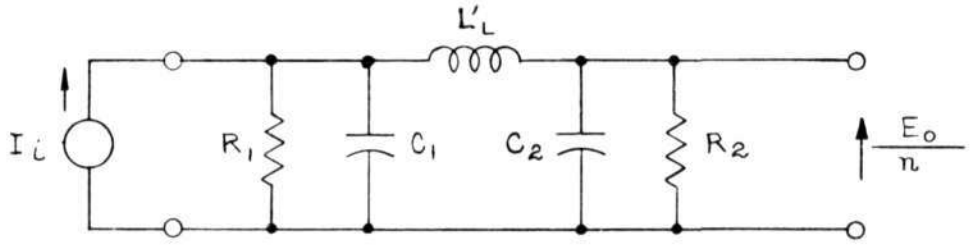

FIG. 17. EQUIVALENT CIRCUIT FOR FREQUENCIES ABOVE MID-BAND OF CIRCUIT IN FIG. 15.

FIGS. 16 & 17

A-30636

APPROVED FOR PUBLIC RELEASE. CASE 06-1104.

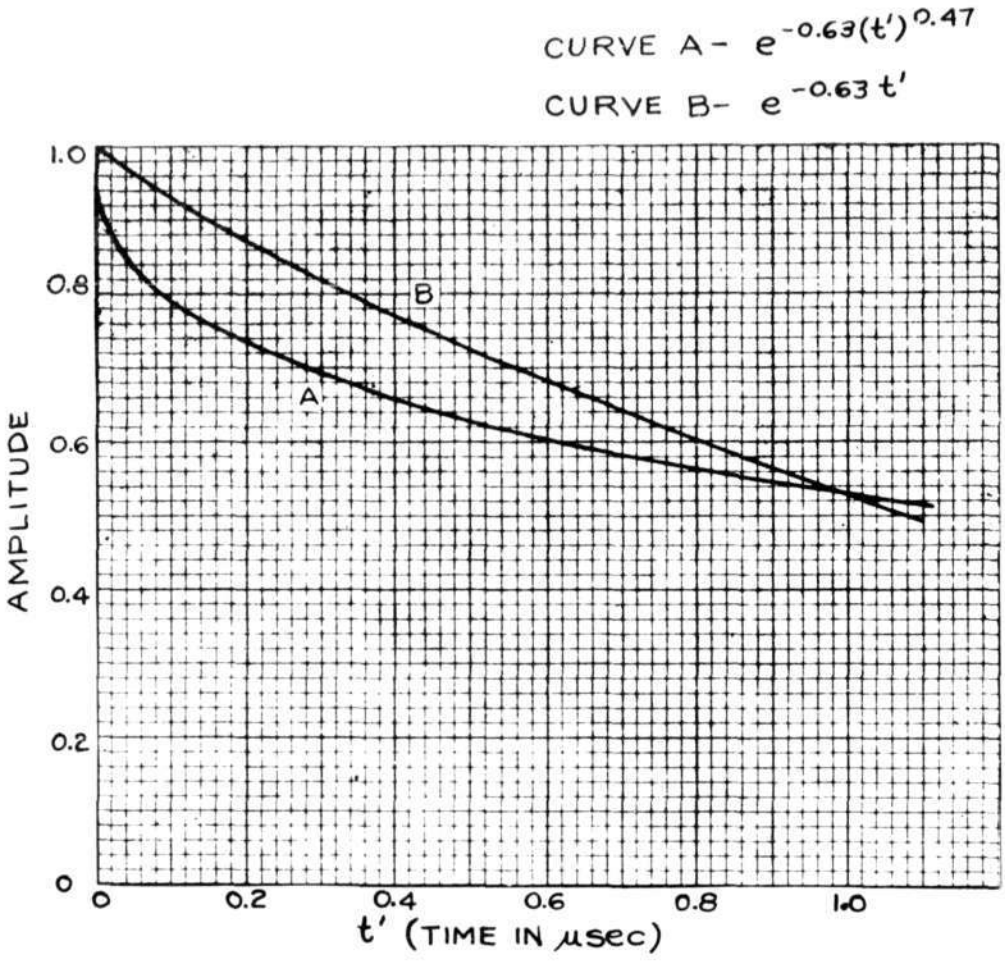

FIG. 18 COMPARISON OF AMPLITUDE DECAY OF A COIL WITH HIPERSIL CORE (CURVE A) WITH ORDINARY EXPONENTIAL DECAY (CURVE B). THE FORMER CHECKS WITH THE ACTUAL PRIMARY INDUCTANCE RESPONSE SHOWN IN PHOTOGRAPH F-6-8, FIG. 54.

A-30765

APPROVED FOR PUBLIC RELEASE. CASE 06-1104.

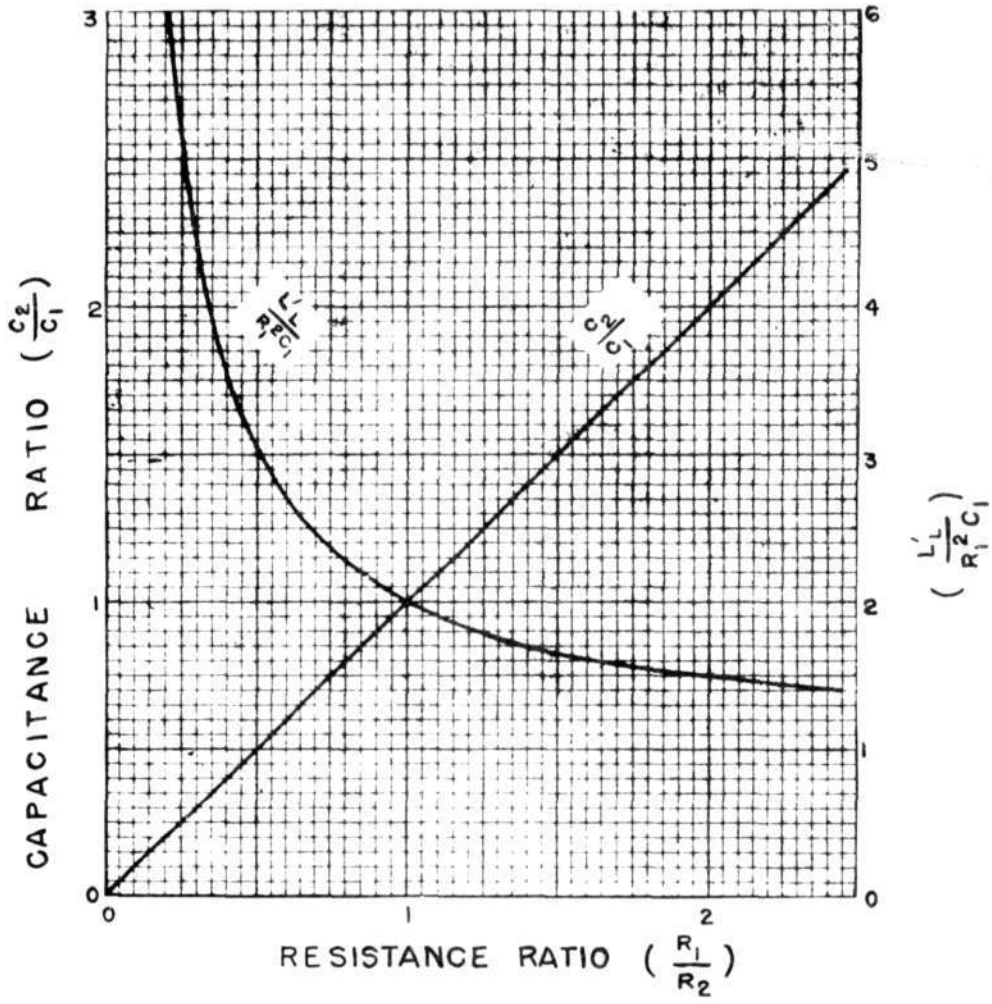

FIG. 19 FIRST SOLUTION FOR TRANSITIONAL RESPONSE OF EQUIVALENT CIRCUIT IN FIG. 17. CAPACITANCE RATIO $(\frac{C_2}{C_1})$ AND $(\frac{L'_L}{R_1^2 C_1})$ PLOTTED AGAINST RESISTANCE RATIO $(\frac{R_1}{R_2})$.

A-30766

APPROVED FOR PUBLIC RELEASE. CASE 06-1104.

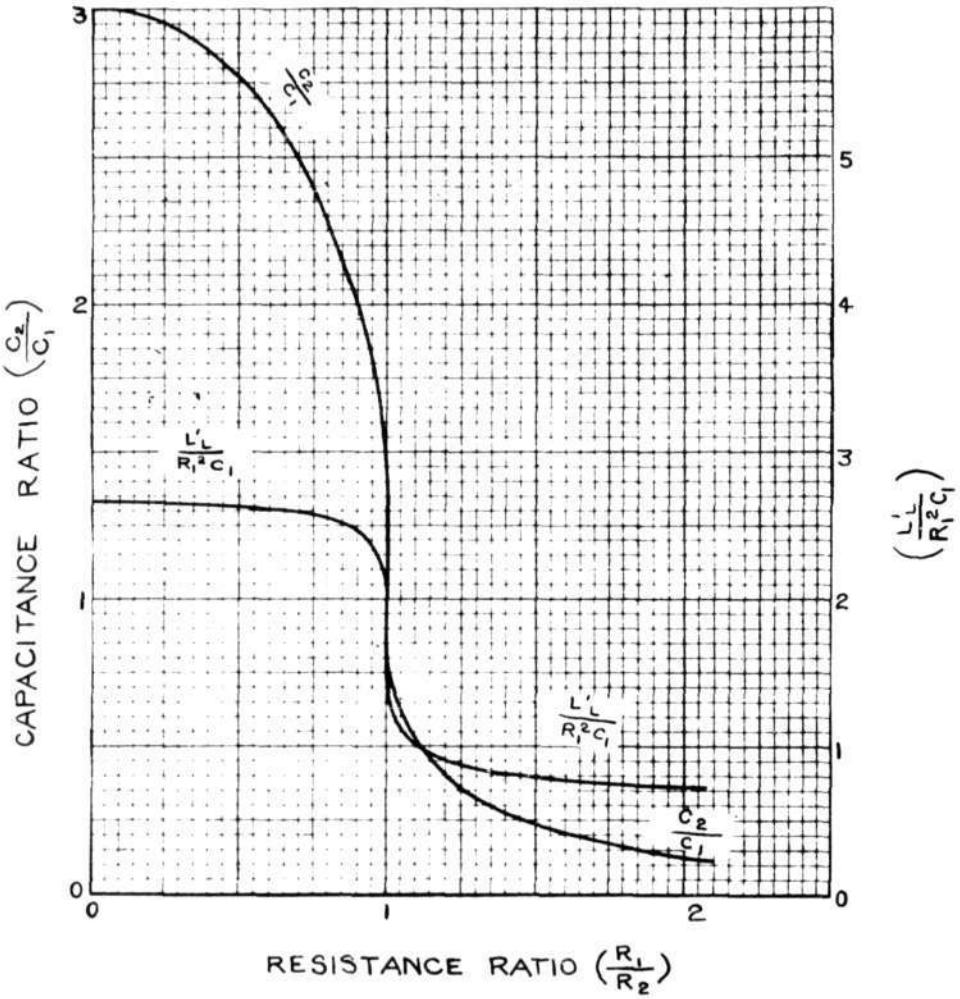

FIG. 20 SECOND SOLUTION FOR TRANSITIONAL RESPONSE OF EQUIVALENT CIRCUIT IN FIG. 17. CAPACITANCE RATIO $\left(\frac{C_2}{C_1}\right)$ AND $\left(\frac{L'_L}{R_1^2 C_1}\right)$ PLOTTED AGAINST RESISTANCE RATIO $\left(\frac{R_1}{R_2}\right)$

A-30767

APPROVED FOR PUBLIC RELEASE. CASE 06-1104.

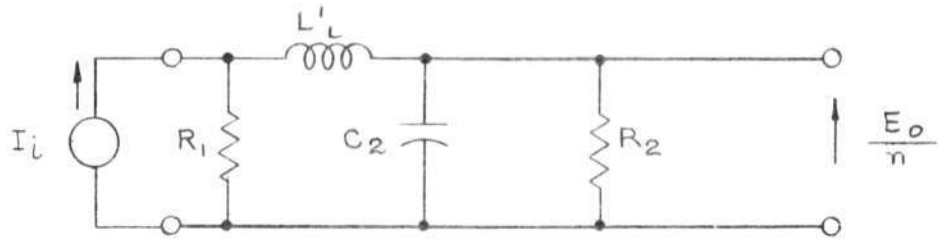

FIG. 21 HIGH FREQUENCY EQUIVALENT CIRCUIT IF C_1 IS NEGLIGIBLE.

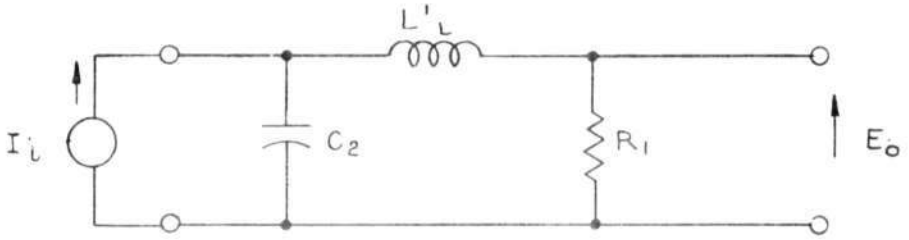

FIG. 22. CIRCUIT WHICH HAS RESPONSE CHARACTERISTICS SIMILAR TO THOSE OF FIG. 21.

FIGS. 21 & 22

A-30[illegible]

APPROVED FOR PUBLIC RELEASE. CASE 06-1104.

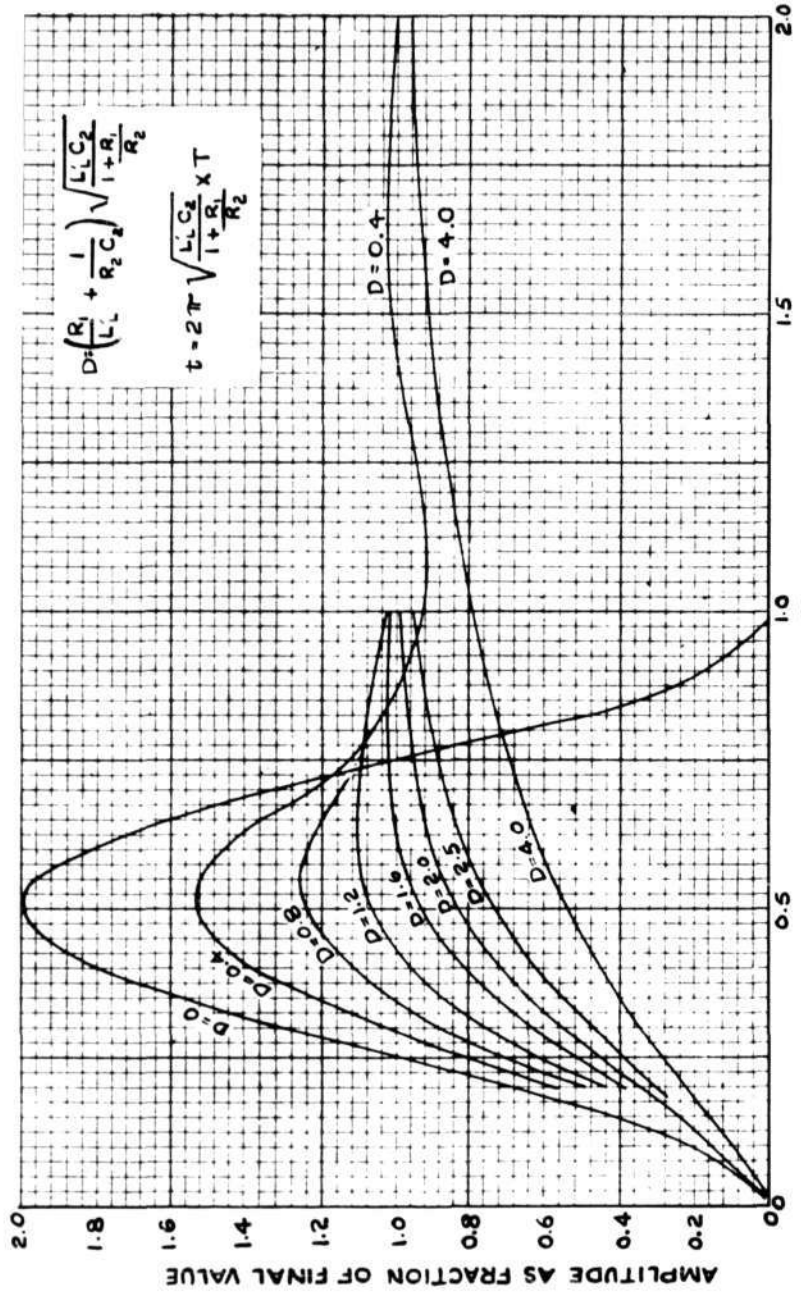

FIG.23 STEP-FUNCTION RESPONSE OF CIRCUIT IN FIG. 21

A-30768

APPROVED FOR PUBLIC RELEASE. CASE 06-1104.

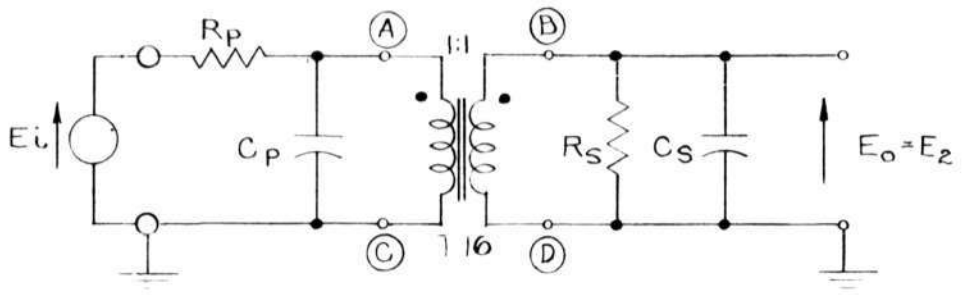

FIG. 24 T16 AS A NON-INVERTER.

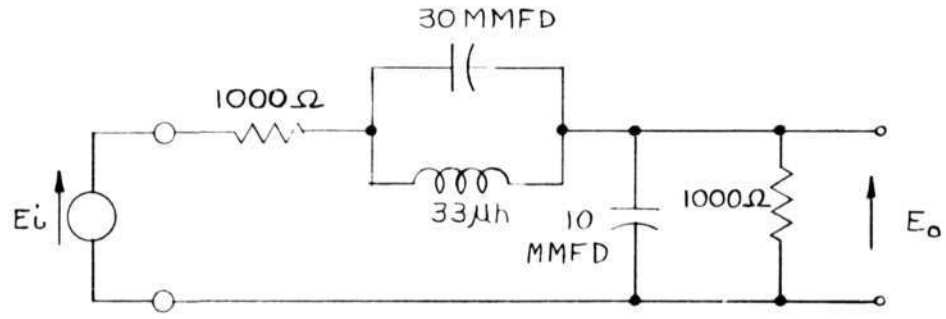

FIG. 25 AN EQUIVALENT CIRCUIT OF FIG. 24 ACCORDING TO SEC. 3.2.

FIGS. 24 & 25

A-30638

APPROVED FOR PUBLIC RELEASE. CASE 06-1104.

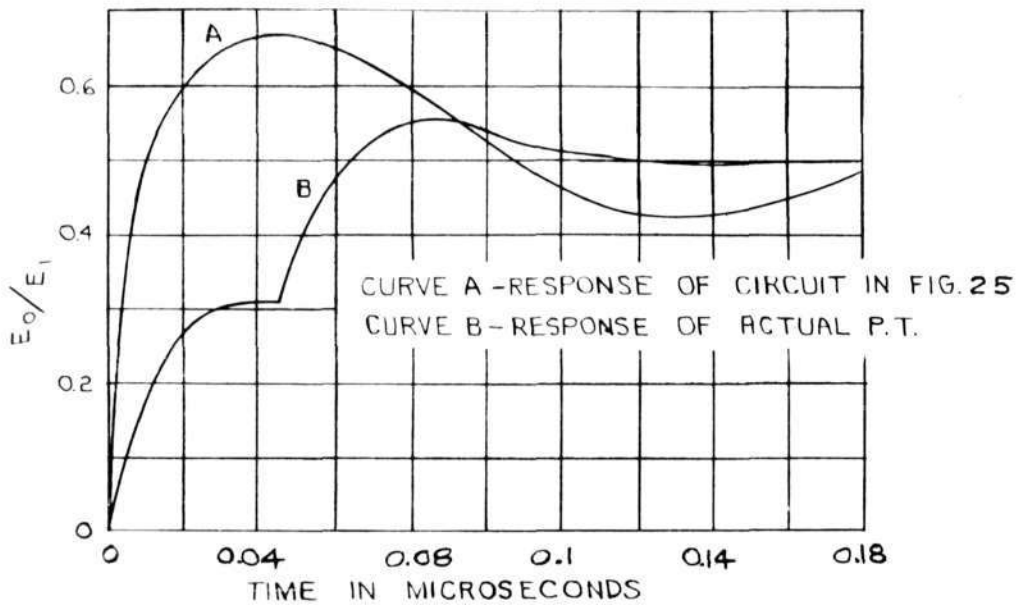

FIG 26 COMPARISON OF OBSERVED RESPONSE OF A NON-INVERTING PULSE TRANSFORMER WITH CALCULATED TRANSIENT RESPONSE OF ITS LUMPED-PARAMETER EQUIVALENT CIRCUIT.

A-30639

APPROVED FOR PUBLIC RELEASE. CASE 06-1104.

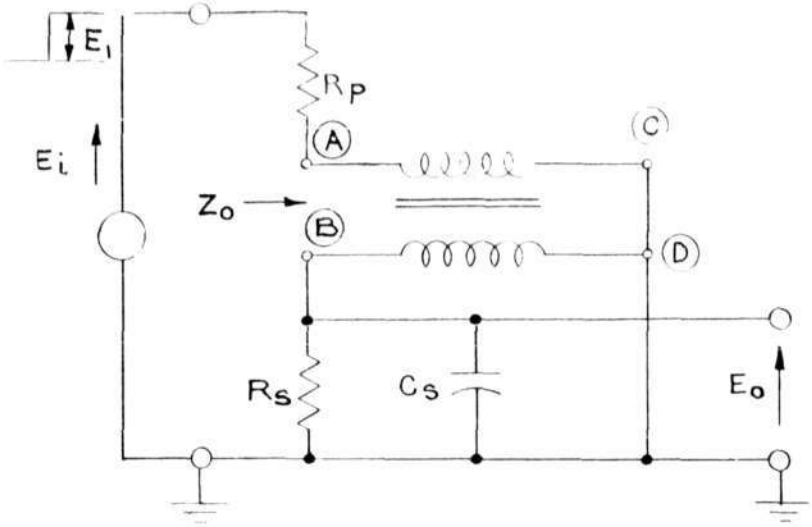

FIG. 27. CIRCUIT OF FIG. 24 REDRAWN TO ILLUSTRATE DELAY LINE EFFECT.

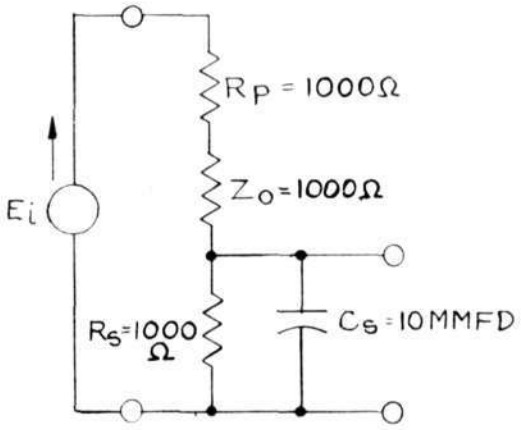

FIG. 28 EQUIVALENT CIRCUIT OF FIG. 27 UNTIL THE FIRST REFLECTION RETURNS TO INPUT TERMINALS.

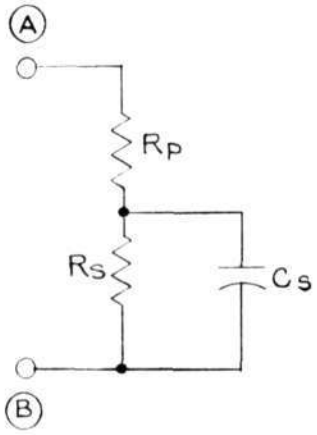

FIG. 29 TERMINATION OF PULSE TRANSFORMER DELAY LINE AT END A B.

A-30640

FIGS. 27, 28, & 29

APPROVED FOR PUBLIC RELEASE. CASE 06-1104.

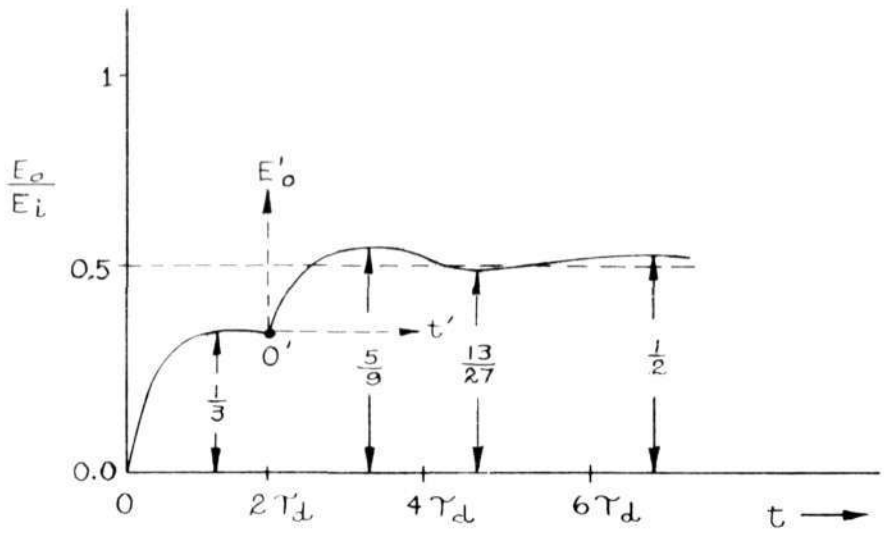

FIG. 30. CALCULATED RESPONSE OF THE CIRCUIT OF FIG. 24 BY DELAY-LINE METHOD.

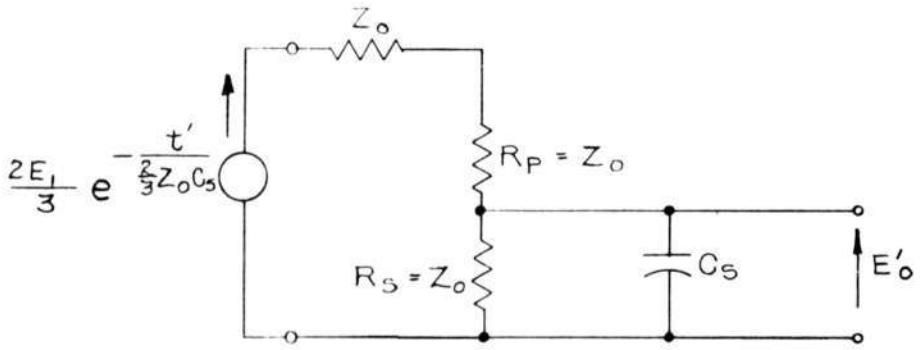

FIG. 31 CIRCUIT FOR CALCULATING WAVE FORM OF SECOND STEP IN RESPONSE CURVE SHOWN IN FIG. 30

FIGS. 30 & 31

A 30641

APPROVED FOR PUBLIC RELEASE. CASE 06-1104.

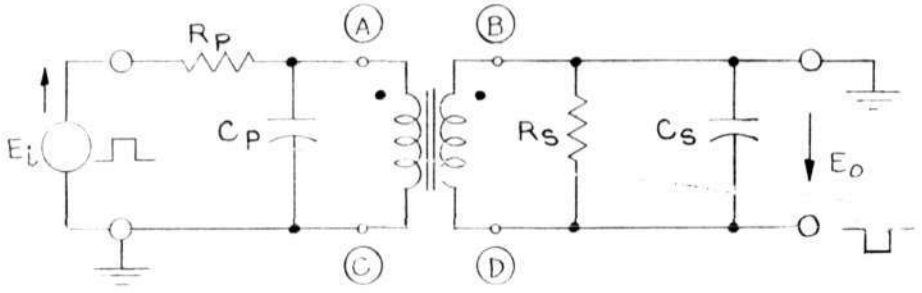

FIG.32 PULSE TRANSFORMER CONNECTED TO ACT AS A PHASE INVERTER.

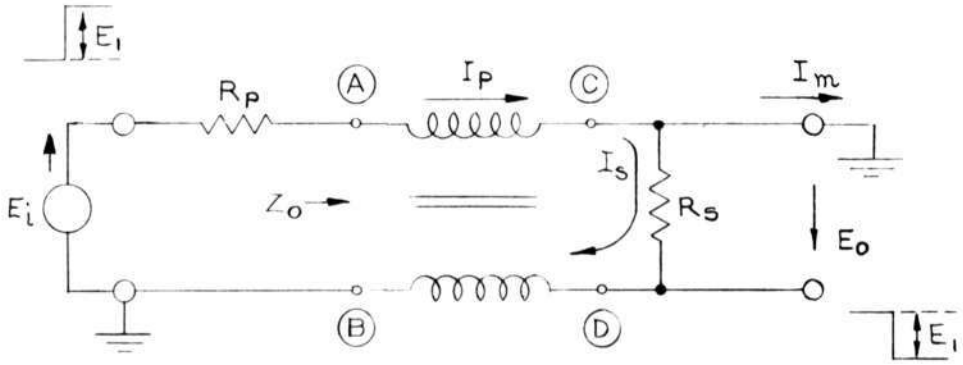

FIG.33 PHASE-INVERTER CIRCUIT REDRAWN TO SHOW DELAY LINE EFFECT. (CAPACITANCES OMITTED)

FIGS. 32 & 33

A-30642

APPROVED FOR PUBLIC RELEASE. CASE 06-1104.

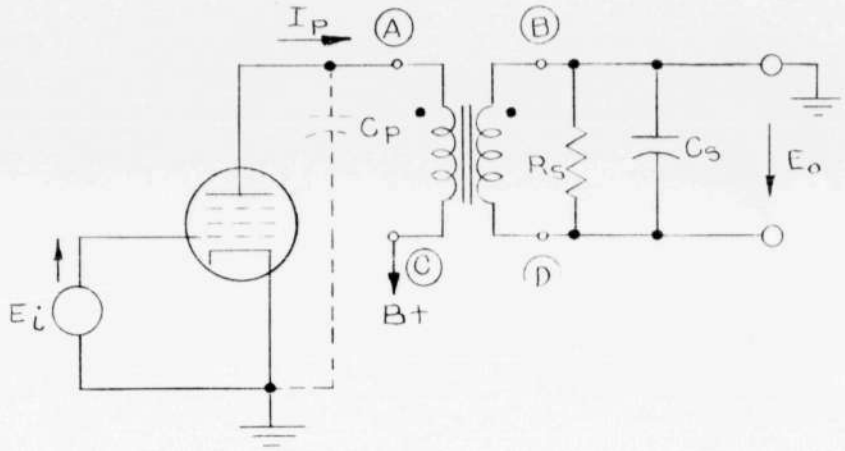

FIG. 34. PHASE-INVERTER CIRCUIT SHOWING DRIVER TUBE.

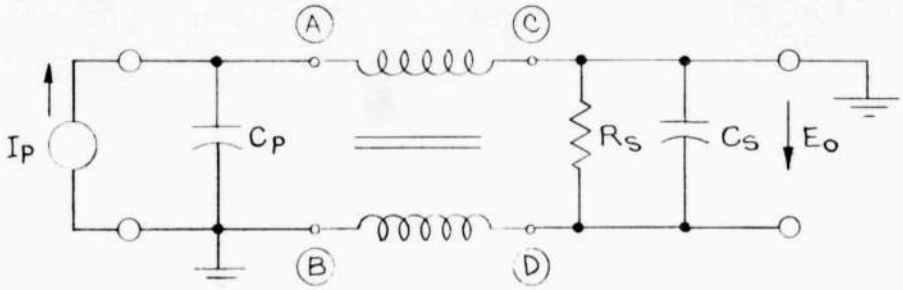

FIG. 35. "DELAY LINE" EQUIVALENT CIRCUIT OF FIG. 34.

FIGS. 34 & 35

A-30643

APPROVED FOR PUBLIC RELEASE. CASE 06-1104.

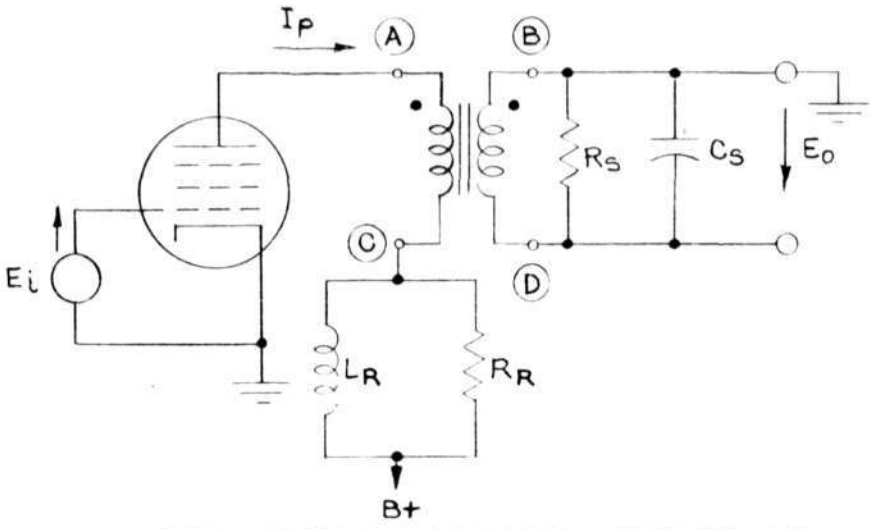

FIG. 36 PHASE-INVERTER CIRCUIT OF FIG. 34 WITH COMPENSATING CIRCUIT.

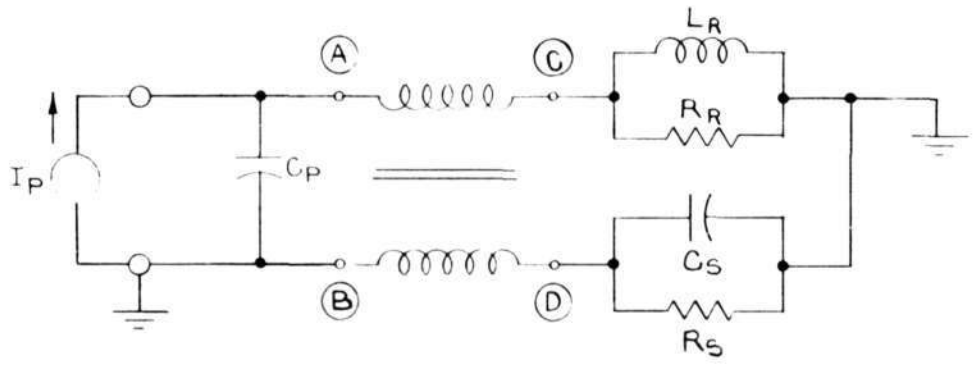

FIG. 37. "DELAY LINE" EQUIVALENT CIRCUIT OF FIG. 36.

A-30644

FIGS. 36 & 37

APPROVED FOR PUBLIC RELEASE. CASE 06-1104.

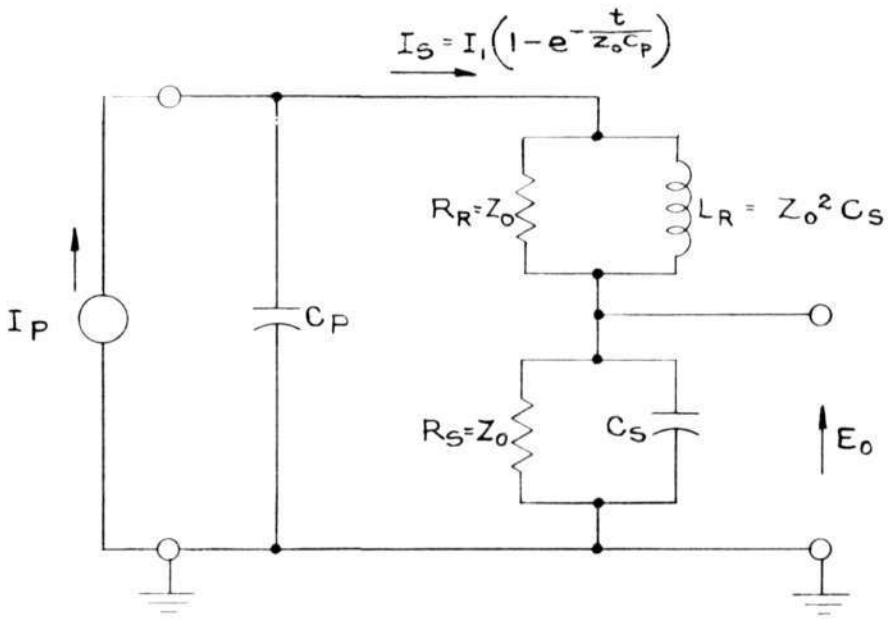

FIG. 38. EQUIVALENT CIRCUIT OF FIG. 37 FOR CALCULATING OUTPUT WAVEFORM WHEN ELEMENTS ARE PROPERLY ADJUSTED.

A-30645

APPROVED FOR PUBLIC RELEASE. CASE 06-1104.

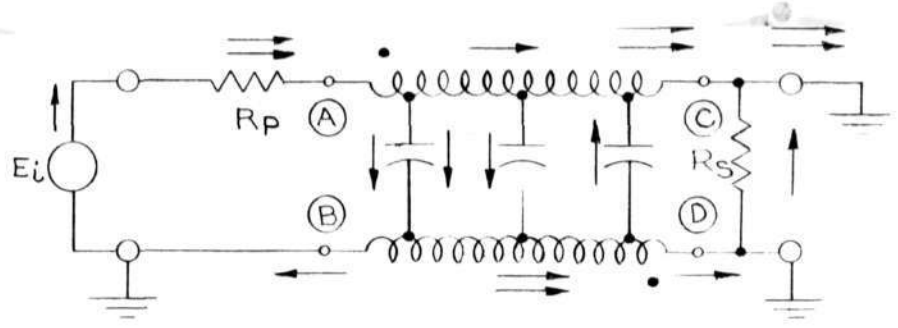

FIG 39. CURRENT DISTRIBUTION IMMEDIATELY AFTER INPUT PULSE IS INTRODUCED.

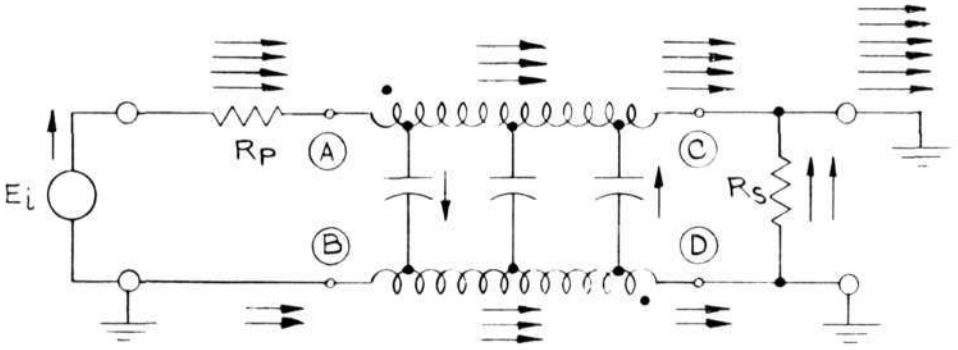

FIG. 40 CURRENT DISTRIBUTION A SHORT TIME AFTER THAT OF FIG 39.

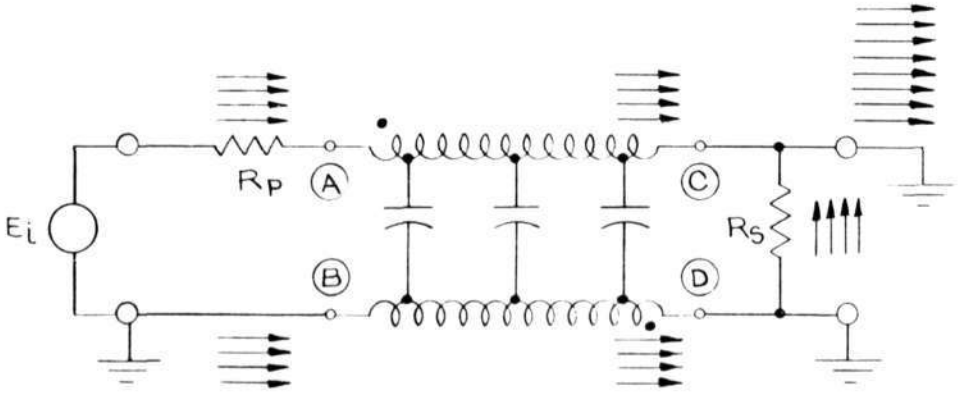

FIG 41. QUASI-STEADY-STATE CURRENTS

FIGS. 39, 40, & 41

A-30646

APPROVED FOR PUBLIC RELEASE. CASE 06-1104.

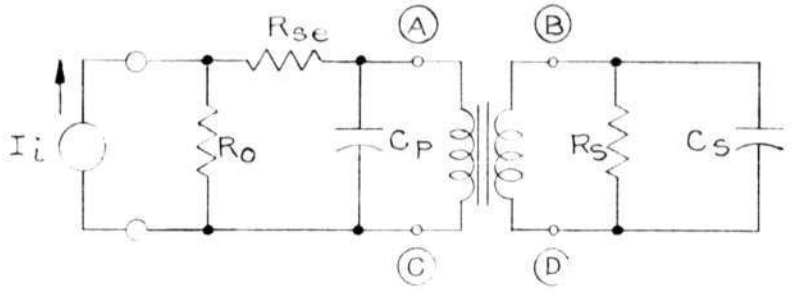

FIG. 42. EXPERIMENTAL CIRCUIT USED IN OBTAINING WAVEFORMS SHOWN IN OSCILLOSCOPE PHOTOGRAPHS. I_i REPRESENTS PULSED PLATE CURRENT FROM A PENTODE (6AG7).

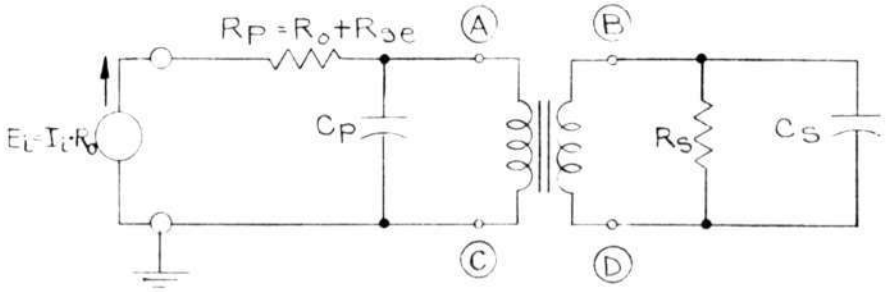

FIG. 43. CIRCUIT OF FIG. 59 WITH CURRENT SOURCE CONVERTED TO A VOLTAGE SOURCE FOR CONVENIENCE IN DISCUSSION.

FIGS. 42 & 43

1-30647

APPROVED FOR PUBLIC RELEASE. CASE 06-1104.

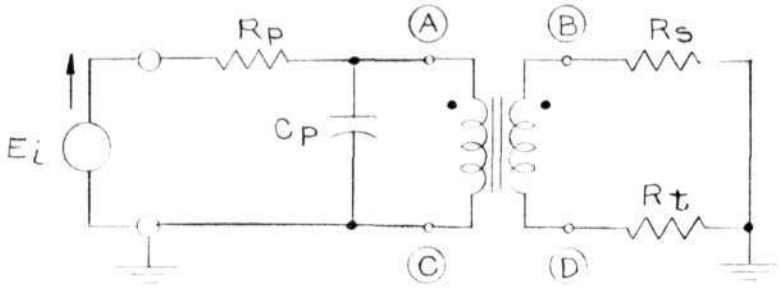

FIG 44 PULSE TRANSFORMER ACTING TO PRODUCE TWO PHASES SIMULTANEOUSLY. (POSITIVE PHASE AT (B), NEGATIVE AT (D).)

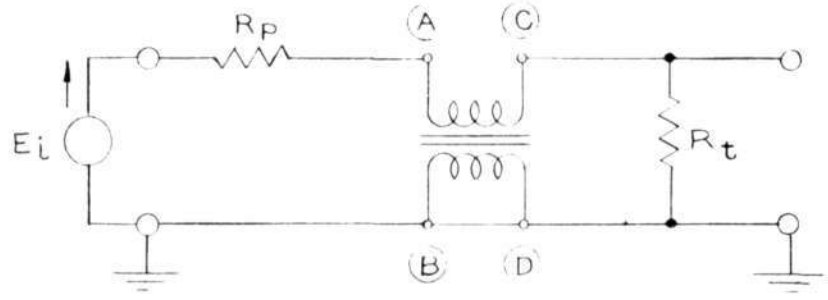

FIG 45 CIRCUIT USED FOR MEASURING CHARACTERISTIC IMPEDANCE

-30648

FIGS. 44 & 45

APPROVED FOR PUBLIC RELEASE. CASE 06-1104.

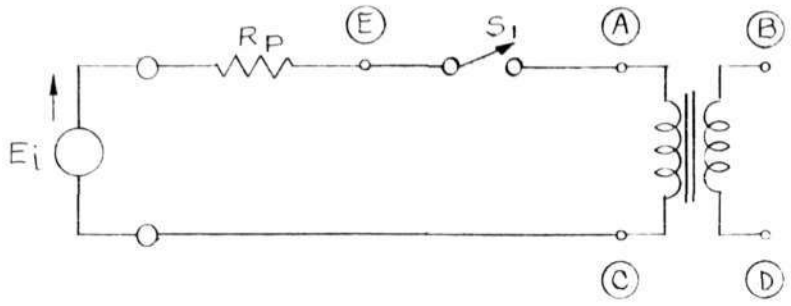

FIG. 46. EXPERIMENTAL CIRCUIT FOR MEASURING WINDING INDUCTANCE

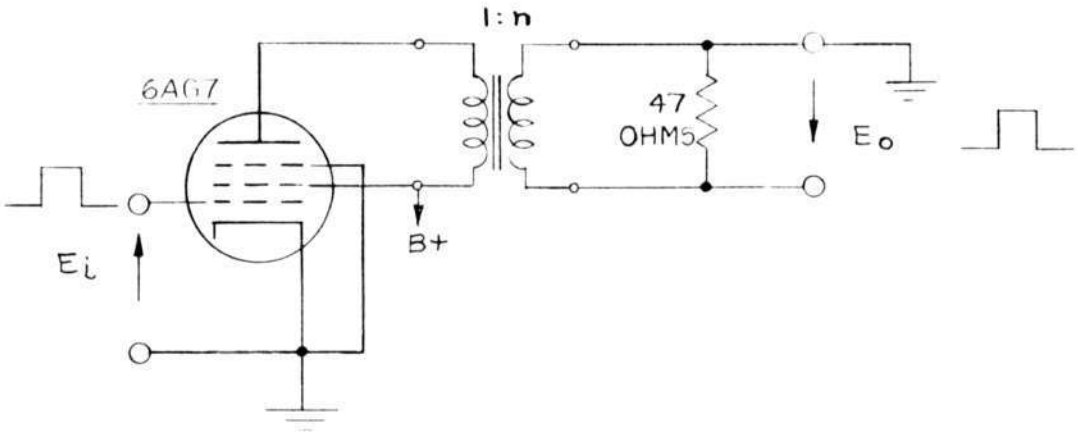

FIG. 47. PULSE TRANSFORMER IN THE PLATE CIRCUIT OF A PENTODE FOR DRIVING A 47-OHM LOAD.

1-30649

FIGS. 46 & 47

APPROVED FOR PUBLIC RELEASE. CASE 06-1104.

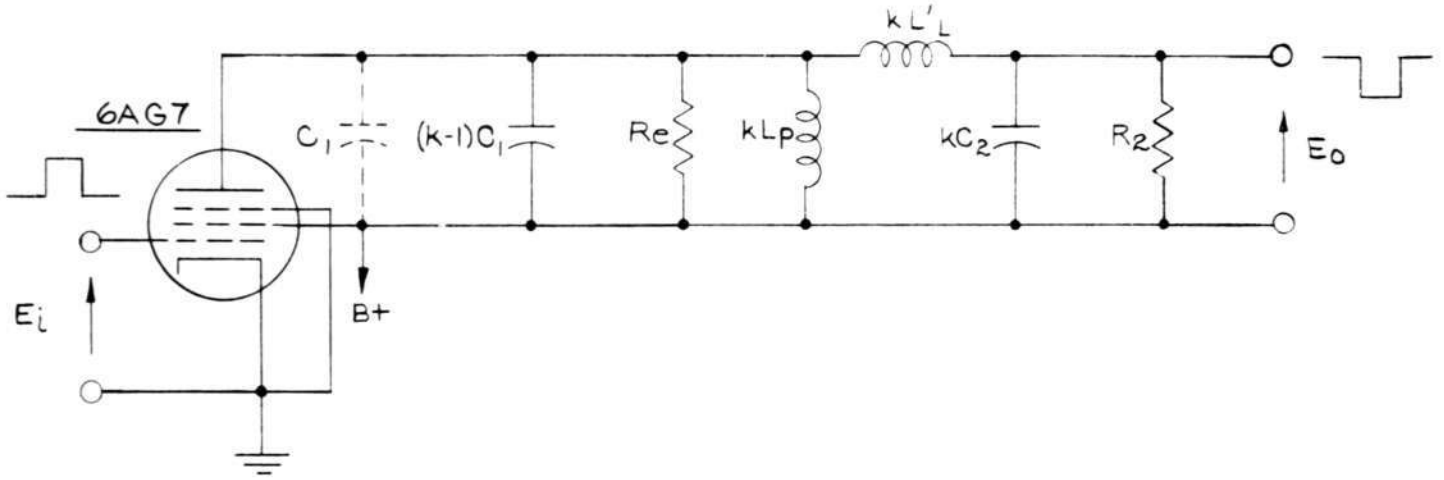

FIG. 48. EXPERIMENTAL CIRCUIT FOR TESTING LOW-FREQUENCY ANALOGUES OF EQUIVALENT CIRCUITS.

APPROVED FOR PUBLIC RELEASE. CASE 06-1104.

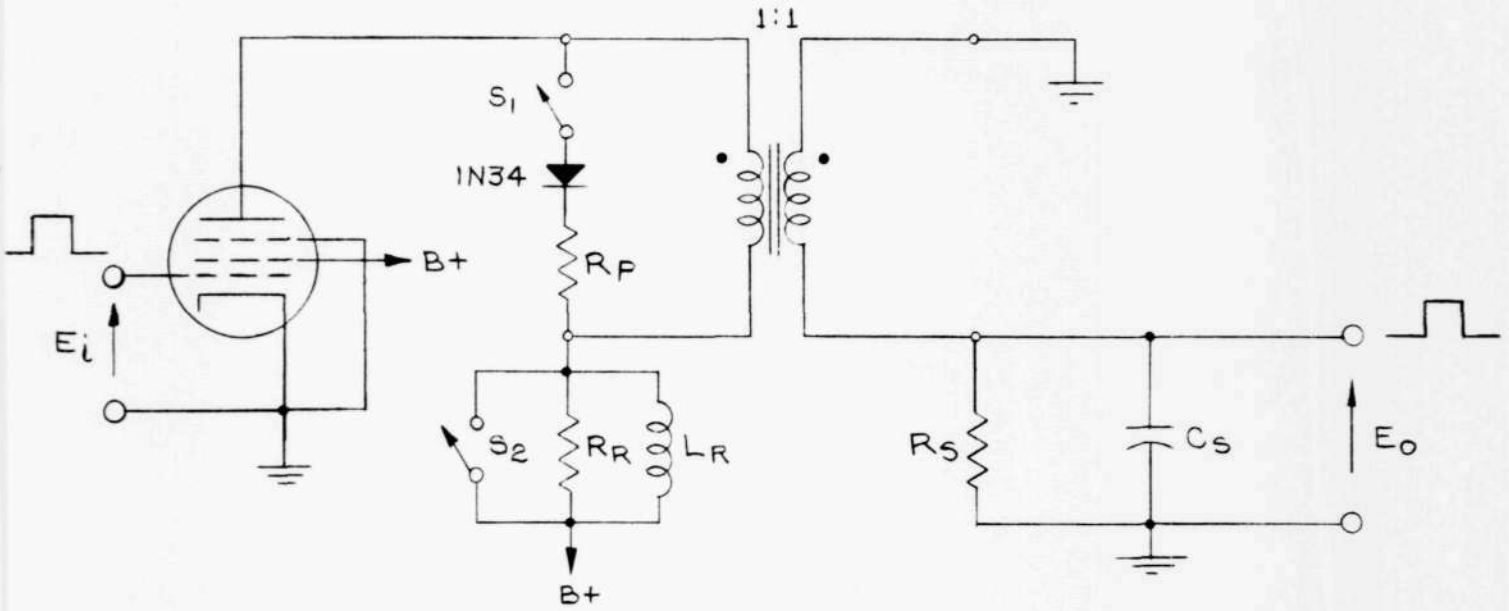

FIG. 49 EXPERIMENTAL CIRCUIT FOR DEMONSTRATING THE EFFECT OF L_R-R_R COMPENSATING NETWORK AND CRYSTAL-DIODE CLIPPING IN THE PRIMARY OF A PHASE-INVERTING PULSE TRANSFORMER

APPROVED FOR PUBLIC RELEASE. CASE 06-1104.

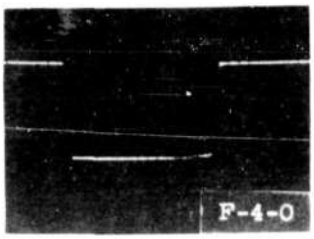

QUARTER-MICROSECOND INPUT PULSE USED FOR PHOTOS IN F-4 AND F-5 SERIES. RISE TIME ABOUT 0.005 MICROSECONDS

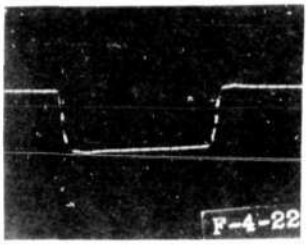

WAVEFORM AT "A", FIG. 43; T16. (R_p = 1100 OHMS, $R_s = R_t$ = 1000 OHMS)

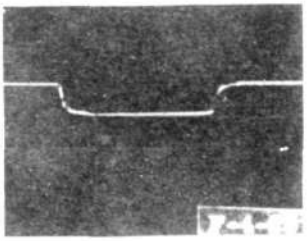

WAVEFORM AT "B", SAME CIRCUIT AS FOR F-4-22

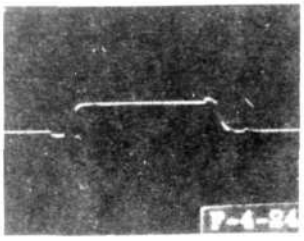

WAVEFORM AT "D" SAME CIRCUIT AS FOR F-4-22

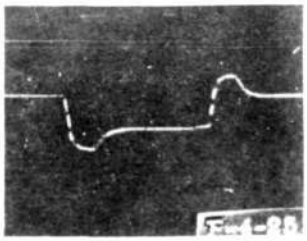

WAVEFORM AT "A", FIG. 43; T16. (R_p = 1100 OHMS, R_t = 500 OHMS)

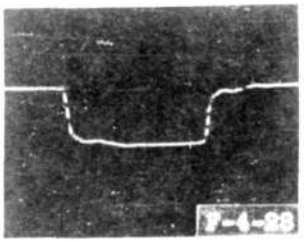

SAME AS F-4-25 EXCEPT R_t = 1500 OHMS

HORIZONTAL SCALE 0.016 MICROSECONDS PER SMALL DIVISION
VERTICAL SCALE 6.6 VOLTS PER SMALL DIVISION

FIG. 50

A-30732

APPROVED FOR PUBLIC RELEASE. CASE 06-1104.

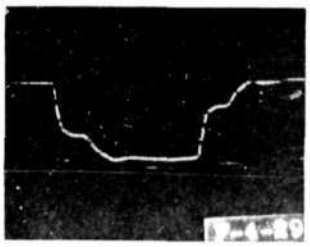

SAME AS F-4-27
EXCEPT
R_t = 4700 OHMS

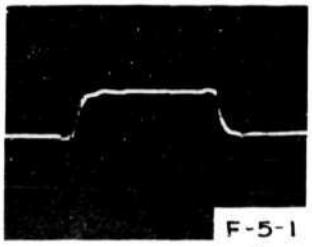

WAVEFORM AT "D",
FIG. 43, WITH "B"
GROUNDED; T16.
(R_p=1100 OHMS,
R_s=1000 OHMS)

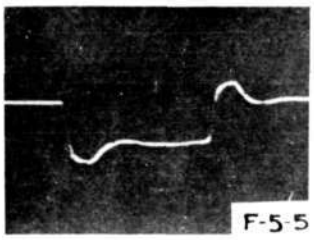

WAVEFORM AT "A",
FIG. 43, WITH "D"
GROUNDED; T16.
(R_p=1100 OHMS,
R_s=1000 OHMS)

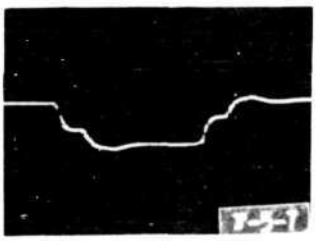

WAVEFORM AT "B",
SAME CIRCUIT
AS FOR F-5-5

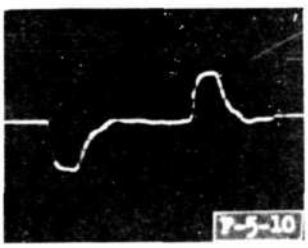

WAVEFORM AT "A,"
FIG. 43; T16.
(R_p=1100 OHMS,
R_t=0)

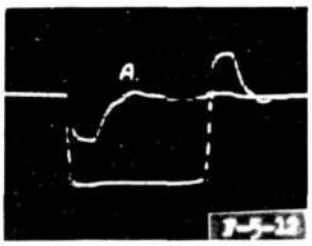

WAVEFORM ACROSS
R_o SUPERIMPOSED
ON WAVEFORM OF
F-5-10

HORIZONTAL SCALE 0.016 MICROSECONDS PER SMALL DIVISION
VERTICAL SCALE 6.6 VOLTS PER SMALL DIVISION

FIG. 51

A-30733

APPROVED FOR PUBLIC RELEASE. CASE 06-1104.

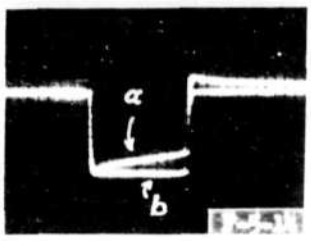

WAVEFORM AT "E",
FIG. 46; T 16.
(a) S_1 CLOSED
(b) S_1 OPEN
HORIZONTAL SCALE
0.1 μSEC. PER DIVISION

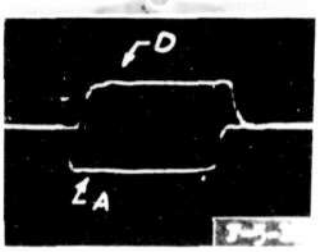

WAVEFORMS AT "A" AND "D",
"B" GROUNDED, FIG. 43; T16.
($R_p = R_s = 1200$ OHMS)

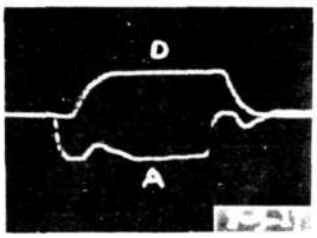

SAME AS F-5-16 EXCEPT
C_s INCREASED BY 20 MMFD

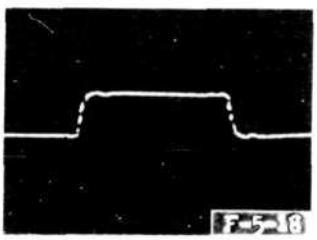

WAVEFORMS AT "D" WITH
"B" GROUNDED, FIG. 43; T 31.
(R_p = 1100 OHMS,
R_s = 1000 OHMS)

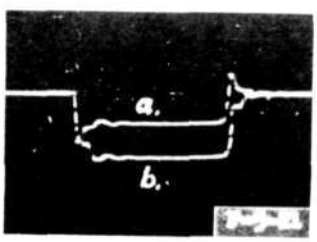

WAVEFORMS AT "A", FIG. 45;
T24, HIGH-VOLTAGE WINDING
GROUNDED. (R_p = 500 OHMS)
(a) R_t = 220 OHMS
(b) R_t = 1000 OHMS

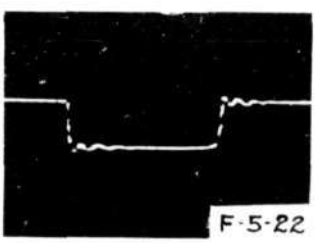

SAME AS F-5-21 EXCEPT
R_t = 470 OHMS

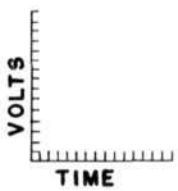

HORIZONTAL SCALE 0.016 MICROSECONDS PER SMALL DIVISION
(EXCEPT WHERE INDICATED)

VERTICAL SCALE 6.6 VOLTS PER SMALL DIVISION

FIG. 52

A-30734

APPROVED FOR PUBLIC RELEASE. CASE 06-1104.

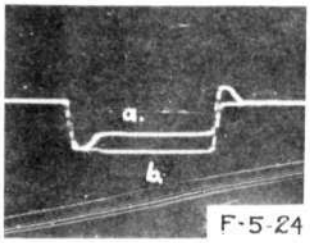

F-5-24

SAME AS F-5-21 EXCEPT LOW-VOLTAGE WINDING GROUNDED.
(a) R_t = 500 OHMS
(b) R_t = 1000 OHMS

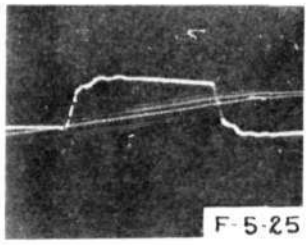

F-5-25

WAVEFORM AT "D", FIG. 43, WITH "B" GROUNDED; T 24 AS STEP-UP INVERTER.
R_p = 1100 OHMS
R_s = 2200 OHMS

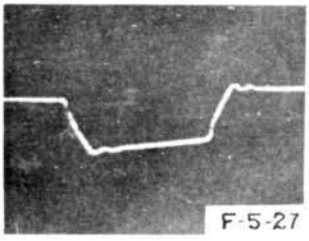

F-5-27

WAVEFORM AT "B" WITH "D" GROUNDED. SAME CIRCUIT AS FOR F-5-25; T 24.

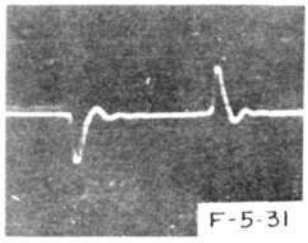

F-5-31

WAVEFORM AT "A," FIG. 45; T 24, HIGH-VOLTAGE WINDING SHORTED TO GROUND.

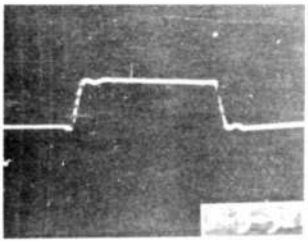

WAVEFORM AT "D", FIG. 44; T 24.
R_p = 500 OHMS
R_s = 1100 OHMS
R_t = 1200 OHMS

A-30735

HORIZONTAL SCALE 0.016 MICROSECONDS PER SMALL DIVISION
VERTICAL SCALE 6.6 VOLTS PER SMALL DIVISION FIG. 53

APPROVED FOR PUBLIC RELEASE. CASE 06-1104.

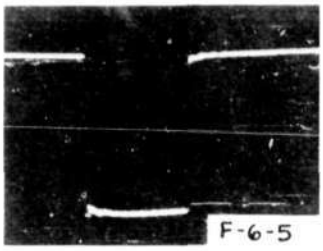

FIVE-MICROSECOND PULSE USED AS INPUT FOR F-6-6,8. HORIZONTAL SCALE 5μSEC PER DIVISION.

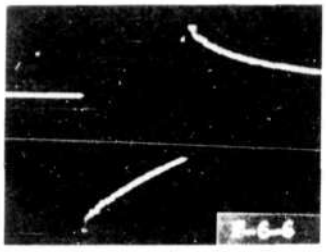

WAVEFORM AT "A", FIG. 46. (S, CLOSED, R_p = 3000 OHMS) T17 WITH MU-METAL CORE

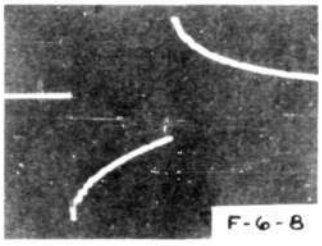

SAME AS F-6-6 EXCEPT HIPERSIL CORE

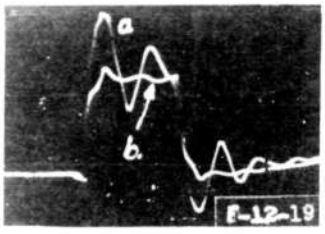

(a) WAVEFORM AT "D", FIG. 45, WITH "B" GROUNDED; 166 AW. (R_{sc} = 0, R_s = ∞, R_c = 100 OHMS)
(b) SAME AS (a) EXCEPT R_{sc} = 390 OHMS.
PULSE DURATION = ¼μSEC

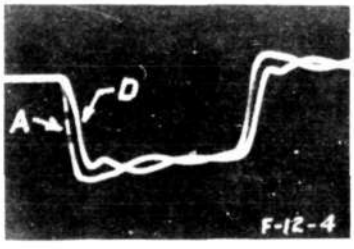

WAVEFORMS AT "A" AND "D", FIG. 43, WITH "B" GROUNDED; T19. R_p = 1100 OHMS, R_s = 1000 OHMS. PULSE DURATION = ¼μSEC

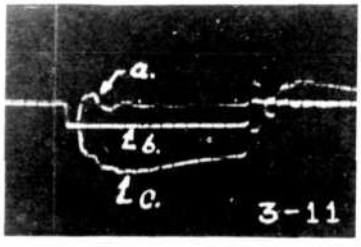

WAVEFORM AT "A", FIG. 43, WITH "B" GROUNDED; 132AW-2. (R = 500 OHMS) (a) R_s = 0 (b) R_s = 180 OHMS (c) R_s = ∞ HORIZONTAL SCALE .016μ SEC PER DIVISION

A - 30736

FIG. 54

APPROVED FOR PUBLIC RELEASE. CASE 06-1104.

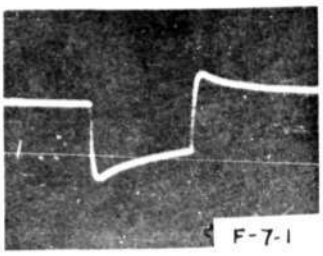

F-7-1

WAVEFORM AT "A", FIG. 4-6.
(S_1 CLOSED, R_p=3000 OHMS)
TI7 WITH HIPERSIL CORE.
PULSE DURATION = 1 μ SEC

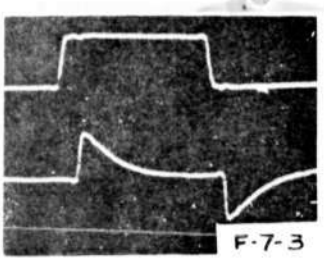

F-7-3

WAVEFORMS AT "D", FIG. 4-3;
TI7 WITH "B" GROUNDED.
(R_p=1100 OHMS, R_s=1000 OHMS)
UPPER TRACE: CORE IN
LOWER TRACE: CORE OUT
PULSE DURATION = $\frac{1}{2}$ μ SEC

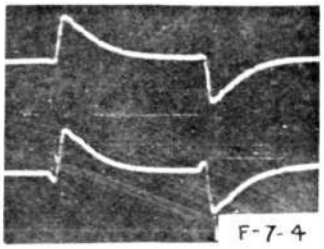

F-7-4

UPPER TRACE: SAME AS
LOWER TRACE IN F-7-3.
LOWER TRACE: ONE WINDING
DISPLACED $\frac{5}{32}$ INCHES

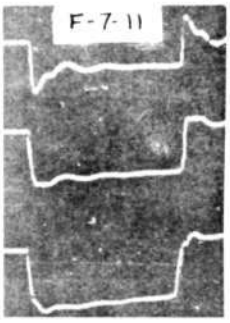

F-7-11

WAVEFORMS AT "A", FIG. 4-3;
TI7 WITH "B" GROUNDED.
(R_p=1100 OHMS)
TOP TRACE: R_s= 470 OHMS
MIDDLE TRACE: R_s=1100 OHMS
BOTTOM TRACE: R_s=2200 OHMS

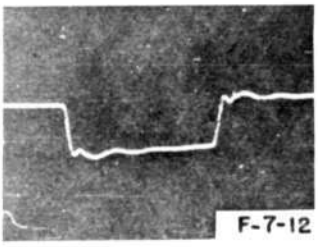

F-7-12

WAVEFORM AT "D", SAME
CIRCUIT AS FOR F-7-11
(R_s =1100 OHMS)

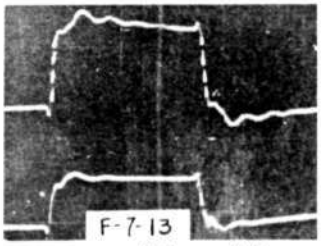

F-7-13

WAVEFORMS AT "B" WITH "D" GROUNDED
SAME CIRCUIT AS FOR F-7-12
UPPER TRACE; $R_s = \infty$
LOWER TRACE: R_s =1100 OHMS

HORIZONTAL SCALE 0.03 MICROSECONDS PER SMALL DIVISION
VERTICAL SCALE 6.6 VOLTS PER DIVISION

FIG. 55

A-30737

APPROVED FOR PUBLIC RELEASE. CASE 06-1104.

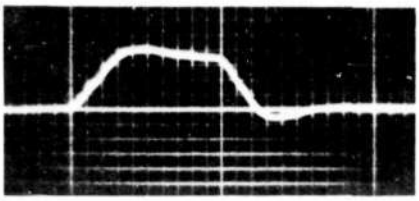

F-103-1
RESPONSE OF T52D5

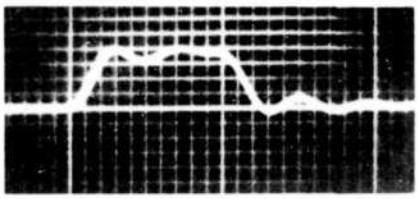

F-103-8
RESPONSE OF LOW-FREQUENCY ANALOGUE OF T52D5

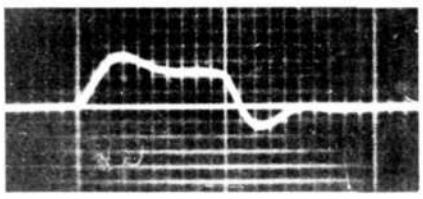

F-103-2
RESPONSE OF T39

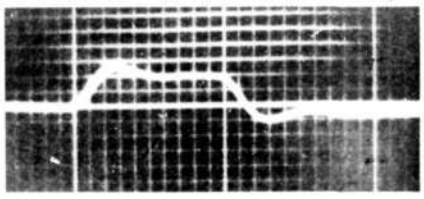

F-103-5
RESPONSE OF LOW-FREQUENCY ANALOGUE OF T39

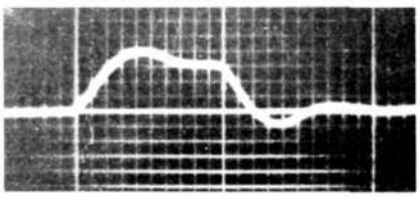

F-103-4
RESPONSE OF T53A

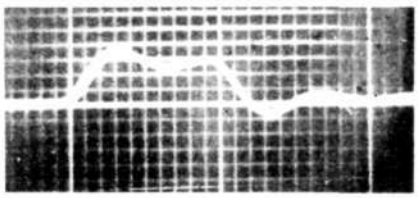

F-103-7
RESPONSE OF LOW-FREQUENCY ANALOGUE OF T53A

HORIZONTAL SCALE 0.023μ SEC PER SMALL DIVISION

HORIZONTAL SCALE 0.53μ SEC PER SMALL DIVISION

VERTICAL SCALE 6.6 VOLTS PER SMALL DIVISION

FIG. 56

A-30738

APPROVED FOR PUBLIC RELEASE. CASE 06-1104.

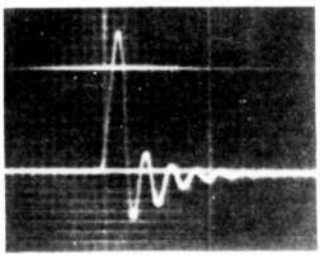

F-118-20
TWENTIETH-MICROSECOND-PULSE RESPONSE OF T66C WITH NO RINGING COMPENSATION.

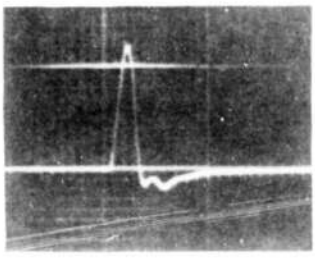

F-118-23
TWENTIETH-MICROSECOND-PULSE RESPONSE OF T66C WITH L_R-R_R CORRECTIVE NETWORK AS SHOWN IN FIG. 49.
(L_R = 10 MICROHENRYS, R_R = 500 OHMS)

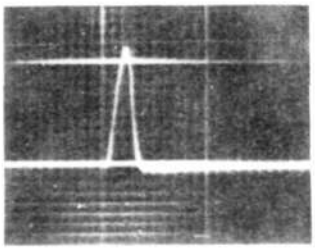

F-118-22
TWENTIETH-MICROSECOND-PULSE RESPONSE OF T66C WITH L_R-R_R NETWORK PLUS A DIODE IN THE PRIMARY CIRCUIT AS IN FIG. 49.
(R_p = 550 OHMS, S_1 CLOSED)

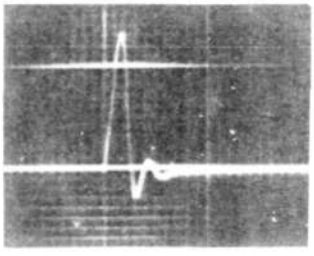

F-118-21
TWENTIETH-MICROSECOND-PULSE RESPONSE OF T66C WITH ONLY DIODE NETWORK IN PRIMARY FIG. 49.
(S_2 CLOSED)

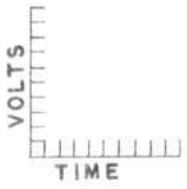

HORIZONTAL SCALE 0.023 MICROSECONDS PER SMALL DIVISION
VERTICAL SCALE 6.6 VOLTS PER SMALL DIVISION

FIG. 57

A-30739

APPROVED FOR PUBLIC RELEASE. CASE 06-1104.

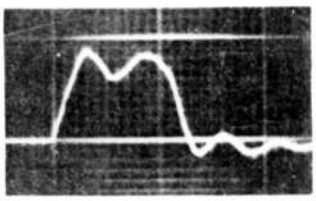

F-118-24
QUARTER-MICROSECOND-PULSE RESPONSE OF T63C2 WITH NO RINGING COMPENSATION

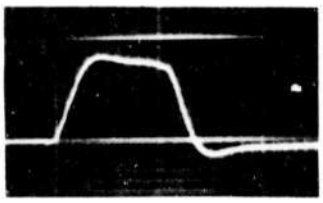

F-118-25
QUARTER-MICROSECOND-PULSE RESPONSE OF T63C2 WITH L_R-R_R CORRECTIVE NETWORK AS SHOWN IN FIG. 49. (L_R = 25 MICROHENRYS, R_R = 1000 OHMS)

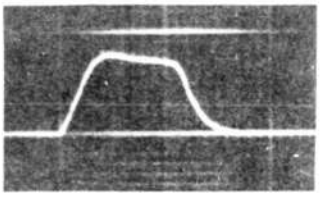

F-118-26
QUARTER-MICROSECOND-PULSE RESPONSE OF T63C2 WITH BOTH L_R-R_R NETWORK AND DIODE ACROSS PRIMARY.

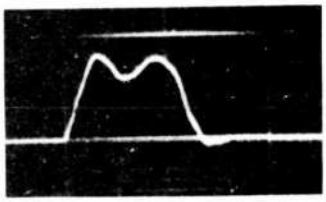

F-118-27
QUARTER-MICROSECOND-PULSE RESPONSE OF T63C2 WITH ONLY DIODE CORRECTION IN PRIMARY, FIG. 49. (S_1 CLOSED)

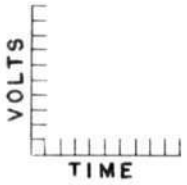

HORIZONTAL SCALE 0.023 μ SEC. PER SMALL DIVISION
VERTICAL SCALE 6.6 VOLTS PER SMALL DIVISION

FIG. 58

A-30740

APPROVED FOR PUBLIC RELEASE. CASE 06-1104.

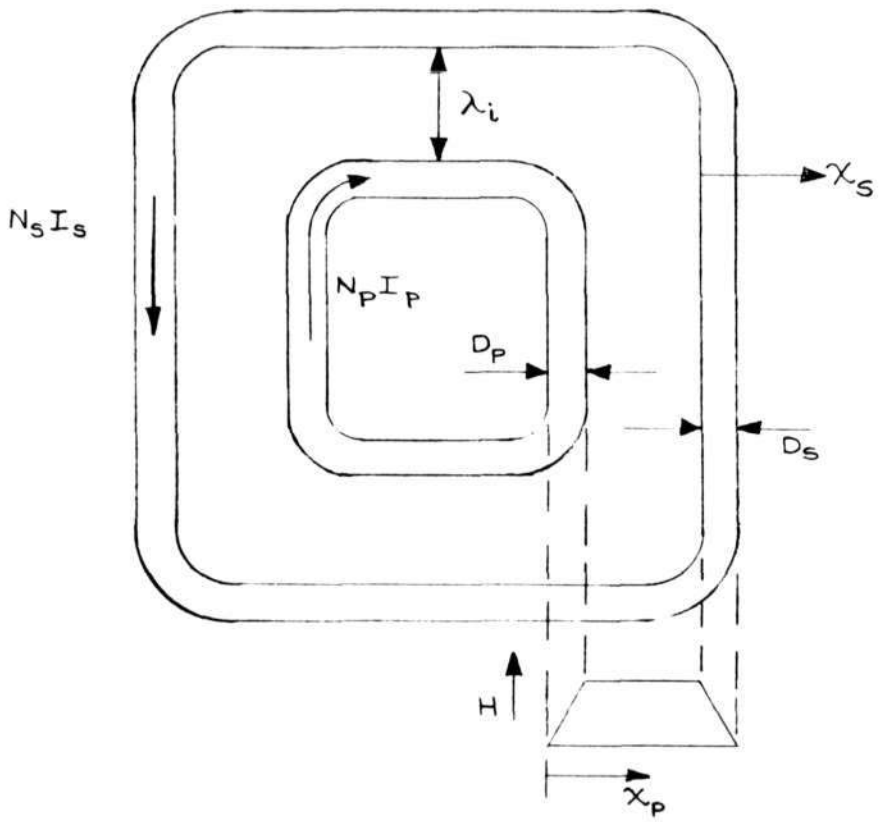

FIG. 59 SCHEMATIC SHOWING LEAKAGE FLUX DISTRIBUTION FOR UNIFORM-FIELD ASSUMPTION.

λ-306652

APPROVED FOR PUBLIC RELEASE. CASE 06-1104.

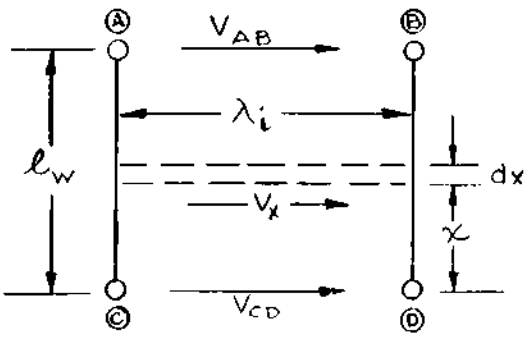

FIG. 60 PULSE TRANSFORMER WINDINGS REPRESENTED BY PARALLEL PLATES.

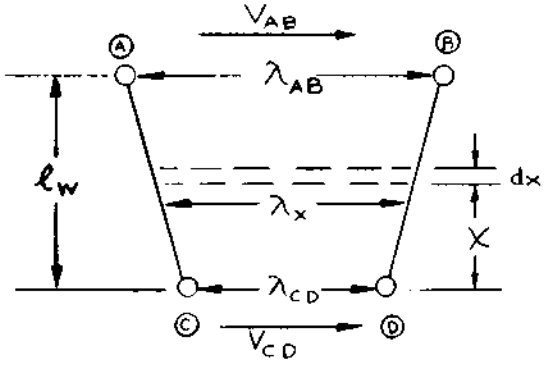

FIG. 61 WINDINGS WITH TAPERED SPACINGS.

1-30653

FIGS. 60 & 61

APPROVED FOR PUBLIC RELEASE. CASE 06-1104.

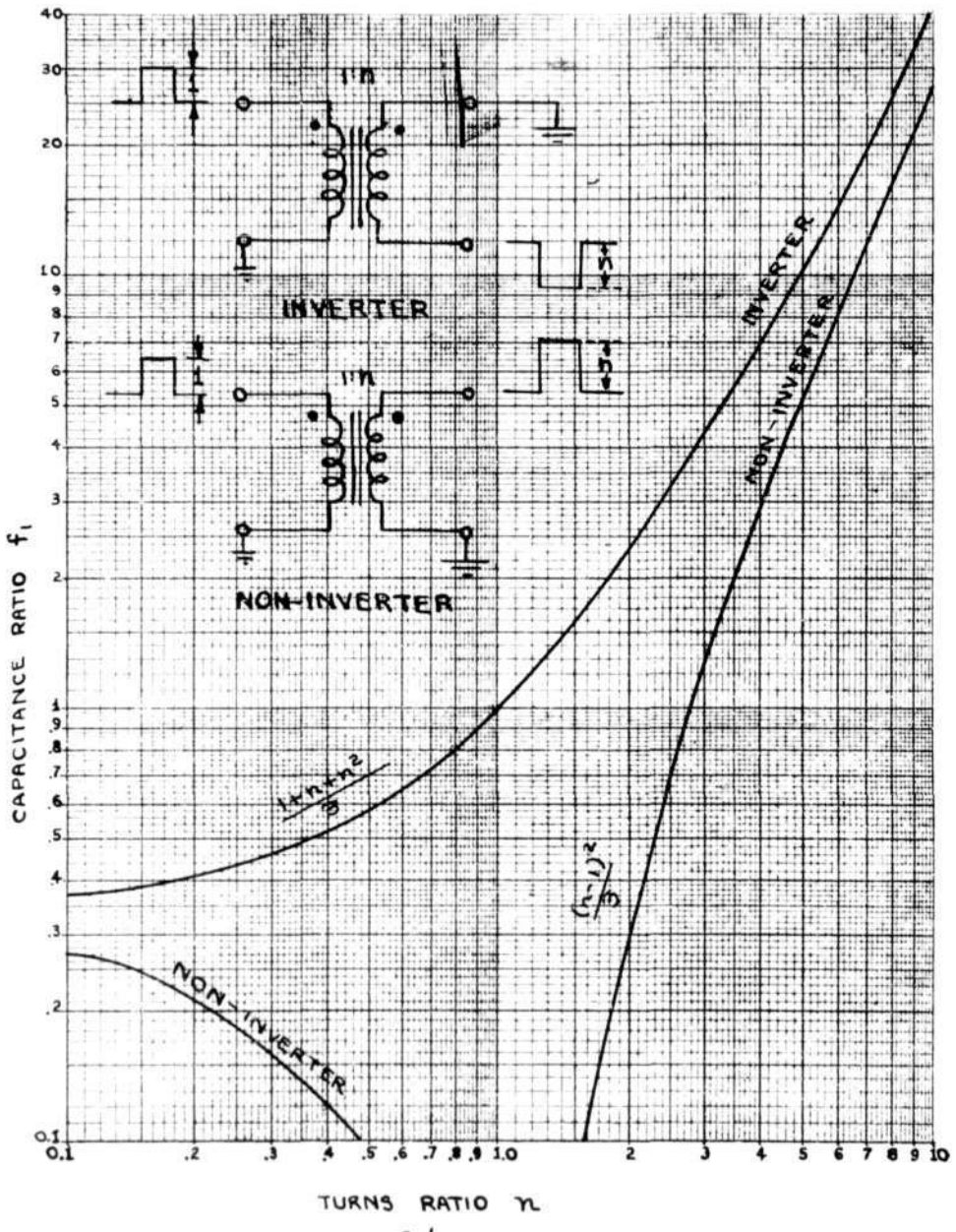

FIG. 62. CAPACITANCE RATIO $\frac{C_D'}{C_1} = f_1'$ PLOTTED AGAINST n

-30769